

Remotely Operated Aerial Vehicles and Their Applications

An Interactive Qualifying Project

Submitted to the Faculty

of the

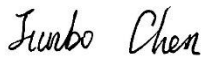
WORCESTER POLYTECHNIC INSTITUTE

in partial fulfillment of the requirements for the degree of

Bachelor of Science

by

Junbo Chen
Robotics Engineering



Ruizhe Chen
Mechanical Engineering



Kezheng Dai
Robotics Engineering



Spiridon Kasapis
Aerospace Engineering



Shihao Xia
Computer Science



January 19, 2017

Approved by:

Prof. M. S. Fofana, Advisor

Mechanical Engineering Department

ABSTRACT

The development of drone technologies is growing rapidly. Various types of drones and unmanned aerial vehicles are used in fields such as photography, transportation, military, and most importantly in search and rescue situations. The objective of this project is to evaluate the developments and applications of unmanned aerial vehicles (UAVs). The effort is mainly focused on the role of UAVs in the application of emergency medical services. A comparison of UAV designs is made in order to locate the most suitable UAV for emergency medical services. A number of UAV designs and their analyses are also evaluated. The designs include components such as UAV structures, flight control systems, instruments layout and applications of UAV heat transfer systems. A survey of various UAV applications in the market and related literature is also carried out. We compare UAV applications and functions in order to locate the most beneficial UAV and component designs for emergency medical services. This comparison provides us an opportunity to produce final design solutions. We use analytical methods such as mathematical modeling, static analysis, and computer aided flow simulations to select and verify the design parameters. These methods are foundational for better understanding of UAV technologies and design techniques. The societal impact of this IQP is that it will enhance the quality of ambulatory care.

TABLE OF CONTENTS

<i>Abstract</i>	<i>ii</i>
<i>Table of Contents</i>	<i>iii</i>
<i>List of Figures</i>	<i>v</i>
<i>List of Tables</i>	<i>viii</i>
CHAPTER 1. INTRODUCTION AND MOTIVATION	1
1. Introduction.....	1
CHAPTER 2. BACKGROUND INFORMATION	3
2. Introduction.....	3
2.1 UAV Analysis.....	3
2.1.1 Types and Usages of UAVs.....	3
2.1.2 UAV Shape Design Based on Speed, Altitude, Payload and Endurance	6
2.1.3 Inner Structural Design of UAVs	14
2.2 Flight Control Systems of UAVs.....	20
2.2.1 Physical Aerodynamic Controlling System.....	20
2.2.2 Physical Control for Each Component	22
2.2.3 Computational Control of Aerodynamic Control System	28
2.2.4 UAV Route Design.....	33
2.3 Power Components, Instruments and Sources of UAVs	36
2.3.2 Electric Motor	43
2.3.3 Internal Combustion and Jet Engines	47
2.3.4 Fuel Engine Power Source.....	53
2.4 Cumulative UAV Comparison.....	54
CHAPTER 3. UAV DESIGN SOLUTIONS	67
3 Introduction.....	67
3.1 Preliminary Design and Design Methodology.....	68
3.1.1 Wings design.....	68
3.1.2 Body Design.....	77
3.2 Search and Rescue Methodologies	80
3.2.1 Transducers and Sensors Descriptions.....	80
3.2.2 Specific Performance Evaluation.....	83
3.2.3 UAV Cooling System	85
3.3 UAV Control and Electric Parts	86
3.3.1 UAV Control Elements.....	86

3.3.2 UAV Control Analysis.....	93
3.4 UAV Data Transmission.....	96
3.4.1 Long Range Remote Control Description.....	96
3.4.2 On Board Computational Systems.....	101
3.4.3 UAV Data and Signal Transmission.....	107
CHAPTER 4. CONCLUSION	108
REFERENCES	109
APPENDICE	114
Dijkstra Functions	114

LIST OF FIGURES

Figure 1: Inspire3 created by DJI Company.....	4
Figure 2: The motor motion analysis of a quadcopter (top view).	4
Figure 3: The cross-section of wing and the air stream around	5
Figure 4: An MQ-1B predator taxis at Creech air force base	5
Figure 5: Parkzone ® Ember modified with articulated wings.....	6
Figure 6: RoboBee, an insect-like flight built by Harvard	6
Figure 7: Examples of wing shapes	7
Figure 8: The overview of X-47A.....	8
Figure 9: The overview of Altair UAV.....	8
Figure 10: The overview of MQ-8	9
Figure 11: The overview of talarion MALE	9
Figure 12: The speed contrast of each shapes of UAV.....	10
Figure 13: The altitude contrast of each shapes of UAV.....	11
Figure 14: The payload contrast of each shapes of UAV.....	11
Figure 15: The endurance contrast of each shapes of UAV.....	12
Figure 16: The overview of qinetiq zephyr	12
Figure 17: The overview of phantom 3 (UAV)	13
Figure 18: The overview of Hobby King™ Bix3 Trainer.....	13
Figure 19: Aircraft Inner structural parts joined together.....	15
Figure 20: Stresses that the drone body experiences	16
Figure 21: A general view of an airplane inner structure.....	17
Figure 22: Types of wings inner structures (cross section).....	17
Figure 23: An airfoil shape in the XFLR5 airfoil design software.....	18
Figure 24: Useful graphs can be plotted with the help of this software.....	18
Figure 25: Inner structure of wing (whole wing)	19
Figure 26: The airplane control parts labeled	20
Figure 27: Top view of a wing with aileron	22
Figure 28: Section view of a wing with aileron.....	23
Figure 29: Section view of plain flaps	24
Figure 30: Section view of split flaps	24
Figure 31: Section view of slotted flaps.....	24
Figure 32: Section view of fowler flaps	25
Figure 33: Best efficiency - for climbing, cruising, descent.....	25
Figure 34: Increased wing area - for take-off and initial climb.....	25
Figure 35: Maximum lift and high drag - approach to landing	26
Figure 36: Maximum drag and reduced lift - for braking on runway	26
Figure 37: Directional control via rudder deflection (top view).....	27
Figure 39: Left is a swept rudder, Right is rectangular rudder (side view).....	27
Figure 40: The section view of a horizontal stabilizer with elevator	28
Figure 41: The top view of a horizontal stabilizer with elevator	28
Figure 42: Negative feedback closed loop for transfer function	29
Figure 43: PID simulation.....	31
Figure 44: Damping ratio simulation.....	33
Figure 45: Relation between UAV and Back-End	34
Figure 46: Example of UAV Orbit (red).....	35

Figure 47: Basic structure of solar power system	37
Figure 48: Structure of MPPT algorithm	38
Figure 49: Contrast basic solar system(Left) and solar system with MMPT(Right).....	38
Figure 50: Fuel cell system construction.....	39
Figure 51: Fuel cell system.....	39
Figure 52: TOF camera abstraction.....	41
Figure 53: MESA imaging 3D TOF Camera SR4000 (ETH, 5m range).....	41
Figure 54: Effects of TOF camera.....	42
Figure 55: Camera function analysis	42
Figure 56: Fuel cell system construction.....	44
Figure 57: The relationship between UAV motor's torque and elements	45
Figure 58: The relationship between UAV power and altitude	46
Figure 59: The relationship between UAV power and speed	46
Figure 60: The relationship between UAV power and payload	47
Figure 61: The relationship between UAV power and weight	47
Figure 62: Full combustion engine diagram	48
Figure 63: 2002 BMW 5-Series Inline-6 Engine	49
Figure 64: Ferrari 360 3586cc Alloy V8 Engine.....	49
Figure 65: Jabiru 3300cc Aircraft Engine	50
Figure 66: Pratt & Whitney R-1340 Radial Engine	50
Figure 67: Centrifugal Turbo Engine.....	51
Figure 68: Turbo-Thrust Engine	52
Figure 69: Turbo-Prop Engine	52
Figure 70: Turbofan Engine	53
Figure 71: The speed performance of each UAV	63
Figure 72: The weight performance of each UAV.....	63
Figure 73: The endurance performance of each UAV.....	64
Figure 74: The altitude performance of each UAV	64
Figure 75: The range performance of each UAV	65
Figure 76: Examples of wings with different aspect ratio.....	68
Figure 77: Examples of the three different wing angle cases.....	69
Figure 78: The plot of aerospace materials with respect to strength and density	70
Figure 79: The XFLR5 analysis procedure for the given Reynolds and Mach numbers	72
Figure 80: The lift coefficient to angle of attack graph for the four NACA airfoils.....	73
Figure 81: The lift to drag ratio for NACA 4412 and NACA 9412 UAVs.....	74
Figure 82: The cross sections of NACA 4412 and NACA 9412 in XFLR5.....	74
Figure 83: The cross section of NACA 9412 in SolidWorks.....	76
Figure 84: The top back view of NACA 9412 and its wingspan length.....	76
Figure 85: The bottom view of NACA 9412 and its wingspan length	77
Figure 86: The top front view of NACA 9412.....	77
Figure 87: The design of UAV model	78
Figure 88: Our model seen from another angle	79
Figure 89: Additional top and side views of the model	79
Figure 90: One Dimensional Structure of an Accelerometer.....	81
Figure 91: The cooling system in the UAV.....	86
Figure 92: The relationship between each element in UAV	87

<i>Figure 93: The relationship between each device</i>	88
<i>Figure 94: 3D angle of view of the UAV control board</i>	88
<i>Figure 95: Application of NVIDIA Jetson TK1</i>	89
<i>Figure 96: 3D angle of view of battery.....</i>	90
<i>Figure 97: Application of battery</i>	90
<i>Figure 98: The 3D angle of view of Arduino Mega.....</i>	91
<i>Figure 99: 3D angle of view of the UAV camera</i>	92
<i>Figure 100: The free body diagram of the UAV.....</i>	95
<i>Figure 101: Basic sketch of MatLab Simulink for speed control</i>	96
<i>Figure 102: 2.4GHz/5.8GHz frequency wireless communication structure.....</i>	97
<i>Figure 103: Structure of UAV-Satellite Communication.....</i>	98
<i>Figure 104: Ranges for various radio frequency</i>	99
<i>Figure 105: Speed for various radio solution.....</i>	100
<i>Figure 106: Power consumption for different frequency</i>	101
<i>Figure 107: Different weights for different components</i>	102
<i>Figure 108: Relations among components in UAV</i>	103
<i>Figure 109: Speed Comparison between CPU and GPU.....</i>	104
<i>Figure 110: Visual Representation of Power Flow[3333]</i>	105
<i>Figure 111: UAV signal transmission structure</i>	107

LIST OF TABLES

<i>Table 1: The performance of each large UAV.....</i>	10
<i>Table 2: The performance of each small UAV.....</i>	14
<i>Table 4: Feedback Controller and Gain.....</i>	30
<i>Table 5: The datasheet of Yeair.....</i>	54
<i>Table 6: The datasheet of MQ-8.....</i>	54
<i>Table 7: The datasheet of MQ-9.....</i>	55
<i>Table 8: The datasheet of CH-3.....</i>	56
<i>Table 9: The datasheet of RQ-21.....</i>	56
<i>Table 10: The datasheet of EHANG 184.....</i>	57
<i>Table 11: The datasheet of Phantom3.....</i>	58
<i>Table 12: The datasheet of S1000+.....</i>	58
<i>Table 13: The datasheet of Precision hawk.....</i>	59
<i>Table 14: The datasheet of Zephyr.....</i>	59
<i>Table 15: The datasheet of Helios.....</i>	60
<i>Table 16: The datasheet of Hale-D.....</i>	61
<i>Table 17: The datasheet of Penguin B.....</i>	61
<i>Table 18: The datasheet of Global Hawk.....</i>	62
<i>Table 19: Cumulative UAV chart.....</i>	65
<i>Table 20: The values of the maximum lift coefficients for selected airfoil.....</i>	73
<i>Table 21: Data description of onboard accelerometers of the UAV [64, 65, 66].....</i>	83
<i>Table 22: Three kinds of gyroscopes that fit for the UAV [67, 68, 69].....</i>	84
<i>Table 23: NVIDIA Jetson TK1 kit content [76].....</i>	89
<i>Table 24: The datasheet of the battery of the UAV.....</i>	91
<i>Table 25: The data contrast of two small electrical board.....</i>	92
<i>Table 26: Example code for PID speed and altitude controller in C programming.....</i>	93
<i>Table 27: PID gain according to Ziegler-Nichols method.....</i>	95
<i>Table 28: The fight mode and speed of the UAV.....</i>	95
<i>Table 29: List of components onboard the UAV.....</i>	102
<i>Table 30: Functions used to control voltage in Linux.....</i>	106

CHAPTER 1. INTRODUCTION AND MOTIVATION

1. Introduction

Throughout the course of human history, harmful accidents, unpredictable attacks, and uncontrollable diseases have been a threat for citizens of the world. The value of human life has increased dramatically in the last Century. Therefore, the need for stronger security is of great concern for many societies around the world. Life expectancy in most of the Western World has nearly doubled in the last 200 years, especially after the Second World War. Governments do their best and spend enormous amounts of wealth to make sure that their citizens live in safe environments. Huge proportions of National budgets go towards medical related research in order to prevent the spread of diseases or find treatments for incurable illnesses. Substantial resources are also spent on the modernization and enforcement of safety systems and rescuing teams. This project focuses on incorporating UAVs into emergency medical services. The advantages of using a UAV include efficiency in terms of search time, risk management and cost reduction. These advantages increase the rate of survival and successful accomplishment of a rescue mission.

The objectives of the IQP are to evaluate a number of UAVs and their applications. The experienced gained from this evaluation is used to design a medical response UAV. The proposed UAV needs to have the ability to provide sufficient information to rescue teams by scanning the scene of an incident using sensors, cameras and other detection instruments. The scanning instruments provide data from the scene to an onboard computer, which builds a 3D image of the scene. Also, these instruments are able to distinguish between humans that need help and those facing possible threats from the surrounding area of the scene. The proposed UAV is capable of operating automatically, and carrying and delivering certain amount of payload to the victims on the scene. To achieve this objective, the IQP team evaluates a number of drones and UAV technologies, and then applies the knowledge gained to the designing of the proposed UAV for emergency medical services. To be more specific, the design process of the UAV involves several iterations. These iterations include, the detailed wing body design, power source selection, onboard electronic devices layout, and flight control mechanisms. The problem statement of the IQP is to evaluate various UAV technologies and their applications, and design a UAV that is able to carry at least two kilograms of payload. This UAV should also have a

minimum operating time limit of thirty minutes, and is able to detect victims who are in danger on the scene of an incident.

In the first Chapter of the report, the authors describe the motivation and the problem statement. The second Chapter introduces a selected number of UAV technologies based on UAV types, applications and capabilities. In order to provide an effective solution, our team analyze the performance of both commercial and military UAVs. In the third Chapter, based on the knowledge amassed in Chapters 1 and 2, the team presents design recommendations including instrument selection criteria, structural design, and flight control theories. We are hopeful that the proposed UAV will strengthen the work of emergency medical services. The medical response UAV can be used to deliver medical supplies such as plasmas, both in a crowded cities or facilities located faraway in the suburbs. In this case, people from different classes or living in different locations and conditions are able to receive the same quality of medical treatments and security. We believe that the proposed UAV design solutions will improve emergency medical services.

CHAPTER 2: BACKGROUND INFORMATION

2. Introduction

As mentioned in Chapter 1, our goal is to evaluate applications and designs of UAVs. It is essential to start with the analysis of UAV structures in order to understand the basic operations and functions. In this Chapter we discuss the different types of existing UAVs and what are the advantages and disadvantages in terms of applications and designs. Moreover, we discuss how the selected UAVs are built, and more specifically, what their outer shapes are and how they change relative to altitude, speed and load. Finally, we focus on the inner structure and computational system design of the UAVs.

2.1 UAV Analysis

2.1.1 Types and Usages of UAVs

UAVs are becoming important applications for many fields and the market for UAVs is growing globally as there is a strong drive to expand the use of UAVs. According to Teal Group's 2014 market study report, the estimate of UAV spending will double over the next decade from current worldwide UAV expenditures of \$6.4 billion annually to \$11.5 billion. A total of \$91 billion is expected in the next ten years [2]. Under the huge amount of market demand, different types of UAV are invented that can be used in different areas such as in industry, commercial, military, searching and rescuing. UAVs have many different applications and they can be categorized in three main kinds: quadcopters (include those with six or eight rotors), fixed-wing aircraft and micro drones [3].

Figure 1 presents quadcopters, which are also called quadrotor helicopters or quadrotors which are multi-rotor helicopters lifted and propelled by four rotors. Quadcopters are mostly small, light weighted with medium speed and altitude. They are all powered by electrical powers. Quadcopters use four motors with four propellers to create thrust and lift force. Figure 2 shows two motors of quadcopters which rotate counter clockwise and the other two motors rotate clockwise. This configuration causes the torque from each motor to cancel by the corresponding motor rotating in the opposite direction. The features of the vertical takeoff and landing and as well as horizontal flight avoiding obstacles, both with characteristics of low speed and high precision, make the quadcopters able to complete missions which require high level of difficult

movement and stability [4].

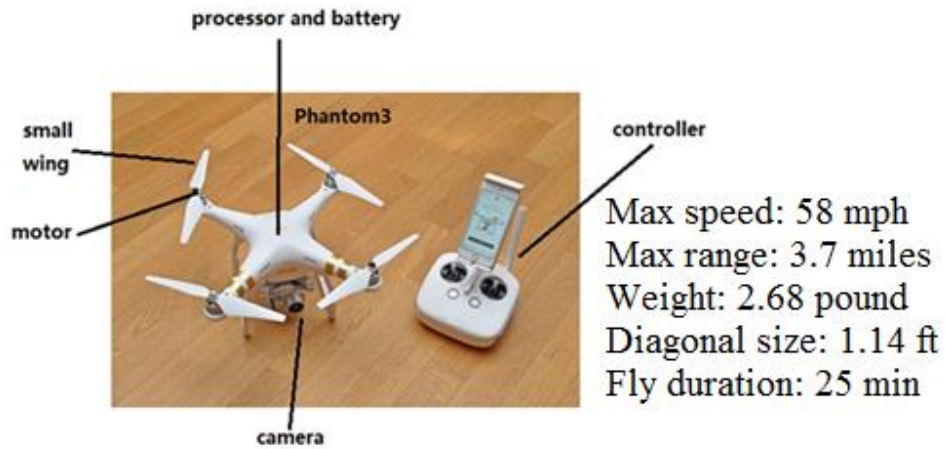


Figure 1: Inspire3 created by DJI Company

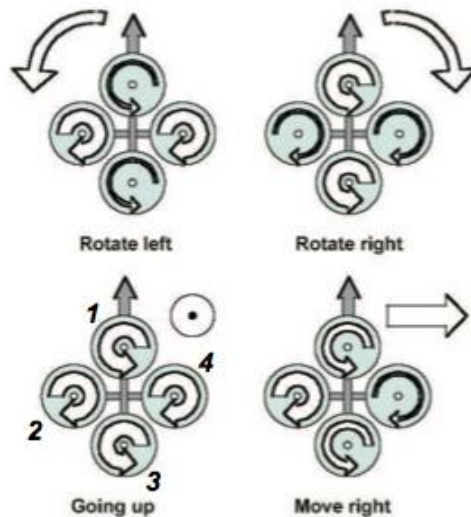


Figure 2: The motor motion analysis of a quadcopter (top view).

People take advantages of the quadcopters' low cost and high stability regimes and utilize them in shooting films, taking pictures and collecting scientific data. For example, the Inspire 3 is a complete ready-to-fly system, with four carbon fiber arms and a full 360 unobstructed view [5]. The Inspire 3 can take 4k high resolution pictures and videos in a distance of five kilometers. It can deliver payloads in a more effective manner than humans are capable of doing.

A fixed-wing aircraft is an aircraft like an airplane shown in Figure 4, which applies Bernoulli's principle by using the special shape of wings to gain lift force. According to the

Bernoulli's principle the pressure in a stream of fluid is reduced as the speed of the flow is increased. In the air stream, the air flows relatively faster at the upper layer of the wing than the lower layer. As a result, the pressure exerted on the upper surface of the wing is smaller than pressure exerted on the lower surface, which pushes the wings upward and makes the aircraft to fly [7].

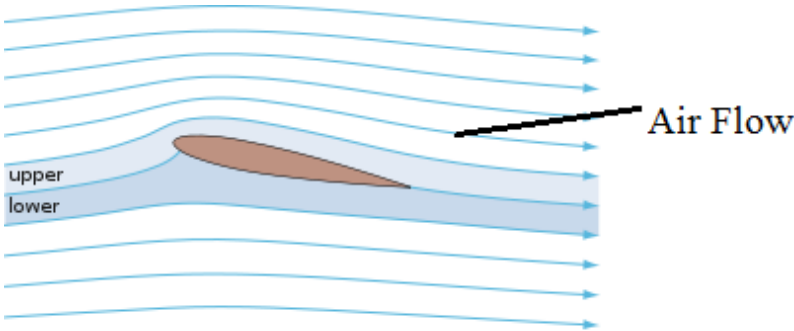


Figure 3: The cross-section of wing and the air stream around

Even though a fixed-wing UAV is difficult to take off and land, yet it has the advantages of flying faster, carrying more payload than quadcopters, staying in a relatively high altitude, and sustaining longer endurance than some other UAVs in the market and relevant literature. Thus, fixed-wing UAV can be used for long range detection, spraying pesticide for crops, providing combat ability for high risk mission. For example, the predator as shown in Figure 4, is medium altitude, long endurance, unmanned aerial vehicle which is used in risky areas where human life may be in danger. The predator is an asset for reconnaissance, surveillance and target acquisition in support of the Joint Force Commander of the United States Military [8].



Figure 4: An MQ-1B predator taxis at Creech air force base

A Micro drone or micro aerial vehicle (MAV) is the UAV with insect-size, and it is typically autonomous. There are two types of micro drone and they are: bird-like flight (see *Figure 5*) and insect-like flight (see *Figure 6*). The wings of the bird-like flight flaps have a low/medium frequency near vertical plane as seen in the *Figure 5*. Lift and thrust forces are generated mainly during the down stroke and the wings can fold back during the upstroke. Thus avoids the producing of any negative (downwards-oriented) lift. The wings of the insect-like flight flaps have a higher frequency within a horizontal or slightly inclined plane, which generates lift strokes in both directions (back and forth) [9].



Figure 5: Parkzone ® Ember modified with articulated wings

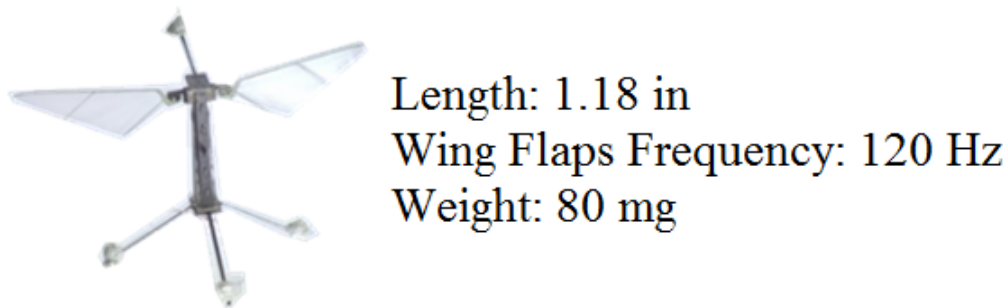


Figure 6: RoboBee, an insect-like flight built by Harvard

This kind of UAV has the advantages of small size and high agility. They can collect information from small holes or tunnels. In military use, they can also be used in reconnaissance without being noticed by enemies. Even though MAV has promising applications, its technology is not mature, and cannot be used in emergency medical services.

2.1.2 UAV Shape Design Based on Speed, Altitude, Payload and Endurance

Currently UAVs are known to have variable performance speed, altitude and payload to accomplish different tasks. Basically, the structure of a UAV is a good determinant of its speed, altitude, payload and endurance. In order to analyze the overall structure of a UAV, these

characteristics and other variables such as the power of the engine should also be considered [10]. We evaluate UAVs which have the same power source. The structure consists of a wing, tail, fuselage and head. Since each UAV has several components and each component can be shaped in many ways, it is difficult to define a specific shape for a UAV. Basically, the wing is one of the most important shapes for the UAV. There are some basic wing shapes [11] as seen in *Figure 7*. The shapes in *Figure 7* are the bases for selecting the case studies in this report.

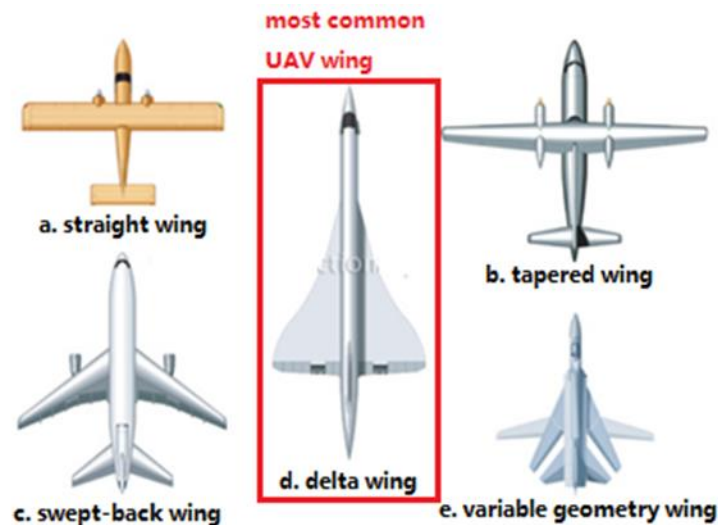


Figure 7: Examples of wing shapes

The first case study of current large UAV is the Northrop Grumman X-47, as shown in *Figure 8*, which is now part of the United States Navy's UCAS-D program. The airframe is a stealthy platform design. It is diamond-kite shaped with a 55° backward sweep on the leading edge and a 35° forward sweep on the trailing edge.

The X-47A has a wingspan of 8.47m and is 8.5m long. It uses a delta wing. The feature of this shape design is that it allows the UAV to fly at high subsonic speeds (greater than 305m/s) and with perfect stealth. However it has limited payload, attitude and endurance.

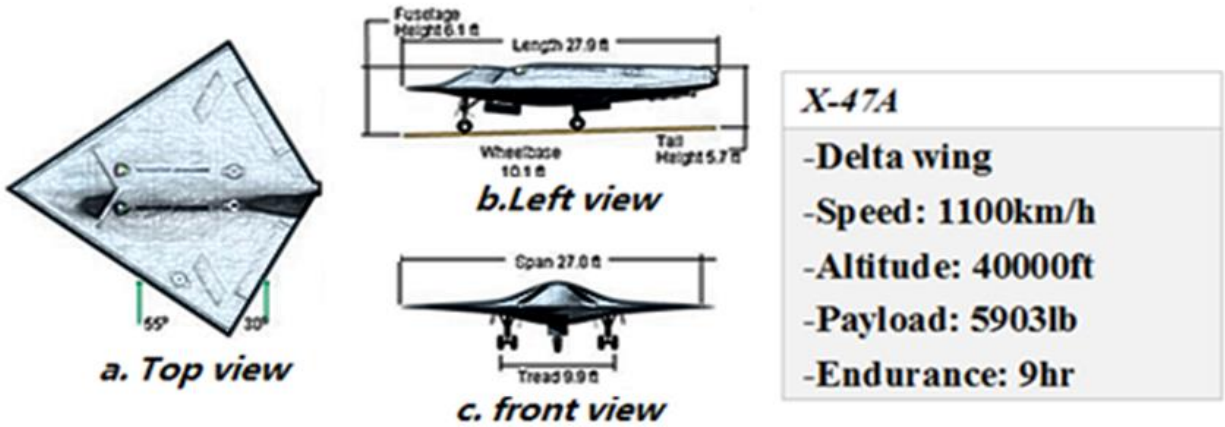


Figure 8: The overview of X-47A

The second case study of current large UAV is Altair, as seen in Figure 9. It is a variant of the improved Predator B UAV, which is designed to perform scientific and commercial research and as well as military intelligence missions. The Altair has a wingspan of 86 ft, can attain an altitude up to 52,000 ft and can remain airborne for well over thirty hours. Also it has six wing stations for external carriage of payloads. It uses tapered wing. The feature of this shape design is that it has extremely high altitude and endurance, good payload but relatively low speed.

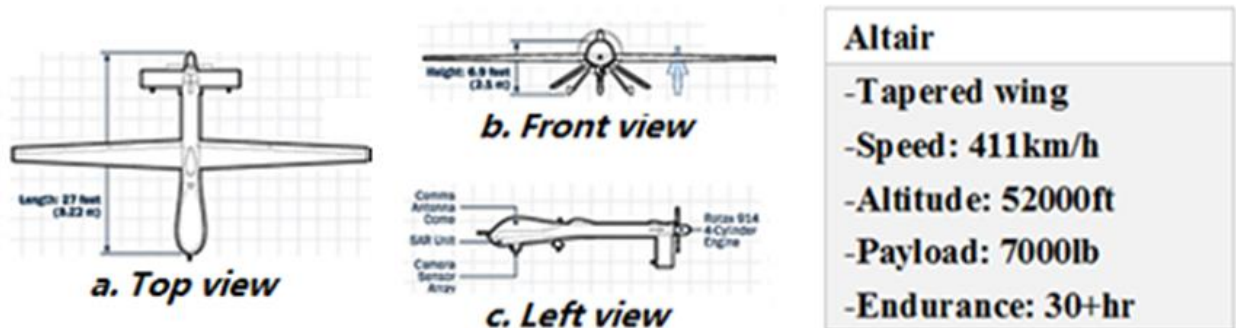


Figure 9: The overview of Altair UAV

The third case study of current large UAV is MQ-8B Fire Scout as seen in Figure 10. It provides unprecedented situation awareness and precision targeting support for the U.S. Navy. The feature of this rotary wing design is that it has the ability to autonomously take off and land from any aviation-capable warship and unprepared landing zones.

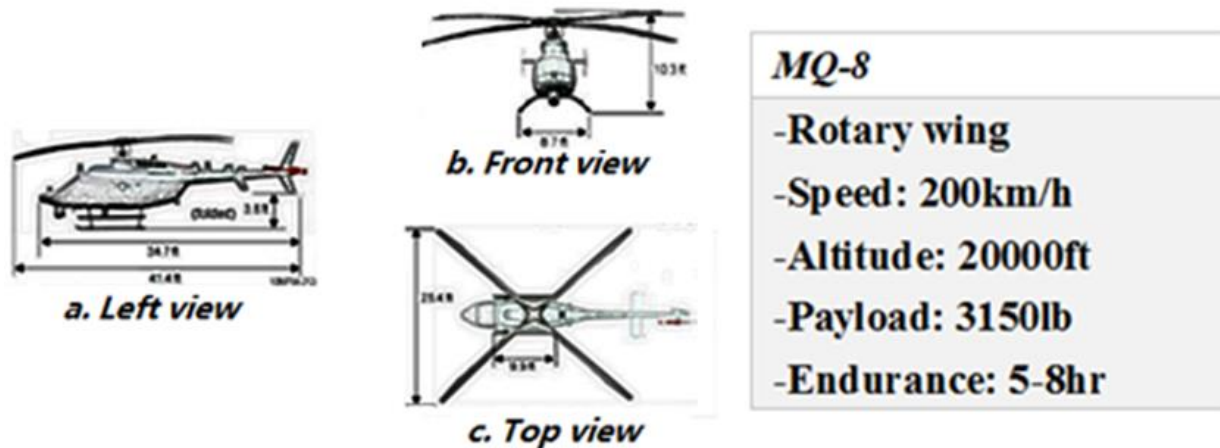


Figure 10: The overview of MQ-8

The fourth case study of current large UAV is Talarion MALE as seen in Figure 11, which is a medium altitude long endurance (MALE) unmanned air vehicle (UAV) designed and manufactured by EADS, which is The Airbus Group. The Talarion MALE has a shape different from the competing global Hawk. The fuselage utilizes a well-streamlined shape with a bulbous nose assembly housing avionics. The feature of this shape design is that it has large payload and relatively high speed.



Figure 11: The overview of talarion MALE

The data, found in Table 1 is the performance of a selected number of UAVs . By using this table, our team obtain specific parameters contrast of differently shaped UAV shown in *Figure 11*. This graph is very useful for future selection of UAV shape. For example, if we want to have a UAV with a good endurance and payload, we can read the chart in Table 1 and find what matches the best to the specifications. The Talarion MALE is the best fit for the specifications. If the UAV environment is rugged and a vertically takeoff and landing are needed, the shape design of the MQ-8 is a good choice [12].

Table 1: The performance of each large UAV

UAV	Speed	Altitude	Payload	Endurance
X-47	1100 km/h	40,000 ft	5,903 lb	9 hr
Altair	411 km/h	52,000 ft	7,000 lb	30+ hr
MQ-8	200 km/h	20,000 ft	3,150 lb	5-8 hr
Talarion MALE	555 km /h	49,213 ft	15,432 lb	20 hr
Barracuda	1,041 km/h	20,000 ft	7,165 lb	4 hr

Figure 12 shows the speed contrast of each shapes of UAV. The shape of X-47 has better speed ranges than the others. It is a good reference of future shape selection.

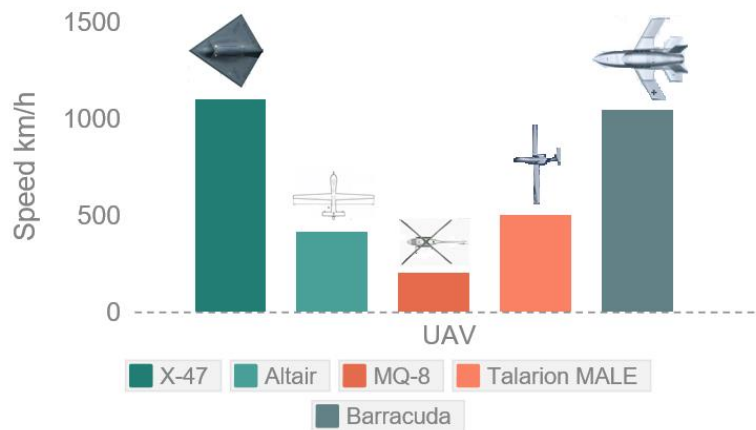


Figure 12: The speed contrast of each shapes of UAV

Figure 13 shows the altitude contrast of each shapes of UAV. The shape of Altair has an advantage of altitude. It is a good reference of future shape selection.

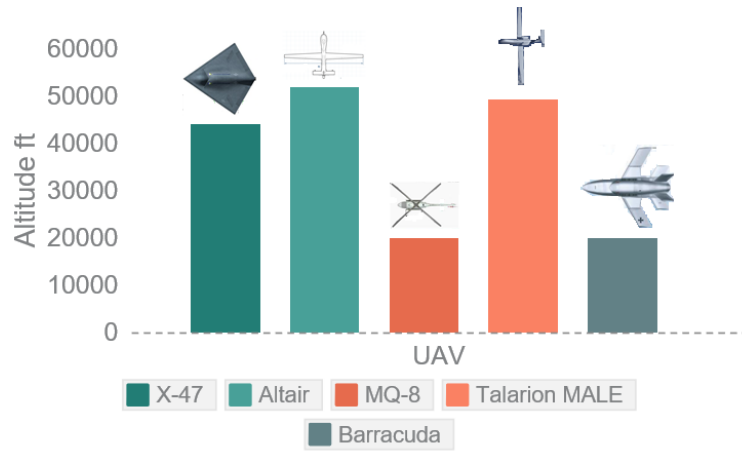


Figure 13: The altitude contrast of each shapes of UAV

Figure 14 presents the payload contrast of each shapes of UAV. The shape of the Talarion Male has an advantage of carrying large payload. It is a good reference of future shape selection.

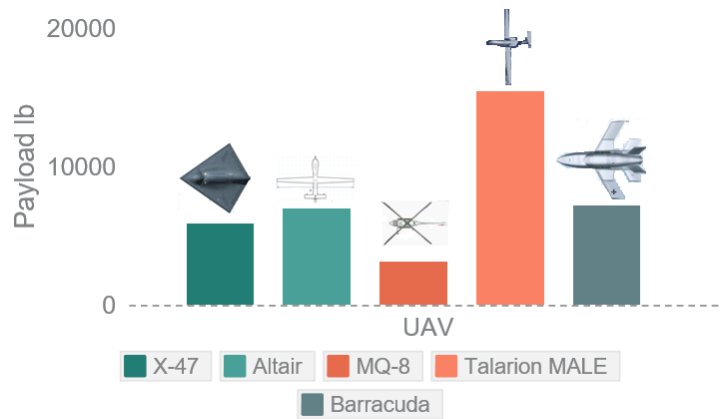


Figure 14: The payload contrast of each shapes of UAV

Figure 15 indicates the endurance contrast of each shapes of UAV. The shape of Altair has an advantage of endurance. It is a good reference of future shape selection.

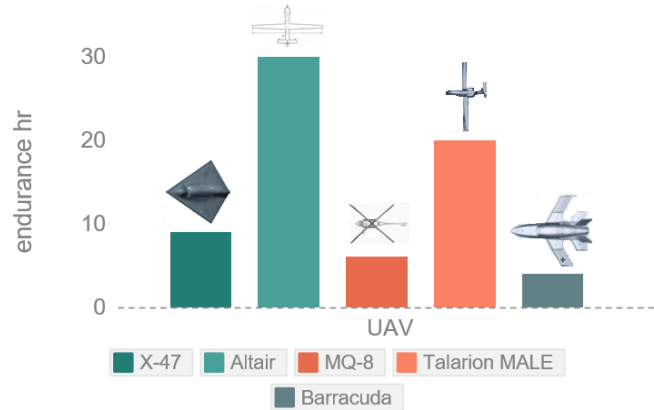


Figure 15: The endurance contrast of each shapes of UAV

Since small UAVs are powered by a weaker electric motors, the speed, altitude, payload, and endurance are extremely lower than for UAV powered by fuel engine. The size of the UAVs are far smaller than the one powered by fuel engine. Therefore, the shape of UAVs are totally different than the large UAV except the Qinetiq Zephyr (lightweight solar-powered UAV). The first case study of current small UAV is the Qinetiq Zephyr as seen in Figure 16. Zephyr uses its state-of-the-art solar cells which spread across the wings of the UAV to recharge high-power lithium-Sulphur batteries and drive two propellers. At night, the energy stored in the batteries is sufficient to maintain Zephyr in the sky. An important characteristic of the shape of this UAV is that it has infinite endurance and very high altitude [13].



Figure 16: The overview of qinetiq zephyr

The second case study of current small UAV is Phantom, the representative of small rotary drone, as seen in Figure 17. Phantom is a series of unmanned aerial vehicles (UAVs) developed by a Chinese company. The body frames are made of composite materials. Propulsion

is provided by four two-blade propellers driven by four electric engines mounted at the ends of the x-shaped body. The feature of the shape of this UAV is that it requires very small take-off and landing area and has good control mechanism.

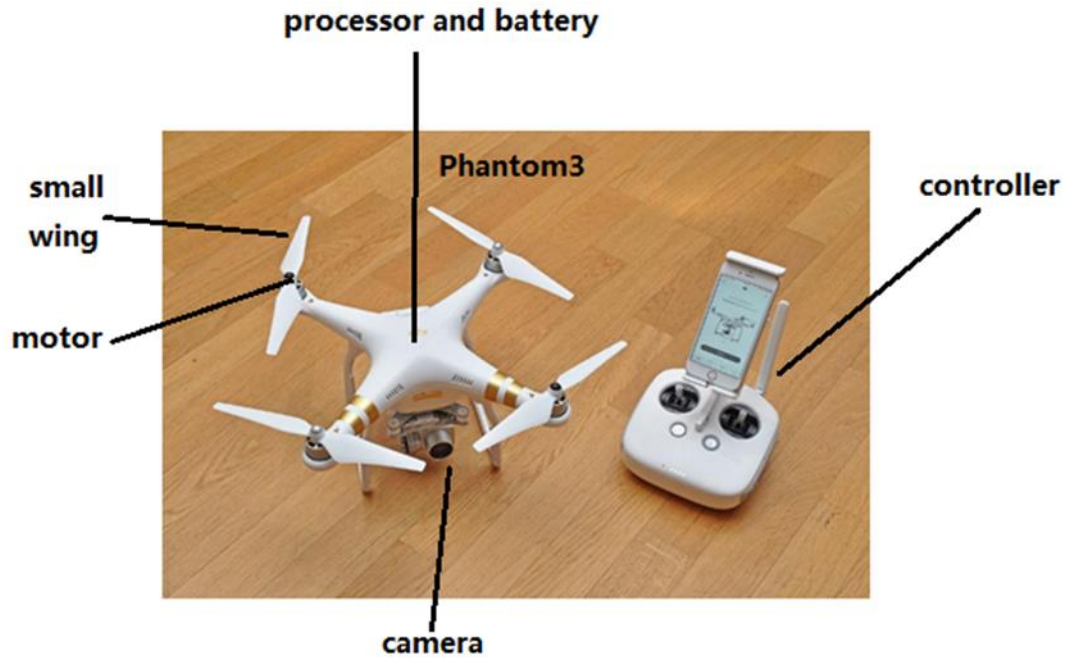


Figure 17: The overview of phantom 3 (UAV)

The third case study of current UAV is the Hobby King™ Bix3 Trainer. This represents a small fix-wing drone. It has 1550 mm large wing for better slow flight and weight capacity and two piece wings for easy transportation. The feature of this shape is that it is very light and has relatively low power and longer endurance. In addition it has higher speed than the shape of rotary wing UAV [14].



Figure 18: The overview of Hobby King™ Bix3 Trainer

Table 2: The performance of each small UAV

UAV	Speed	Altitude	Payload	Endurance
Zephyr	56 km/h	70,000 ft	117 lb	infinite
Phantom3	25.6km/h	1,640 ft	2.82 lb	0.41 hr
Hobby King™ Bix3 Trainer	45km/h	3,000 ft	1.96 lb	0.83 hr

The datasheet as seen in Table 2 is the performance of small shaped UAVs. This Table is useful for the selection of the UAV shape and structure. For example, an electrically powered UAV can reach high speeds seen in Table 2. A good choice is to use a similar shape as the Hobby King™ Bix3 Trainer, which is a fixed-wing UAV [15].

2.1.3 Inner Structural Design of UAVs

To be able to craft a fully functional UAV, it is necessary to have a deep knowledge on how aircrafts are structured. A drone's structure differs from this of a conventional airplane as it doesn't carry people. The inner body of a drone is filled with equipment which are necessary for the drone to fly, communicate and navigate itself. Detecting instruments will also be included in the UAV, as detection of people is the main desirable operation. The main question to be answered in this section is how UAV manufacturers decide to arrange all of the above equipment in their vehicle's body [16].

The methods of building an aircraft are similar. However, there is a huge difference between the man-piloted aircrafts and UAVs. During the manufacturing process, a man-piloted aircraft structure is designed to protect human and also provide additional comfort. More specifically, the fuselage must provide a pressured environment with certain level of humidity, and also absorbs vibration generated by the high speed air flow. An UAV fuselage contains equipment and cargo, which means the inner frame is only required to handle stresses due to the air pressure. There are several types of UAV fuselage that are commonly being used in the field. They are high density foam fuselage, composite material hollow fuselage, composite material with inner frame fuselage, and pure metal frame fuselage. The high density foam fuselage and the composite material hollow fuselage are usually used for small remotely controlled aircrafts.

The composite material with inner frame fuselage and the pure metal frame fuselage are more often used for larger fixed-wing UAVs, because they are able to handle more stress while in the air, thereby allowing the aircraft to carry more weight and do high force load maneuvers [17].

For a small UAV, the main objective of body structure is lightweight. The material of body structure is plastic or wood. For example, Balsa wood provided a solid and light base for the access panels and tied the structure together, providing more strength than others. It is efficient to use glue or screw, nut to combine the fuselage together. Basically, the glue has the advantage of light, small space. The screw and nut have the advantage of durable, stiffness. Both of these UAVs can play a significant role in linkage connection. However, for a large UAV, the material of fuselage becomes more complicated. In general, fuselage is built by metal frames improved the strength, which can finally led all-metal aircraft with metal covering all surfaces. On the other hand, some UAV fuselages are constructed with composite materials for main part. It allows a higher pressurization levels and lower weight. Because of the complexity of fuselage, the fuselage of a UAV should be constructed in basically three different methods and they are truss, stressed surface material.

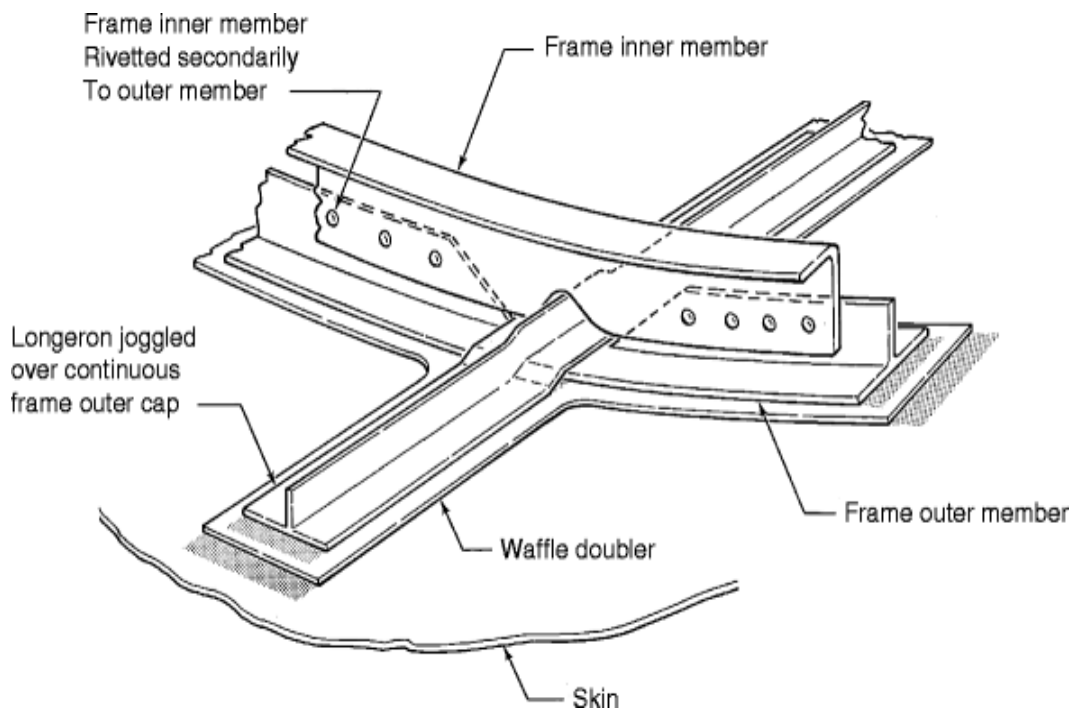


Figure 19: Aircraft Inner structural parts joined together

There are several components that are used in a common aircraft fuselage frame which are skin, ribs, spars, doublers and membranes. Aircraft frames are able to handle different types

of forces such as shear force, tension, bending force, compression force and torsion, shown in Figure 20. Specifically, the skin is the outer surface of the aircraft, which allows the air to flow through smoothly while distributing air pressure loads evenly onto the inner frame. Ribs and spears are usually mounted vertically to each other and these two components are able to handle stresses while the aircraft is in the air. A doubler is a reinforcement for the ribs and spears of the aircraft. Additionally, it is able to amortize the air pressure load to the inner frame. A member is usually a connection on the rib or spear, which connects different components together while distributing the load evenly by either glue or rivets. Additionally, there are some areas of an aircraft frame which need special reinforcements such as the connection between wings and body structure, fuel tank and engines. There are several reinforcement methods for each case, shown in Figure 21. For the connection between wings and body, composite materials are often used to handle extra tension at the structure of the connections and also to reduce uncontrollable vibrations caused by turbulences. Fire proof materials are often used to protect the fuel tank. Heat resistant ceramics are often used to isolate heat generated components by the main engines [18].

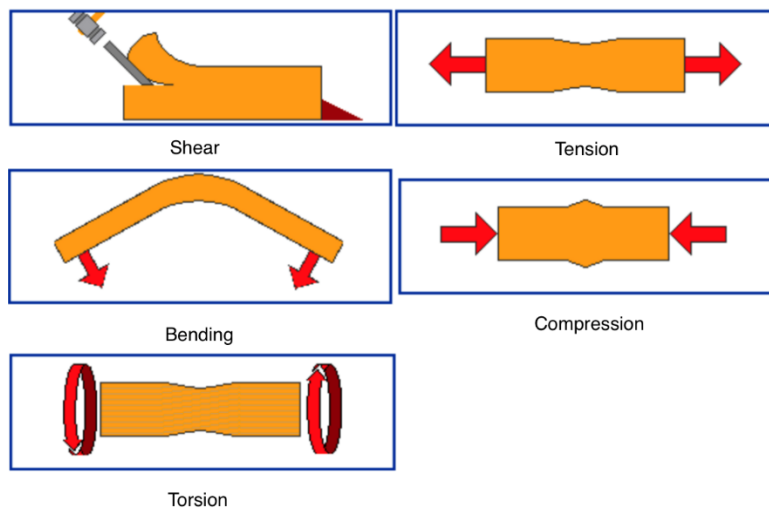


Figure 20: Stresses that the drone body experiences

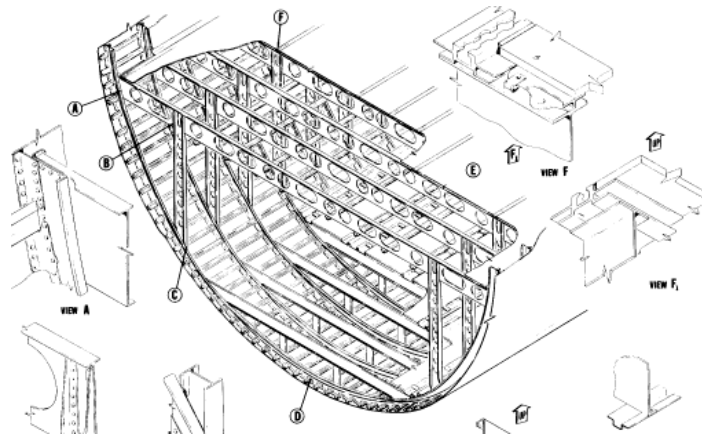


Figure 21: A general view of an airplane inner structure

The design of the wings are the most complicated portion of an UAV. There are several types of wings that are used by a man-piloted aircraft such as vertical stabilizer, horizontal stabilizer and two major wings. Aircraft wings may also include elevators, rudders, flaps, ailerons, and speed brakes which handle most of the load of the aircraft and provide maneuver abilities to the aircraft. There are several types of inner structures that designers are able to choose from (see Figure 22). Four types of designs, which are commonly used in the field of aircraft design are rib-spar structure, composite material structure, hollow wing structure, and high density foam structure [19].

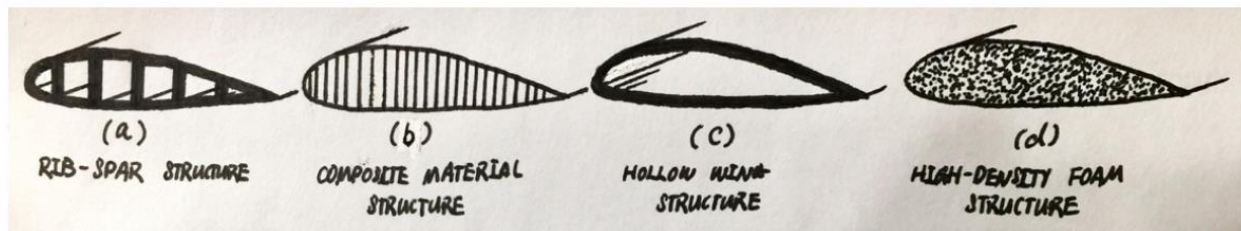


Figure 22: Types of wings inner structures (cross section)

In order to design heavy duty wings, the first step is to find the airfoil shape that is preferred for the given specifications. Different airfoil shapes result to different lift and drag forces. We first have to know what the total weight of the proposed UAV should be. With this knowledge, we can calculate the lift force needed to get it in the air. XFLR5 is the software we use to analyze airfoil types and shapes to find the one that matches the design specifications. Using this software our team customize the shape of the airfoil of the UAV. An example of the

XFLR5 airfoil data processing is listed as follow. For the Boeing Commercial Airplane Company model 737 airfoils, the software generates the following shape [20]:

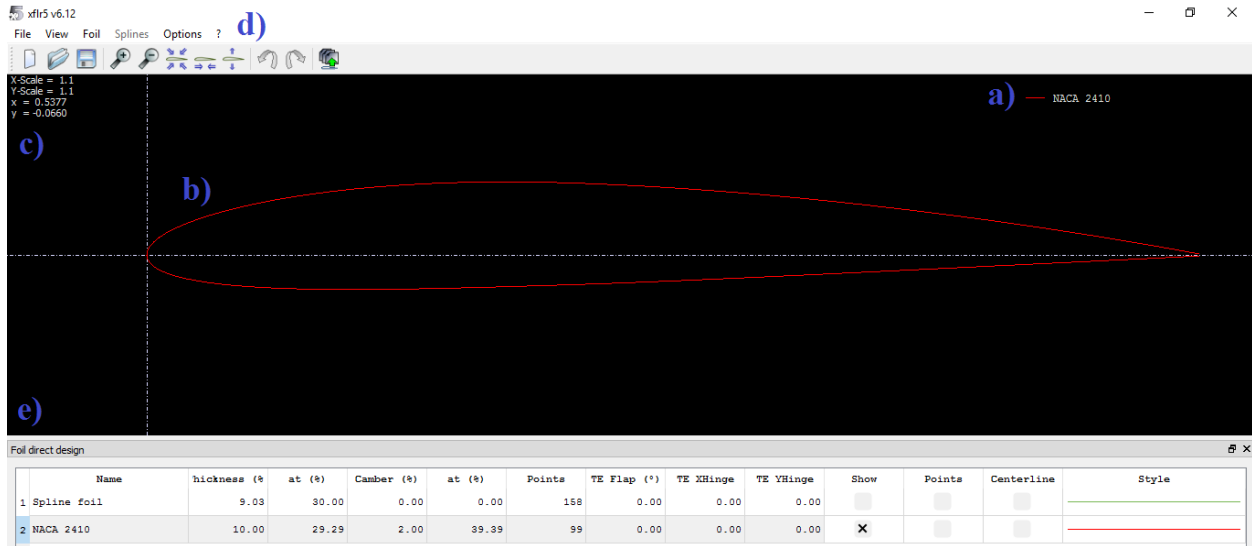


Figure 23: An airfoil shape in the XFLR5 airfoil design software

For the specific airfoil chosen, we generate a variety of plots of the lift coefficient and angle of attack for given Reynold's numbers.

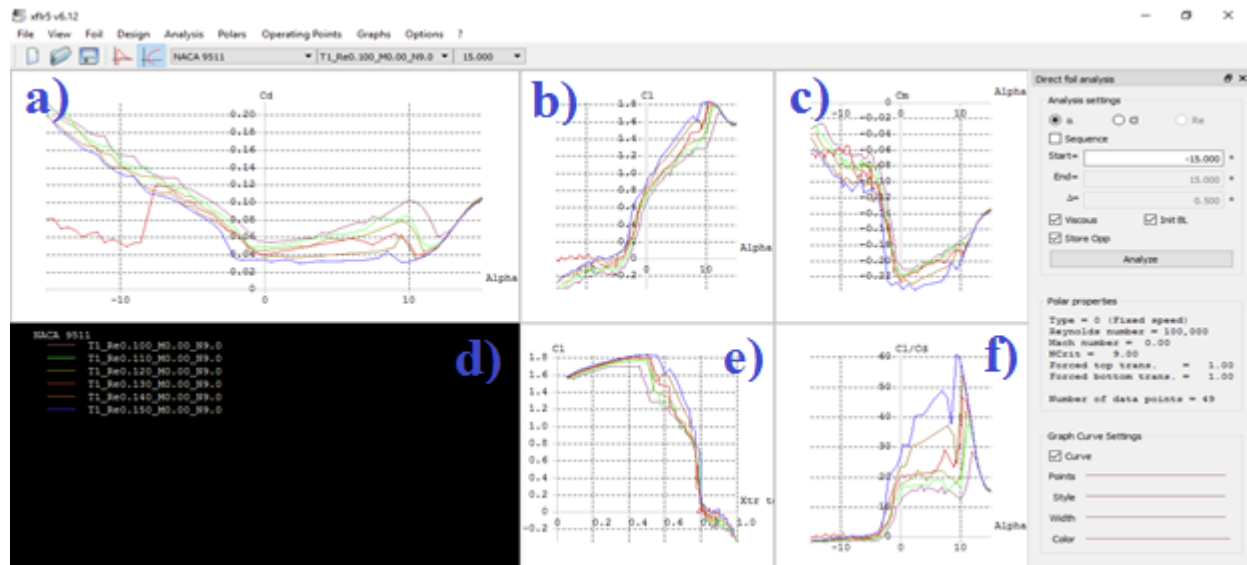


Figure 24: Useful graphs can be plotted with the help of this software.

Our first concern though, is the lift we want our wings to generate. To do so we will be using two basic equations. The first and most basic equations used is related with the lift coefficient. The inner structures of an UAV's wings are similar to an actual airplane, which include skin, ribs, spars, leading and trailing edges. More specifically, by analyzing each section individually and assuming the direction the aircraft goes is the X axis which is horizontal to the paper, the skin covers the entire inner structure of the wing, transforms the air pressure difference into lift and drag, and spreads the road of air pressure difference onto the inner structure of the wings. The ribs, which can be seen in *Figure 25*, handles most of the vertical loads due to the air pressure differences, usually lie almost vertically towards the X axis. The ribs also need to be patterned by the shape of the wings; specifically, no ribs that are in a wing structure must be placed all the way from the base to the tip of the wing. Spares are usually mounted vertical to the ribs of the aircraft and they must be placed perfectly perpendicular to the X axis. They handle most of the load from the air pressure which comes from the front of the wing and the turbulence generated at the tip of the wing. In another words, spars prevent the distortion of the wing structure. The leading and trailing edges are placed at the front and back of the wing. Specifically, the leading edge cuts through the air and spreads the load of front air flowing pressure evenly to spars and ribs, and the trailing edge smoothness the airflow. The wings of an aircraft not only handle the load due to the air pressure and also they carry multiple hydraulic systems. Also, the wings mount aerodynamic controlling components (flaps, ailerons, and speed brakes), and most commonly carrying fuel. The design of wings is indeed crucial for a high performance aircraft [21].

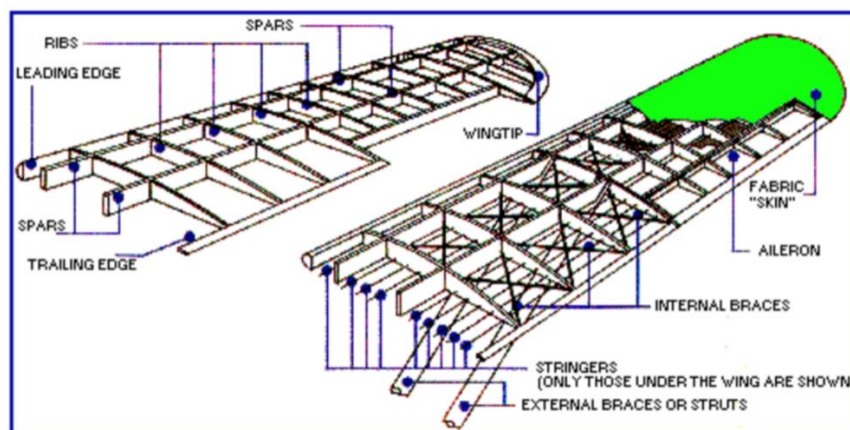


Figure 25: Inner structure of wing (whole wing)

2.2 Flight Control Systems of UAVs

In the sections above, we describe some of the major functions of the components of UAVs. In this section, we describe the relationship between each component and the actual flight control mechanisms. There are three axes that an aircraft can rotate: x , y , z (Figure 26) [22].

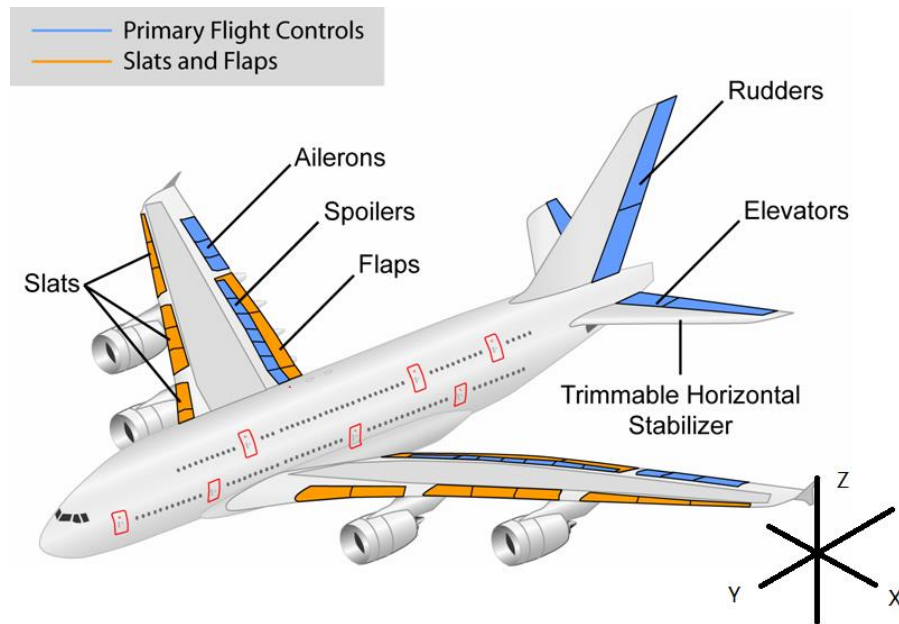


Figure 26: The airplane control parts labeled

The ailerons control the rotation of the aircraft in y axis, elevators control the rotation in x axis, and rudders control the rotation in z axis. In other words, ailerons control the roll rotation, elevators control the pitch rotation, and rudders control the yaw rotation. Additionally, the Y axis is in the direction of the nose of the aircraft, X axis points along with the wings.

2.2.1 Physical Aerodynamic Controlling System

The physical aerodynamic controlling system is involved in controlling the aircraft either on the ground or while flying. The physical aerodynamic controlling components include flaps, slats, elevators, ailerons, spoiler panel, vortex generators, thrust reverser, and the wing tip. Each component plays a crucial role in controlling the aircraft. However, depending on the type of the aircraft which involves the size and the weight, some of the components could be combined together or even eliminated [23]. Specifically, two pairs of flaps can be combined as one. Flaps

are usually mounted at the end of the wings. The major role of the flaps is to increase the wing surface area, which helps the aircraft generate the larger amount of upward lift while flying at a lower speed. There are several types of flaps used on passenger planes, which are high-speed flaps and low-speed flaps. They are both called ailerons. The high-speed flaps are used to adjust aircraft's position and direction. The low-speed flaps are generally used in the takeoff and landing process. Additionally, there are at least two sets of high and low-speed flaps which are installed into the main wing of an aircraft. High-speed flaps are able to maneuver upward and downward the wing. In the contrast, the low-speed flaps are only eligible of bending downward the aircraft. In other words, high-speed flaps can be used to reduce aircraft speed and generate more lift. Low speed flaps cannot be used to adjust the aircraft position. There is a speed limit of the low-speed flaps. If the low-speed flaps are extended under a high-speed flight condition, the connection between the flaps and the wings may be damaged and even tear off from the wings. The physical control theory of both types of the wings are the same. Once a set of flaps are extended, it increases the wing surface area and creates a low-pressure area above the wing, which pushes the aircraft maneuver towards that direction. Once a set of low-speed flaps of both wings are extended to the same direction, with a high angle of attack, the flaps create an airbag above the aircraft. This generates a larger low pressure area above the wings and also allows the aircraft to maneuver at a much lower speed [24]. Slats are similar to the flaps. The only difference between them is that the slats are mounted at the front tip of the wings. Slats are often used during takeoff and the final landing process. They increase the wing surface by extending forward. The major difference between flaps and slats is only high-speed flaps can be used during the high-speed maneuver. However, the slats can be used under various conditions, especially for military aircraft during high-speed turning maneuver, slats are often extended to increase the wing surface area and reduce surface vortices due to the high angle of attack.

There are usually two sets of wings on a single aircraft, the one mounted at the tail of the aircraft are the elevators. The elevators act like a smaller version of the main wings. However, elevators are able to rotate about the aircraft body in a certain angle no larger than 15 degrees. The main purpose of the elevators is to stabilize the aircraft horizontally and also to distribute the total gravitational force on the wings. The elevators allow the aircraft to handle sophisticated airflow conditions while flying in the air. In other words, angled elevators allow the aircraft flies with an angle of attack. This helps the wings to reduce to generate required lift in order to

maintain the altitude [25]. The vertical stabilizer is often used to balance the aircraft vertically, which is known as the rudder. The vertical stabilizer operates similar to the wings. The vertical stabilizer cuts through the air in a relevant speed and generate an equivalent amount of force to each side of the stabilizer in order to hold the aircraft in a steady position. While the rudder is being pushed to one direction, the vertical stabilizer generates a low-pressure area in the inverse direction, which will force the aircraft to turn into the low-pressure zone. For some special cases, the vertical stabilizer can be combined with the elevators in a smaller sized aircraft. One significant point must be mentioned and that is the vertical stabilizer cannot be used continuously back and forth while flying. In the contrast, the tensile force exists on the connection of the vertical stabilizer will increase. This may cause overloading on the connection between the vertical stabilizer and the fuselage, which leads to mechanical failure [26].

The spoiler panels are known as speed brakes. They can either be mounted onto the wings of the aircraft or the fuselage. The spoiler panels are used to increase the drag and decrease the upward lift of aircraft. The spoiler panels are often used to decrease altitude while in the air and increase the drag and downward force during the breaking process of the aircraft on the ground. The spoiler panel guides the airflow upward the aircraft, which increases the front surface area of the aircraft and generates a large amount of downward force to the aircraft. For a lighter and smaller aircraft, the spoiler panel can be eliminated due to the lower momentum the aircraft needs to handle.

2.2.2 Physical Control for Each Component

There are several factors that influence the performance of the aileron. They are the aileron platform area (S_a), aileron chord/span (C_a/b_a), the maximum up and down aileron deflection (A_{up}) and (A_{down}) and the location of the inner edge of the aileron along the wing span (b_{ai}) see Figure 27 and 28.

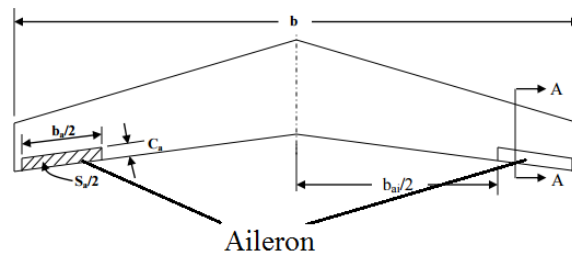


Figure 27: Top view of a wing with aileron

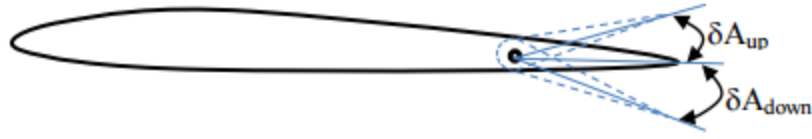


Figure 28: Section view of a wing with aileron

The typical values get from “Air Flow Applications on Fighter Jets” for these factors are as follows: $S_a/S = 0.05\sim 0.1$, $b_a/b = 0.2\sim 0.3$, $C_a/C = 0.15\sim 0.25$, $b_a/b = 0.6\sim 0.8$ and $A_{\max} = \pm 30$ degrees. These represent the area of the aileron is between 5%~10% of the airfoil area. The aileron to wing chord ratio is between 15%~25%. [27].

Flaps of fixed wings UAV are used to increase and decrease the effective curvature of the wing. That can change the maximum lift coefficient of the aircraft and thereby reduce its stalling speed. The maximum lift coefficient is a dimensionless coefficient which is determined by the shape of the airfoil and the angle of attack in [28]. It is determined by the equation

$$C_L = \frac{L}{\frac{1}{2}\rho v^2 S} = \frac{2L}{\rho v^2 S} = \frac{L}{qS}$$

Where L is the lift force, ρ is the fluid density, v is the true air speed, S is the relevant plan area. Therefore, we can find the fluid dynamic pressure is:

$$q = \frac{2}{\rho} * v^2$$

There are also many kinds of flaps, and all kinds of the flaps are changed or combined by four primary flaps: plain flap, split flap, slotted flap, and fowler flap [29]. The plain flap is a simple component. In *figure 29* it shows an example of plain flap. The black line is the section view of a wing, the green dot line is the boundary layer of air and red line labels the weak pressure zone. The rear portion of the airfoil rotates downwards on a simple hinge mounted at the front of the flap. This can decrease the amount of lift created and create a large drag force backward. In this case, the aircraft can descend quickly without increasing the airspeed. This movement is used when an aircraft is in a relatively at high altitude and wants to land soon.

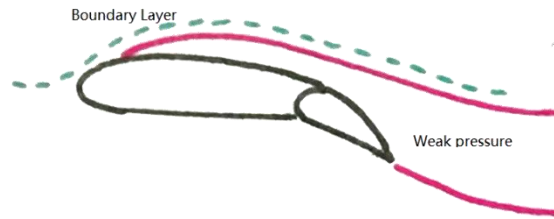


Figure 29: Section view of plain flaps

The split flap is the rear portion of the lower surface of the airfoil which hinges downwards from the leading edge of the flap, while the upper surface remains immobile shown in figure 30. This can also create a large drag force toward backward but create a slightly more lift than plain flaps [30]. This kind of flaps sometimes has the same function as a spoiler, but pretty uncommon these days.

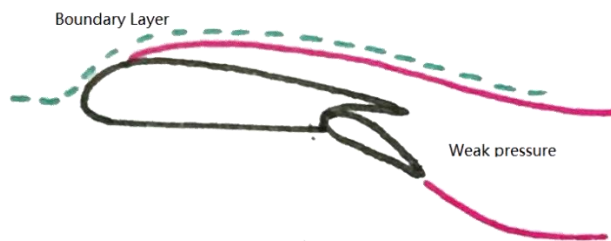


Figure 30: Section view of split flaps

In Figure 30, it is an example of slotted flap. The slotted flap has a gap between the flap and the wing. This gap forces high pressure air from below the wing over the flap. It helps the airflow remain attached to the flap, increases lift compare to the split flap and decreases the drag force created by the hinging of the flaps.

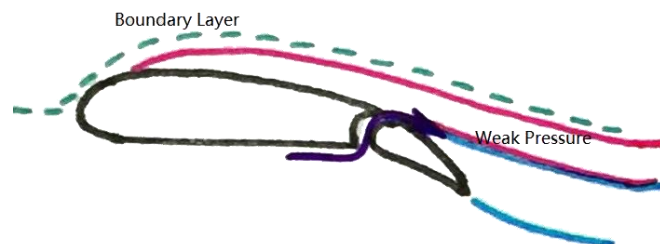


Figure 31: Section view of slotted flaps

The fowler flap is a series of slotted flap combined together, as shown in Figure 32. At first stage of the extension, the flaps create a large amount of lift, but small drag force. As the flaps keep on extending, the lift force increases by small amount but creates a large amount of drag force [31]. This kind of flap can fit both for climbing and descending.



Figure 32: Section view of fowler flaps

The most commonly used flap is a combination of the fowler flap and slotted flap. This combinational flap has all the property the flaps above have. When all the flaps are not extended, as shown in Figure 33, the airfoil has good efficiency. This can be used when climbing, cruising and descent.

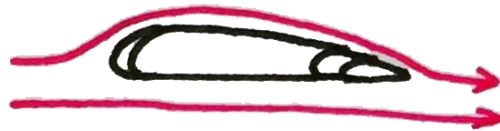


Figure 33: Best efficiency - for climbing, cruising, descent

When the flaps are extended and increased, as shown in Figure 34, the wing area without creating slots, they can create a high lift and low drag in low air speed. This can be used when takeoff and initial climb [32].

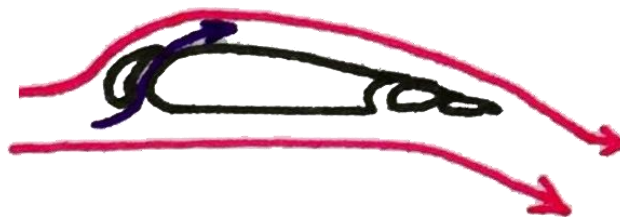


Figure 34: Increased wing area - for take-off and initial climb

When the flaps are fully extended, as shown in *Figure 35*, both the lift and drag forces reach their maximum point. This is used for landing.

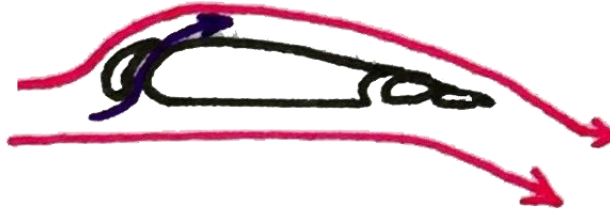


Figure 35: Maximum lift and high drag - approach to landing

The spoiler is a device intended to reduce the lift and increase the drag of an airfoil. This is used when braking the aircraft on the runway and descending. When the aircraft flies in a relatively high altitude and wants to decrease altitude quickly, the spoiler is extended normally without exceeding 3-5 degrees. When the spoiler is fully extended, as shown in *Figure 36*, it can create a large force downward and press the aircraft on the ground. In this case, the aircraft can remain on the runway while decreasing its speed quickly [33].

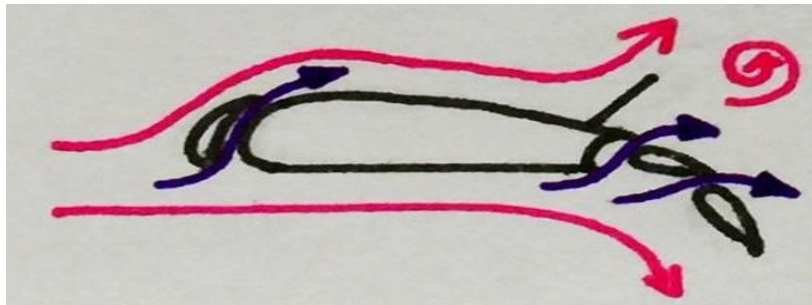


Figure 36: Maximum drag and reduced lift - for braking on runway

Rudder is a moveable surface located at the end of vertical stabilizer, as shown in *Figure 37*. It is used to control rotation about the z axis. When the rudder is rotated, a lift force is created and rotation of the aircraft around the center of gravity occurs.

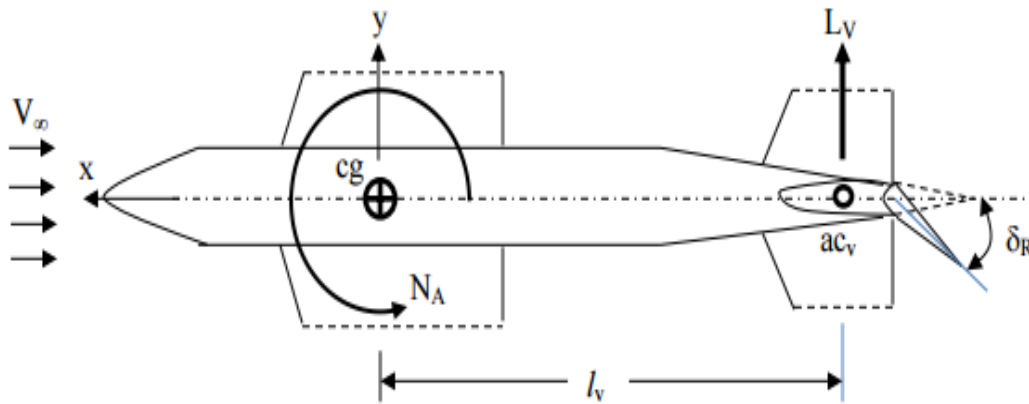


Figure 37: Directional control via rudder deflection (top view)

There are two basic designs of the rudder. One is swept rudder, shown in Figure 38, another one is rectangular rudder, shown in Figure 39. There are also many parameters that must be determined when designing a rudder. The rudder area (S_r), rudder chord (C_r), rudder span (b_r), the maximum rudder deflection (R_{max}), and the location of inboard edge of the rudder (b_{ri}) are some of these parameters.

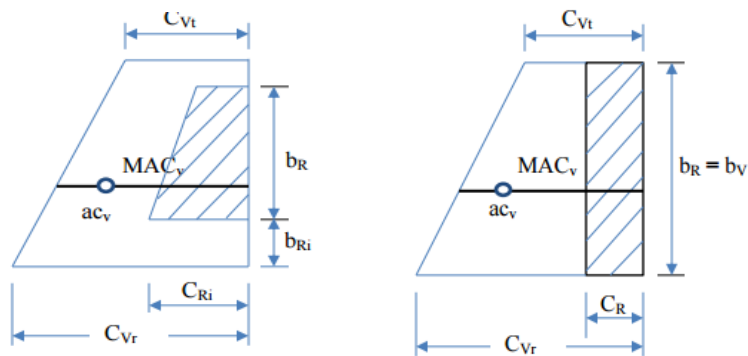


Figure 38: Left is a swept rudder, Right is rectangular rudder (side view)

Elevators are normally hinge to the tail plane or horizontal stabilizer, shown in figure 40 and 41. Sometimes it can also be a stabilizer which means the whole horizontal stabilizer can rotate as elevators. It controls the x axis rotation which is the angle of attack of the aircraft. For the designing of the elevators, four parameters determine the performance of the elevators and they are the elevator area (S), elevator chord (C), elevator span (b_E), and maximum elevator

deflection (E_{max}). There are also several typical values for these parameters as follows: $S_E/S = 0.15$ to 0.4 , $b_E/b = 0.8$ - 1 , $C_E/C = 0.2$ - 0.4 , and $2 E_{max_up} = -25$ degrees, $E_{max_down} = +20$ degrees [34].

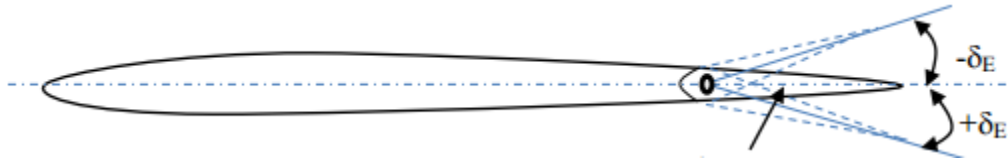


Figure 39: The section view of a horizontal stabilizer with elevator

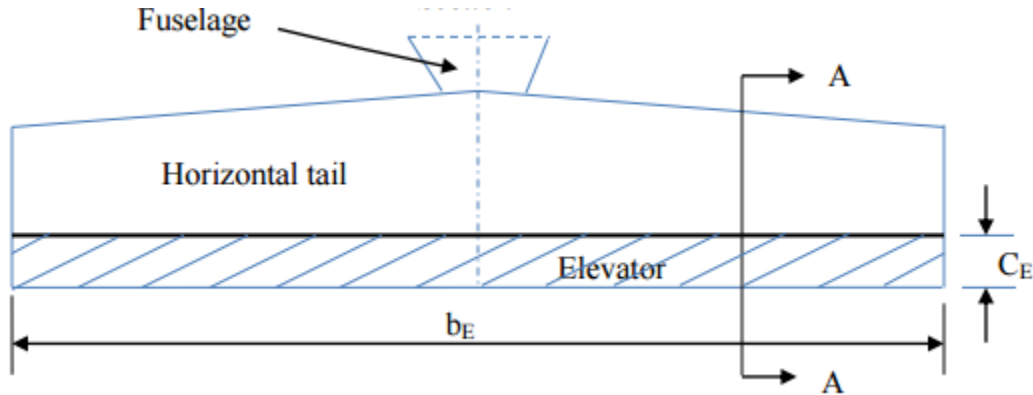


Figure 40: The top view of a horizontal stabilizer with elevator

According to the values shown above, the area of the elevator is 15% ~ 40% of the horizontal stabilizer. The length of span of the aircraft is 80% ~ 100% of the total span length. The elevators' chord is 0.2 ~ 0.4 multiplier relative to the total chord length. And the angle limits are 25 degrees to up and 20 degrees to down.

2.2.3 Computational Control of Aerodynamic Control System

For an UAV, the altitude and speed are two key elements in the control system. *Figure 41* is an example of negative feedback system, which is described in the frequency domain. $R(s)$ is the input function, $X(s)$ is the output function, $H(s)$ is the transfer function in feedback path. Since the UAVs may be powered by electro-motor or fuel engine, the input function can be unit step input, unit impulse input, sinusoidal and cosine input, which can be a representative of voltage supply or valve switch. The output function can be speed or altitude. In addition, height

sensor and speed sensor in the UAV can obtain information about current speed or altitude, and send back such information to a PID controller [35].

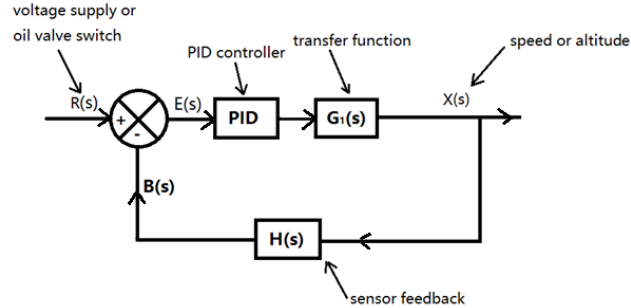


Figure 41: Negative feedback closed loop for transfer function

From Figure 41, it is easy to get the open loop, closed loop and error transfer functions. These transfer functions are the basis for the simulation and are very important in control system. Open loop transfer function is given by

$$\frac{B(s)}{E(s)} = G(s)H(s) \quad (2)$$

It is the ratio of the measured feedback to the error signal with all the initial conditions being zero. Closed loop transfer function is defined by

$$\frac{X(s)}{R(s)} = \frac{G(s)}{1 + G(s)H(s)} \quad (3)$$

It is the ratio of output X(s) to the input R(s). Error transfer function is defined by

$$\frac{E(s)}{R(s)} = \frac{1}{1 + G(s)H(s)} \quad (4)$$

It is the ratio of error signal to the output with all the initial conditions being zero. The next part is to analyze the PID controller and influence of damping on the output response. The PID controller consists of proportional, integral and derivative elements. P is the value of the error, I is the past values of the error and D is the possible future values of the error according to its current rate of change. The PID equation, which is shown in equation (5), states that K_p is proportional gain, K_i is the integral gain and K_d is the derivative gain. It is widely used in the

feedback control study of systems. Some applications might require using only one or two terms of the PID to provide the appropriate system control. This can be done by setting the other parameters to zero. A PID controller may be called a PI, PD, P or I controller in the absence of the respective control actions [37].

$$u(t) = K_p e(t) + K_i \int_0^t e(\tau) d\tau + K_d \frac{de(t)}{dt} \quad (5)$$

PID equation shown in equation (6) can be changed into transfer function, which can be used in the control analysis:

$$G_{PID}(s) = \frac{U(s)}{E(s)} = k_p + \frac{k_i}{s} + k_d s \quad (6)$$

This is the example of operational-amplifier circuits design period from the circuit seen in Table4 we can get the value of K_p in (7), K_i in (8), K_d in (9) for resistance and capacitance.

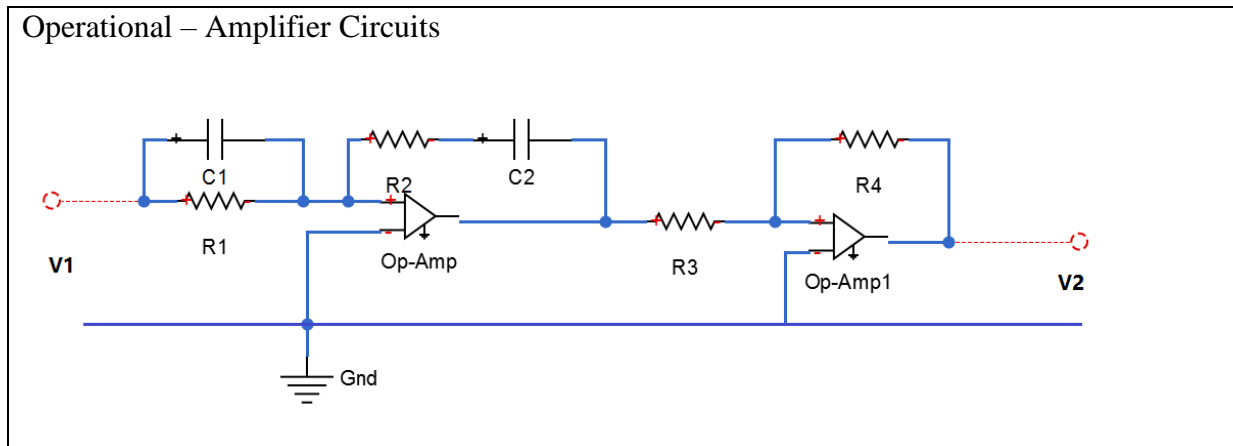
$$k_p = \frac{R_4(R_1C_1 + R_2C_2)}{R_1R_3C_2} \quad (7)$$

$$k_i = \frac{R_4(R_1C_1 + R_2C_2)}{R_1R_3C_2} \left(\frac{1}{(R_1C_3 + R_2C_2)} \right) \quad (8)$$

$$k_d = \frac{R_4(R_1C_1 + R_2C_2)}{R_1R_3C_2} \left(\frac{R_1R_2C_1C_2}{(R_1C_1 + R_2C_2)} \right) \quad (9)$$

The following table is the feedback controller and gain:

Table 3: Feedback Controller and Gain



The UAV system can control the speed and altitude by adjusting values of K_p , K_i , K_d . The *Figure 42* is an example of PID simulation. From this graph, amplitude performs underdamped, undamped and overdamped by different value of K_p , K_i , K_d . When $K_p = 100$, $K_i = 5$, $K_d = 50$, it is overdamped, which is a good example of controlling UAV at certain speed or altitude [38].

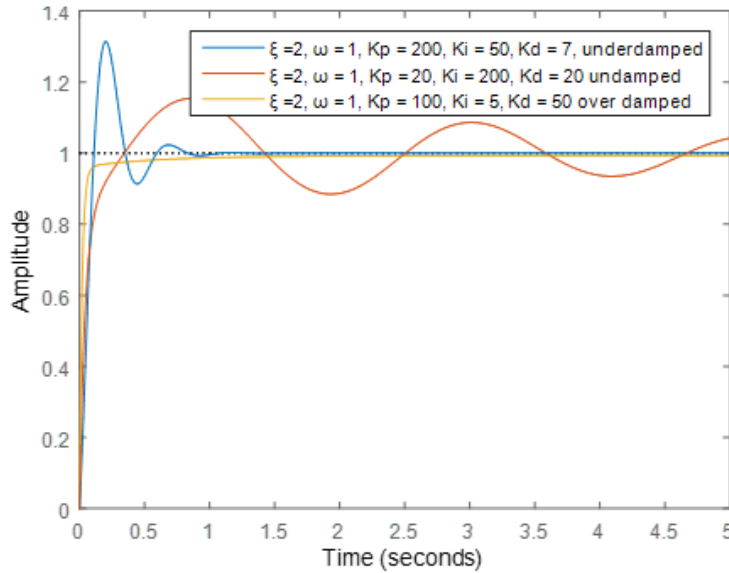


Figure 42: PID simulation

The damping analysis can be therefore carried out. The equation in (10) is an example of a second order transfer function. All the second order equations can be used by this model. It is a basic analysis and model of control systems.

$$\ddot{x}(t) + 2\xi\omega\dot{x}(t) + \omega^2_n x(t) = \omega^2_n r(t) \quad (10)$$

There are several cases from this equation and they are: overdamping, critical damping, underdamping and undamped. First one is underdamping case, from the calculation below, ξ should be in the interval 0 and 1 to make the system stable.

$$\begin{aligned}
x(t) &= \mathcal{L}^{-1}\left(\frac{1}{s}\right) - \mathcal{L}^{-1}\left(\frac{s + \xi\omega_n}{(s + \xi\omega_n)^2 + \omega_d^2}\right) - \frac{\xi\omega_n}{\omega_d}\mathcal{L}^{-1}\left(\frac{\omega_d}{(s + \xi\omega_n)^2 + \omega_d^2}\right) \\
&= 1 - e^{-\xi\omega_n t} \cos \omega_d t - \frac{\xi\omega_n}{\omega_d} e^{-\xi\omega_n t} \sin \omega_d t \\
&= 1 - e^{-\xi\omega_n t} \left(\cos \omega_d t - \frac{\xi}{\sqrt{1 - \xi^2}} \sin \omega_d t \right) \\
&= 1 - \frac{e^{-\xi\omega_n t}}{\sqrt{1 - \xi^2}} \sin(\omega_d t + \varphi), \quad \varphi = \arctan\left(\frac{\sqrt{1 - \xi^2}}{\xi}\right), \quad \omega_d = \omega_n \sqrt{1 - \xi^2},
\end{aligned} \tag{11}$$

Equation (1) is the underdamping response to a unit step function. Second one is critical damping, from the calculation below where ξ should be exactly 1 to make the system in critical damping in (12).

$$\left. \begin{aligned}
s_{1,2} &= -\xi\omega_n \pm \omega_n \sqrt{\xi^2 - 1} = -\xi\omega_n, \quad \text{for } |\xi| = 1, \quad s_1 = s_2 = -\xi\omega_n < 0 \\
\xi &= \frac{c}{c_{crit}} = 1, \quad c_{crit} = 2\sqrt{mk} = 2m\omega_n, \quad \omega_n = \sqrt{\frac{k}{m}}, \quad m \neq 0
\end{aligned} \right\}, \tag{12}$$

Third case is overdamping and from the calculation below ξ should be greater than.

$$\left. \begin{aligned}
s_{1,2} &= -\xi\omega_n \pm \omega_n \sqrt{\xi^2 - 1}, \quad \lambda_1 < 0, \quad \lambda_2 < 0 \\
s_1 &= -\xi\omega_n + \omega_n \sqrt{\xi^2 - 1}, \quad s_2 = -\xi\omega_n - \omega_n \sqrt{\xi^2 - 1} \\
\xi &= \frac{c}{c_{crit}} > 1, \quad c_{crit} = 2\sqrt{mk} = 2m\omega_n, \quad \omega_n = \sqrt{\frac{k}{m}}, \quad m \neq 0,
\end{aligned} \right\}, \tag{13}$$

The last case is undamped, and ξ should be exactly 0. Each case has different response as seen in *Figure 43*. Simulation shows that for ξ being in the interval 0 and 1, the system is stable.

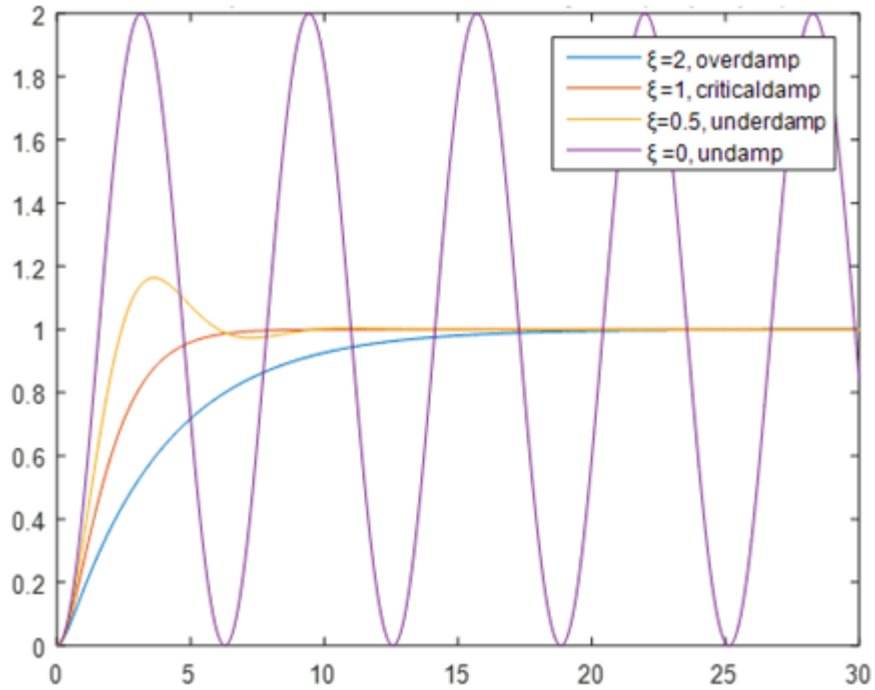


Figure 43: Damping ratio simulation

2.2.4 UAV Route Design

The UAV route design plays a critical role in UAV designs. The selection of routings is directly related to the efficiency of UAVs. Under real search and rescue operations, less effective operation procedure may cause the life of survivors. This is the reason for our team to think about route design carefully. Typically, there are two main ways to control the path of UAV. First is manually controlling the UAV through a computer. Second is by presetting the path, such as a set of GPS location and let the UAV automatically circle along the path. Choosing between these two ways depends on different situations. Specifically, when the range of the searching location is not known, some locations with high possibilities of finding survivors will be assumed. Additionally, switching to manual operation at the base station is when signals of survivors are detected [41]. Once an UAV is operated manually, it can be controlled by the real-time video streaming system and directional instructions which in turn adjust the direction and altitude of the UAV. Figure 45 shows the components which support the communication between the UAV and base station.

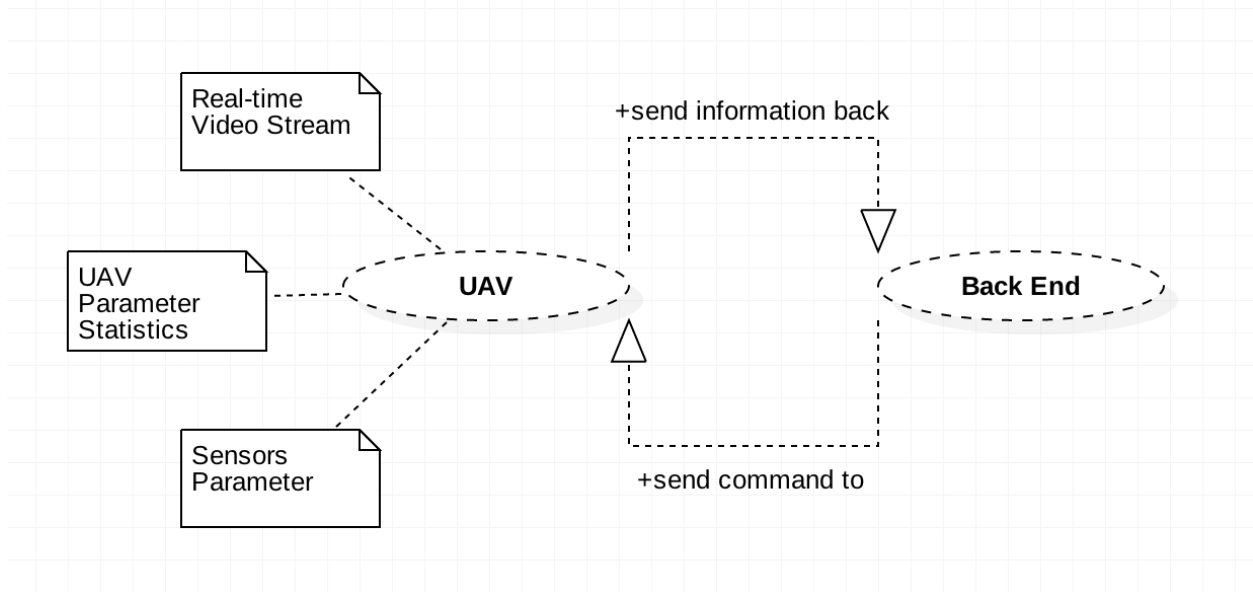


Figure 44: Relation between UAV and Back-End

There are several advantages of using manual mode. First of all, people can discover the real-time situations through watching the video stream sent back from the UAV. Detailed information can help the UAV operator and rescuers to make timely and effective decisions. Second, the base station may notice some details that the sensors on the scene may not recognize. The disadvantages of manual mode are the high cost of systems management and security. For some manual operations, operating time could be several hours and weeks. Long time highly concentrated working distribution would decrease the sensitivity of operators. This is critical to rescuing missions. In order to minimize manual mode operations, auto mode, which is known to have several features, is used. While an UAV is operated under automatic mode, there is no need of operators to manage the operating procedures. The UAV will fly along the designed path and keep searching for the survivors on the ground through many powerful sensors mounted on it. On the other hand automatic operation requires user inputs and operating procedures such a path information control the UAV [42]. Figure 46 presents the paths of the UAV of an accident scene where the red points indicate the location of the UAV along the path.

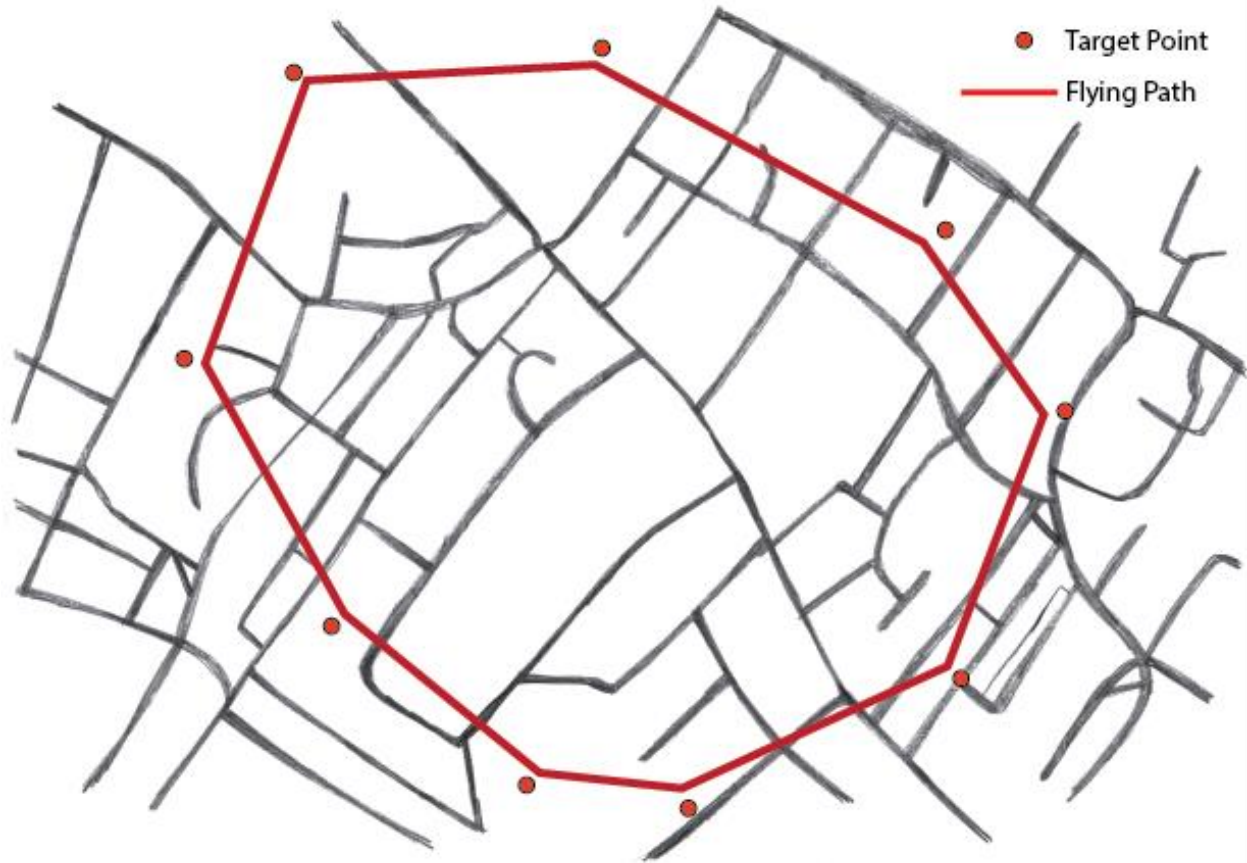


Figure 45: Example of UAV Orbit (red)

The UAV will automatically calculate the angle and altitude for the next point in its orbit. Although there are many sensors on UAV, some large algorithms and machine cannot be carried by UAV because of size limit. According to that, when flying, UAV will continue to send real time images and video streaming back to the station in order to be analyzed by experts and other powerful tools.

While the UAV is running the auto mode, accuracy is one of the biggest problem. The UAV is easily out of its orbit by environmental factor such as wind and rain. Only one subtle error on direction will cause huge uncertainty on its air route. However, GPS gives the great help to fix the uncertainty. Even the UAV is beyond its original route, when it comes to the next coordinate, the UAV will fix the error between the current route and the original route. This feature guarantees the accuracy of flying in auto mode [43]. After the operator has set up the destination points, the UAV therefore needs to calculate the shortest path among these points. There are many graph searching algorithms are often being applied such as Dijkstra's algorithm.

Specifically, given a graph with V , the number of nodes, and E , the number of edges. Dijkstra's algorithm has $O(V^2)$ running time. Actually this complexity can be improved by using min-priority queue structure. The implementation based on a min-priority queue implemented by a Fibonacci heap and running in $O(E + V\log(V))$ [44].

2.3 Power Components, Instruments and Sources of UAVs

The selection of electrical power source for an in-flight computer and operation depend upon weight, efficiency, flexibility, quality, stability, and cost. Weight is a crucial factor when considering a power system on UAV. The UAV, subtle difference on weight can lead significant effects on efficiency. Especially, the power system mainly runs on battery, and weight can decide the capacity of the whole power system. Efficiency is calculated by actual electrical output divided by total electrical output. As a component of the whole system, improving efficiency as much as possible can benefit system's operation. Less redundant waste on transition and rational power arrangement are two ways to improve whole system. Flexibility in power system is regarded as an ability to respond to the change in demand. The UAV is a highly multi-used vehicle. Electrical power source for the UAV should have ability to meet different requirements in different environment. The quality of a power system is important for stability. During an operation, unexpected collision or vibration caused by extreme weather conditions may damage the physical structure. High quality structure material ensures the UAV working properly in different environment so that support stable power to let every component in system working. The cost of these materials are spread from several dollars to thousand dollars. Different price of power source has different ways to use. However, our team chooses a power source according to how much it is suitable for the UAV and related operation but no depending on high cost [45].

Solar power system is not an ideal power solution for UAV. For capacity, while operating in daytime, solar power system can use the sun to operate the UAV without limit. However, solar energy is not available at all times. It ensures the operation of the UAV being executed without additional fuel input. This kind of time limit will influence the utilization of an UAV. When the emergency occurs in night time, power will be the biggest problem for the UAV. However, if the solar system cooperate with the power system based on chemical battery, the problem can be solved. Tradeoffs are the cost and weight. Using solar system means we should incorporate some

solar panels into the UAV. In order to get the maximum utilization of the sun, suitable solar panels on top of the wings are required. The body area must be increased that the UAV can get maximum irradiating area. The disadvantage of this is more solar panel will increase the weight of the UAV. This means consumed rate of power will increasing so that operating time will be decreasing. We have to make a tradeoff between the utilization and weight. So under limit irradiating area to maximize the utilization of solar power is the problem we are facing. Maximize the utility of solar power when it's available is one way to improve efficiency of power system, such as maximum receiving power from solar panel [46].

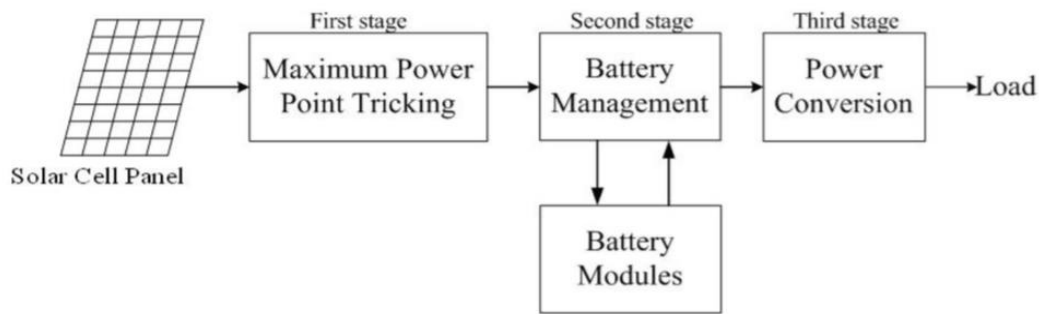


Figure 46: Basic structure of solar power system

According to the *Figure 46*, solar system is divided into three parts. First part is maximum power point tracking, second part is communication between battery management and battery modules. Third part is the transfer of the solar power to the electrical power in order to support the whole system. Maximum power point tracking (MPPT) algorithm, can support help on tracking the maximum power point. Detailed structure of the power system is shown as follows [47]:

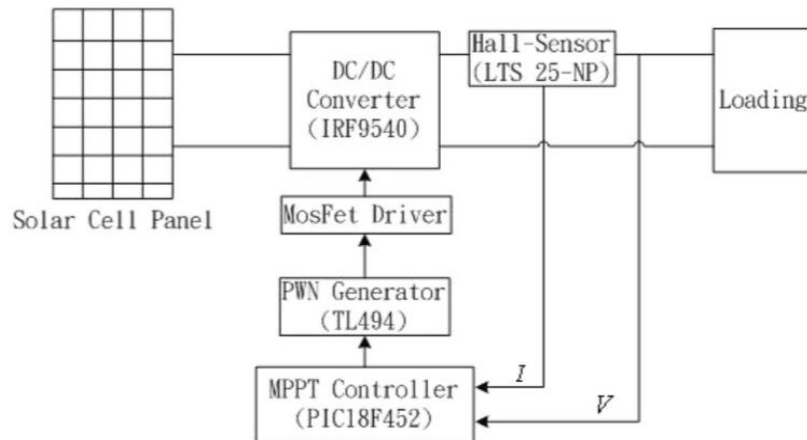


Figure 47: Structure of MPPT algorithm

The effects with basic solar system with MPPT is shown in Figure 49.

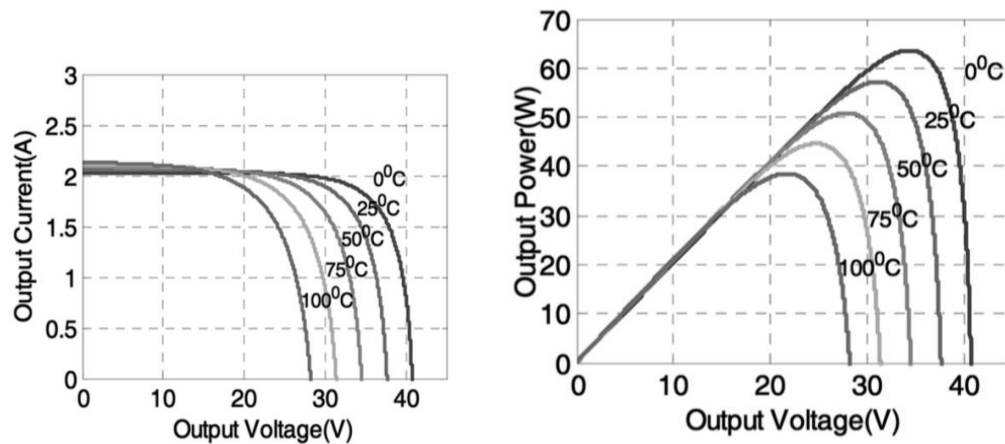


Figure 48: Contrast basic solar system(Left) and solar system with MMPT(Right)

As shown in Figure 48, the solar system with MMPT can produce large power output. Fuel is a traditional and popular way to generate power. The use of fuel cell in UAVs can give UAV stable and abundant power. Chemical generator has pretty high efficiency and utilization. It allows UAV flying at much higher altitude, typically, five thousands meters. Strong power also can support UAV carrying more heavy equipment such as high resolution camera, powerful embedded system or sophisticating flying control devices. Another advantage is stability. Fuel cell can sustain harsh environmental conditions such as cold, hot and humidity [48].

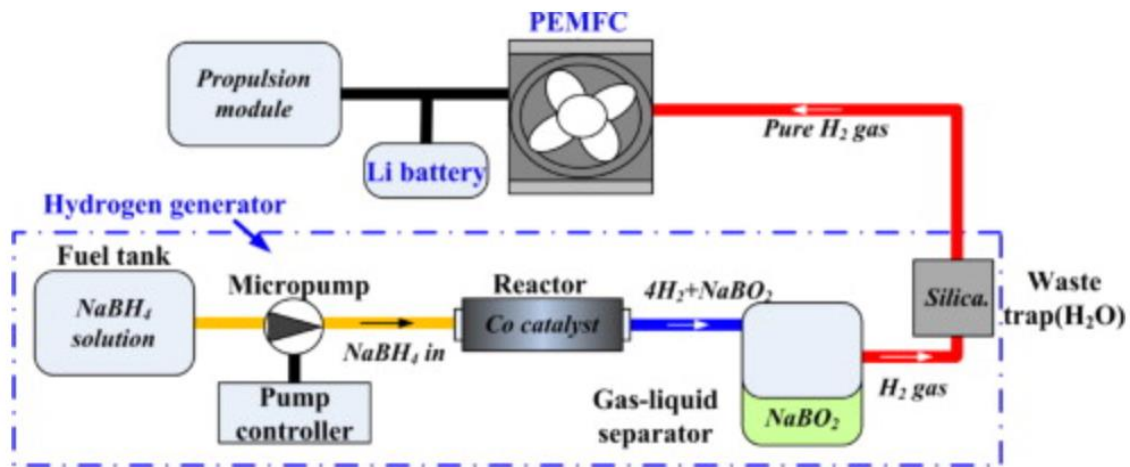


Figure 49: Fuel cell system construction

As shown in Figure 49, the principle fuel cell system is presented. The fuel tanks transfer the chemical energy by reacting with hydrogen gas and produce electricity through the PEMFC which is a turbine converts flow energy to electrons.

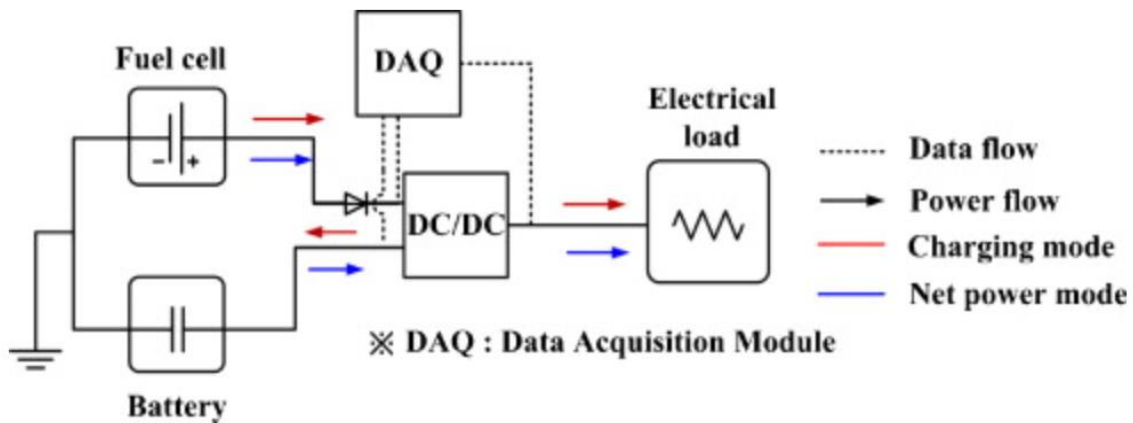


Figure 50: Fuel cell system

Usually, only using videos and photos captured by a UAV is not suitable for operator to mastering a typical situation. A three dimensional map can help people analyze situation in a forwarding and precise way. The goal is to scan a large area to three dimensional map from an UAV or groups of UAVs flight instruments. Usually, using one single depth camera, an UAV is

able to obtain a three dimensional model from a specific object. Specifically, the UAV needs at least 4 images from 4 different directions (front, rear, sides), even a 360 degree video. However, if there are multiple camera working together, the situation will be much different [49].

In a common three dimensional scanning system, setting proper light condition, stable movement of camera and measured camera degrees are required conditions. There are various situations needs be considered. Especially, scanning large area from a UAV will not have these comfortable condition. When flying, camera, which is tightly set up on the UAV, will endure unpredictable shaking because of unstable air current. This will cause the images or videos being recorded from unexpected degree, which increase the difficulty for distracting 3 dimensional information [50]. Lighting condition is also a factor that cannot be ignored. Well-setting lighting condition will reduce complexity of analyzing images. One of the most important problem is that lighting can easily impact result returned by the algorithm which used to distract depth information from images. In this project, camera will face infinitely different lighting condition. Factors like sunlight, weather, humidity and haze can influence quality of recordings, which can lead to imprecise information.

The number of cameras plays an important role in this project. There are two different combination. First is that let each UAV's independently scan a part of an area then combine them together after scanning. Second is use group of UAV scan an area together at the same time then keep going to the next area. Each combination will use different algorithm to deal with different data. For now, it is hard to say which one is better than the other without numerical experiments [51]. For single camera, there are several ways to achieve third model. These include:

1. Use Time-of-Flight camera, which can measure depth at some specific rates (Reconstruction).
2. Use laser distance measuring and regular high resolution camera (Reconstruction).
3. Use regular high resolution camera and connect them together (Non-reconstruction).

For 1, Time-of-Flight camera, which as known as depth camera, can use laser light to get distance information in the real time. Its cost is more expansive than that of regular high solution camera. For 2, cost is low, but difficulty for mapping depth to images and parsing them is higher than 1. For 3, cost is lowest, but there is no guarantee on precise of result. Small changes in environment conditions will cause unexpected result. Furthermore, non-reconstruction merely

give us something seems like three dimensional model. We can directly measure length or position precisely by using this method [52].

The three dimensional Time-of-Flight (TOF) technology is revolutionizing the machine vision industry by providing 3D imaging using a low-cost CMOS pixel array together with an active modulated light source. Compact construction, easy-of-use, together with high accuracy and frame-rate makes TOF cameras an attractive solution for a wide range of applications.

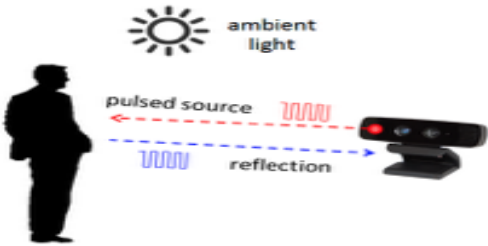


Figure 51: TOF camera abstraction

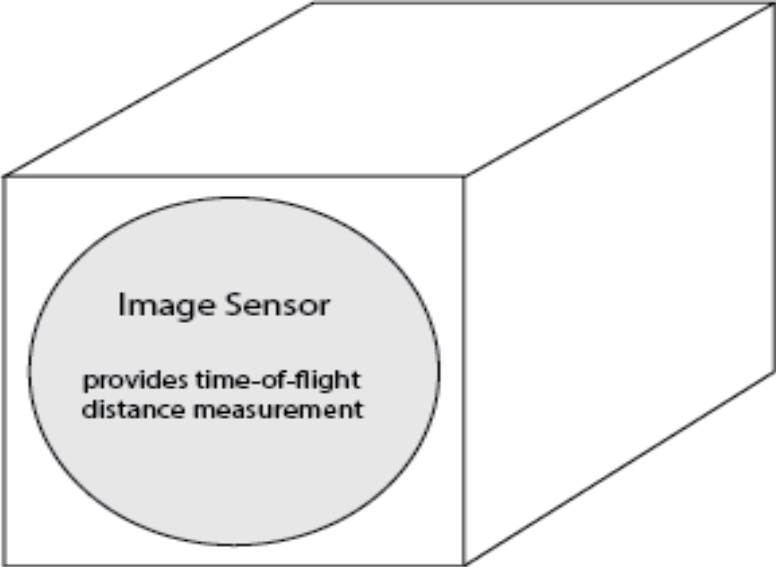


Figure 52: MESA imaging 3D TOF Camera SR4000 (ETH, 5m range)



Figure 53: Effects of TOF camera

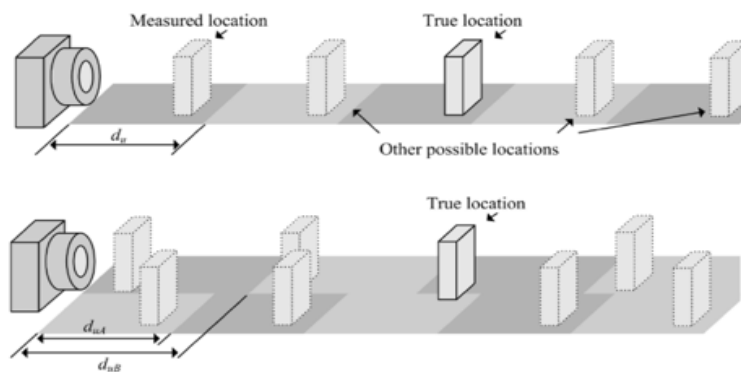


Figure 54: Camera function analysis

One of the largest problems with the TOF camera is its cost, which is normally above \$2300. The low cost approach is to actually use a regular camera, which is usually under \$300 with 1080p resolution. This is used to record and use algorithm and laser light simultaneously analyze depth information. The cost of laser sensor is depending on its type. Different type has different maximum supported receiving range, which is actual flying height of UAV. When a regular camera is working, laser sensor works at the same time. Theoretically, if we know actual depth of one pixel on image, we can know the rest of them. There are two kinds of 3D algorithms: reconstruction and non-reconstruction. Reconstruction means at first transfer data to point cloud, and use algorithm to reconstruct 3D model from point cloud data.

Equation for Reconstruction Map from Video:

For $i = 1:36$ frames

$$Cube_{init}\{i\}(x, y, z) = I_{segment}\{i\}(x, y) \times \begin{pmatrix} \frac{Dis+z}{Dis} & 0 & 0 \\ 0 & \frac{Dis+z}{Dis} & 0 \\ 0 & 0 & 1 \end{pmatrix}$$

$$Cube_{rotated}\{i\}(x, y, z) = Cube_{init}\{i\}(x, y, z) \times \begin{pmatrix} 1 & 0 & 0 \\ 0 & \cos(10^\circ \times i) & -\sin(10^\circ \times i) \\ 0 & \sin(10^\circ \times i) & \cos(10^\circ \times i) \end{pmatrix}$$

$$Cube_{segment}\{i\}(x, y, z) = Threshold(Cube_{rotated}\{i\}(x, y, z))$$

end

$$Cube_{finalmodel} = \bigcap_{i=1}^{36} Cube_{segment}\{i\}$$

Note: Operator \times represent affine transformation with tfm matrix (\cdot)

Non-construction way is directly using continuous data from regular camera connect them together. However, this way can give us precise vector position, which is fatal factor in this project.

2.3.2 Electric Motor

The electrical motor is a device that brought about one of the largest advancements in the engineering field. In the field of UAV, it is commonly applied in the small size of UAV. The electrical motor consists of DC motor, AC motor and special motor. And the AC motor consists of synchronous motor, one phase induction motor, and three phase induction motor. Figure 56 shows the image of T-motor, the structure of DC motor, which is widely used in UAV power source. There are many parts in it [53]:

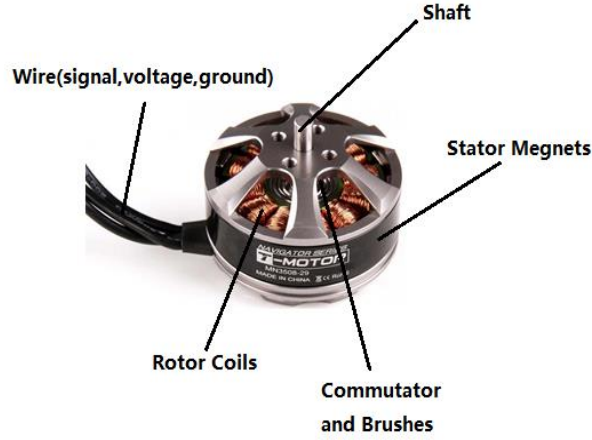


Figure 55: Fuel cell system construction

The motor that used by UAV will be supplied by the DC power supply source. To the DC motor we have a shaft which is attached to it. At the end of the shaft we have the pin which have the rotor attached to it. It may or may not have the bearings to it. Let internal resistance of the motor by R_a . And K_t torque constant, which is the ratio of motor output torque to input current. K_a is back EMF constant, which is the ratio of voltage to angular speed. V_t is the terminate voltage. The relationship is

$$\tau_{out} = \frac{K_a K_t}{R_a} + \frac{K_t}{R_a} V_t \quad (14)$$

The total current with load is proportional to the output torque like equation (13).

$$I_{load} = \frac{\tau_{out}}{K_t} \quad (13)$$

The total torque is therefore

$$\sum \xi = \xi_m - \xi_d - \xi_s \quad (14)$$

Where T_d is the damping Torque, and where $\zeta_d = C_t$, and $\zeta_s = K_t \theta$

So the equation is like equation (15)

$$J\ddot{\theta} + c_t\dot{\theta} + k_t = K_m i \quad (15)$$

The motor torque has relationships with motor current, efficiency, speed and output power, which is showing in the *Figure 56*. The torque is proportional to the current, inversely proportional to speed. The output power is maximum at the mid of the torque. This graph can help us for the future UAV motor selection. The axis represents the number of elements and torque output.

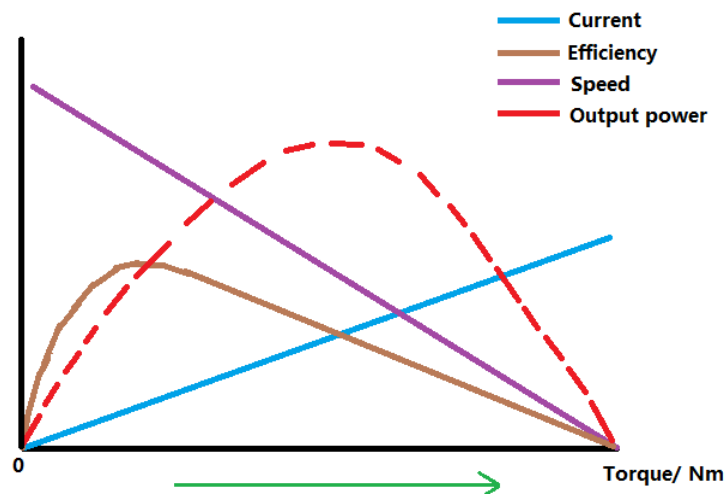


Figure 56: The relationship between UAV motor's torque and elements

The power source is one of the most importance aspects for the UAV motor, so our team did the case study and found that relationship between the UAV power and other performance. The source of these data is collected from many datasheets of UAV. *Figure 56* is the result of that. *Figure 57* is the relationship between UAV power and altitude. It is a good reference of the future motor power selection base on the altitude.

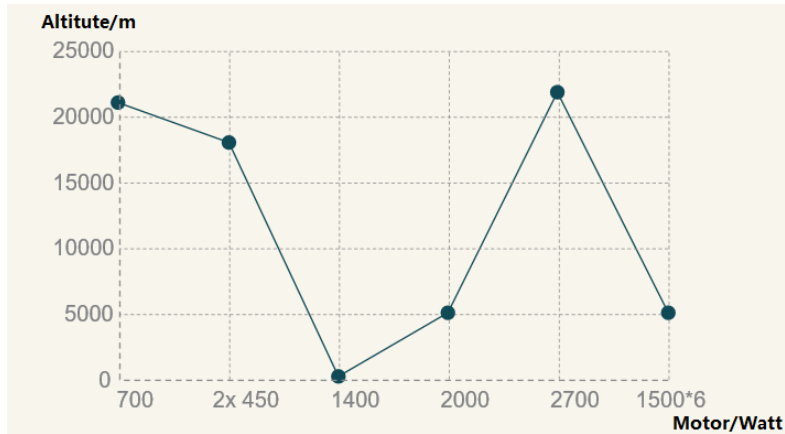


Figure 57: The relationship between UAV power and altitude

Figure 58 is the relationship between UAV power and speed. It is a good reference of the future motor power selection base on the speed.

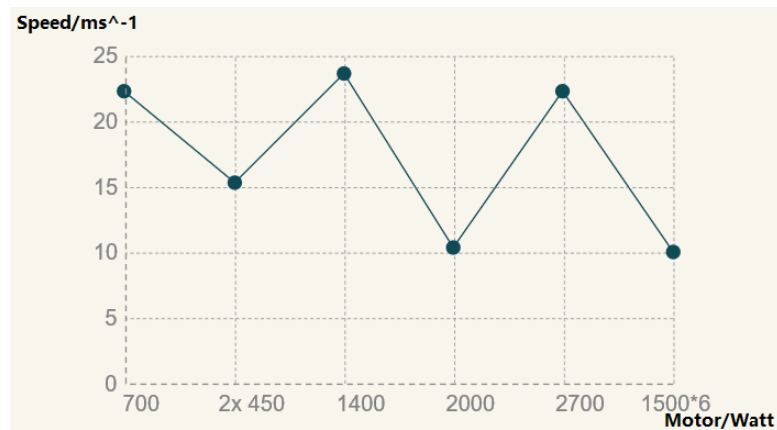


Figure 58: The relationship between UAV power and speed

Figure 59 shows the relationship between UAV power and payload. It is a good reference of the future motor power selection base on the payload.

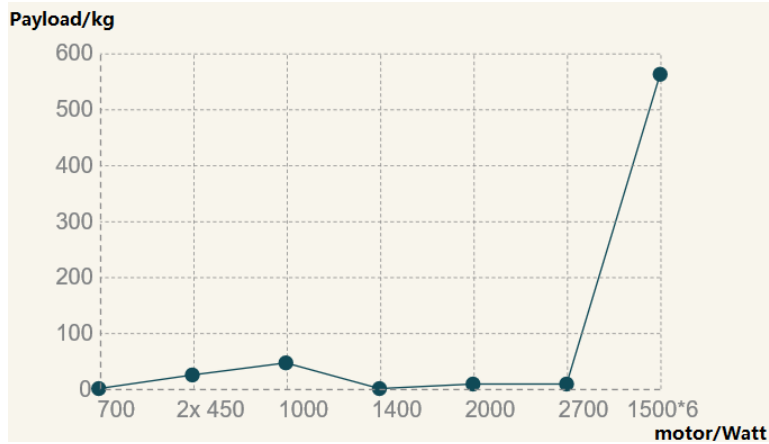


Figure 59: The relationship between UAV power and payload

Figure 60 is the relationship between UAV power and weight. It is a good reference of the future motor power selection base on the weight.

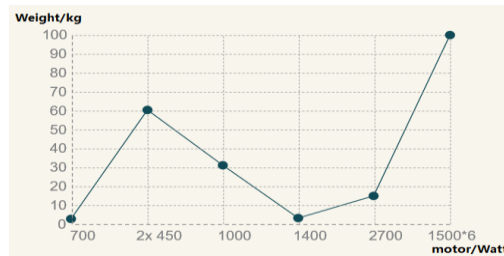


Figure 60: The relationship between UAV power and weight

2.3.3 Internal Combustion and Jet Engines

From the very beginning of aviation history, airplanes used internal combustion engines to turn propellers and generate thrust. Internal combustion engines were used for the first flight in human history, this of the Wright brothers, and still in our days, many private airplanes and general aviation aircrafts use the same principle. These engines are similar to the ones used in automobiles and in this section I will be discussing the fundamentals of their function. When studying such engines, we are interested in two kinds of operations, the mechanical and thermodynamics. Both processes make the engines to produce the useful work we are looking for. The mechanical design of these engines is similar to the ones that are used in automobile industry, most widely known to engineers as four stroke or four cylinder engines. In order for these engines to work, a mixture of fuel and air has to enter in the cylinder where the combustion

process will occur, forcing the pistons to move back and forth. This motion is then transferred to the power stroke where the piston turns a crank which converts the linear piston motion into circular, which is connected to the propellers through shafts. This repeated cycle motion was developed by the German engineer Dr. N. A. Otto and that why we also refer to it as the Otto Cycle. The general and complete view of the engine is the one that follows:

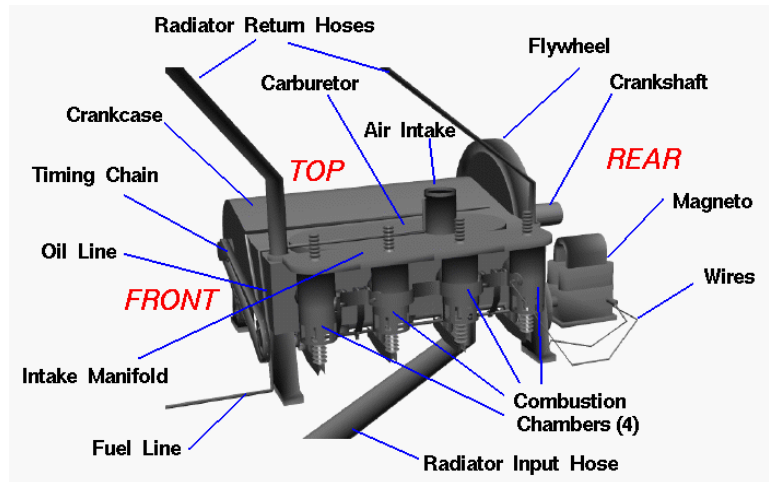


Figure 61: Full combustion engine diagram

As we can clearly see at the design picture above, the engine is composed of several parts. Starting from the fuel storage tank, a hose called fuel line goes to the intake manifold in order to supply it with fuel. The intake manifold is the part where the fuel is distributed evenly into the four cylinders, and the carburetor is the component that blend the fuel with air -supplied from the air intake- and inject this mixture into the cylinders. The cylinders also known as combustion chambers, is the place where the burning of the fuel occurs in order to convert chemical energy to mechanical. Other parts are the crankcase where the crankshaft is located. The crankshaft is the mechanical part that converts the reciprocating motion of the pistons to rotational motion. The timing chain is a belt that synchronizes the rotation of the crankshaft and the camshaft so that the engine's valves open and close at the proper times during each cylinder's intake and exhaust strokes. The last two main parts are the flywheel and the magneto. The flywheel is rotating mechanical device which stores rotational energy in order for the system to continue rotating even when the pistons are in the process of compressing a fresh charge of air

and fuel. Finally, the magneto is an electrical device that provides current for the ignition system of the pistons.

There is a variety of reciprocating piston engines that were mainly used to power aircrafts. The different types of engines depend mostly on the formation of the pistons around the crankshaft. Thus, we have the in-line engine, where the cylinders are located in a line on top of the crankshaft, the V-engine where the cylinders have a V shape on top of the crankshaft and the horizontally opposed engine where the cylinders are connected horizontally to the crankshaft. The last two categories are the radial and the rotary engine, where the combustion chambers are placed around the crankshaft and the main difference is that for the rotary engine, the crankshaft is fixed to the airframe and the propeller is fixed to the engine case, so that the crankcase and cylinders rotate.

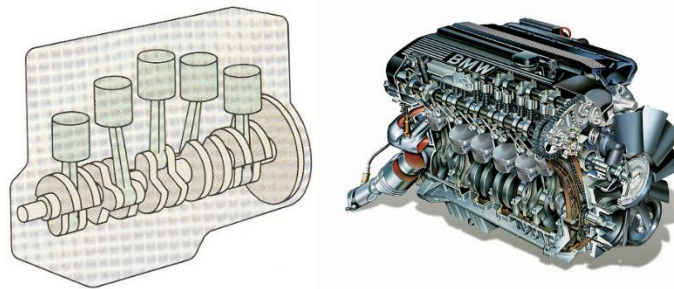


Figure 62: 2002 BMW 5-Series Inline-6 Engine

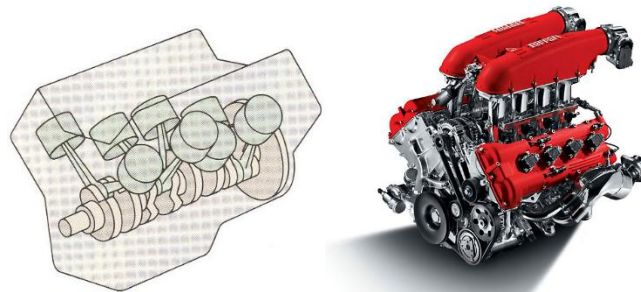


Figure 63: Ferrari 360 3586cc Alloy V8 Engine

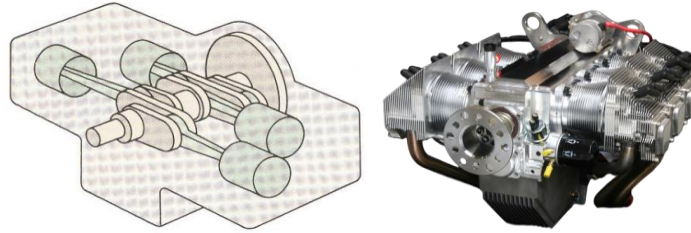


Figure 64: Jabiru 3300cc Aircraft Engine

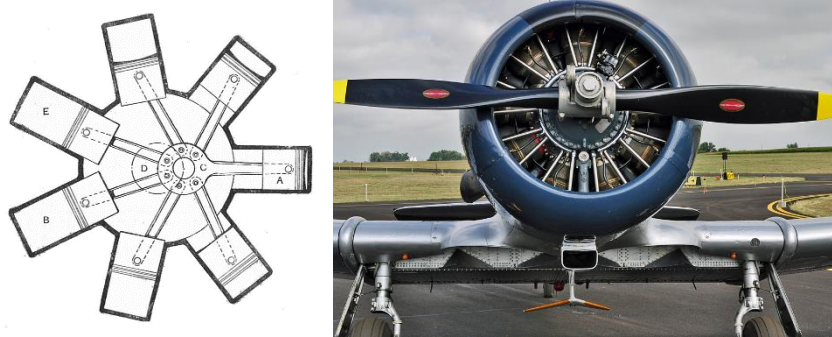


Figure 65: Pratt & Whitney R-1340 Radial Engine

Concluding, internal combustion engines were widely used in military and commercial aviation, but when it comes into smaller aircrafts, their increased weight makes it difficult to be carried by a drone, and so electrical engines are preferred. There has been an effort though to supply drones with internal combustion engines. A team of German engineers recently launched a project on the Kickstarter website, where they built a UAV which uses both an electrical motor and small fuel combustion engines to power the aircraft. They claim that this innovation increases air time, speed and payload [54].

There are four different kinds of turbo engines that are directly powered by the thermal expansion of the fuel, which are turbofan, turbojet, turboprop, and ramjet engines. Based on the internal structures and physical application of these four types of power sources, the turbofan, turbojet, turboprop engines can be placed under the same category and the ramjet engine can be placed in another. Although there are a large difference on the performances of these engines, some engines can be combined in certain specific usage and application.

First and foremost, the turbofan, turbojet, turboprop engines are called turbo engines. All turbo engines uses similar structure in order to provide the aircraft relevant thrust; specifically, they all involve a compressor, combustion chambers, and turbines. The operation theories of

these components of any kind of turbo engine is equivalent as the cylinder engines. Specifically, the gas chamber opening operation is equivalent as the front opening of a turbo engine; while the piston moves upwards which compress the air is equivalent as the compressor; the firing operation is equivalent as the fuel burning in the combustion chamber; and the piston moves towards the center of the engine is equivalent as the high-temperature air pushes the turbine blades.

On the other hand, there are several categories under the same engine type. Also, all three types of turbo engines are applicable to UAVs based on the physical specifications. By only looking at the active mechanical portion the engine, which are the compressor, combustion chambers, and turbines. There are three main types of structures that are being used fairly often in the field, which are centrifugal, single shaft, and double shaft. The centrifugal turbofan engine is often used in the smaller aircraft with reverently slower air speed. As shown in *Figure 66* the airflow is being deviated to outside boundary of the engine by the centripetal force generated by the compressor [55].

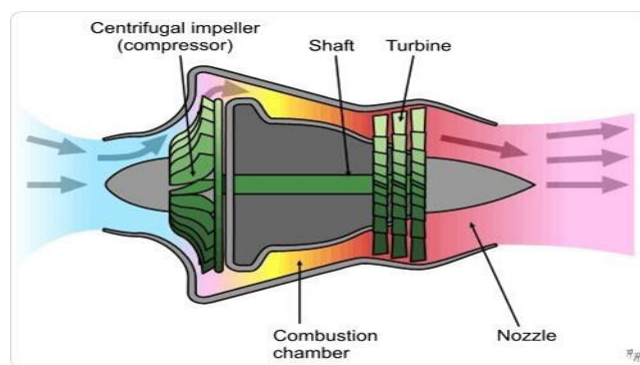


Figure 66: Centrifugal Turbo Engine

The advantage of this engine is this structure allows the engineers to design a shorter and smaller engine with less mechanical components. However, due to the shape of the compressor and the path of the airflow the engine has a chamber inside which has no use; in other words, this structure may cause large air resistance and excessive space occupation inside of the aircraft. The single and double shaft turbo engines both has a linear airflow, air enters straight to the engine, compressed by the compressor, ignited in the combustion chamber, pushes the turbine blades and exist the engine from the exit nozzle under maximum velocity. The difference between the single

and double shaft turbo engines is in the single shaft turbofan engine, the front fan, compressor, and the turbine are mounted on a single shaft; in the contrast, the double shaft turbo engine has two shafts are mounted on the same axis one over another. More specifically, there are two sets of turbine blades in the turbine stage, which are high-pressure turbine and low-pressure turbine; the compressor and the high-pressure turbine are mounted on the same shaft called high-pressure shaft; the front fan and the low-pressure turbine are mounted on one shaft called low-pressure shaft. The major reason using the double shaft turbo engine is crucial; the single shaft turbo engines has the same turbine-compressor speed, which causes vibration and reach velocity limit while operating under a high air thickness or density. The double shaft turbo engine allows a differential speed between the compressor and the turbine disk, which provides the front fan consistent power and rotation [56].

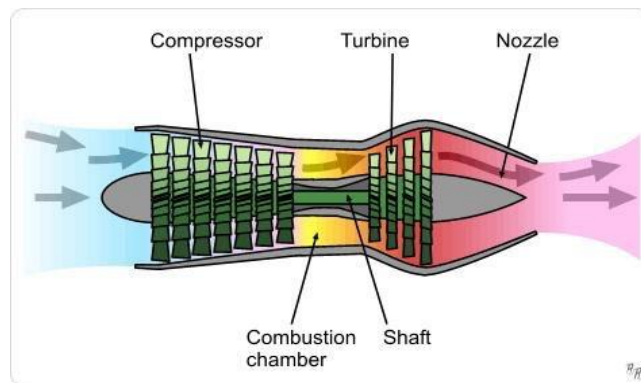


Figure 67: Turbo-Thrust Engine

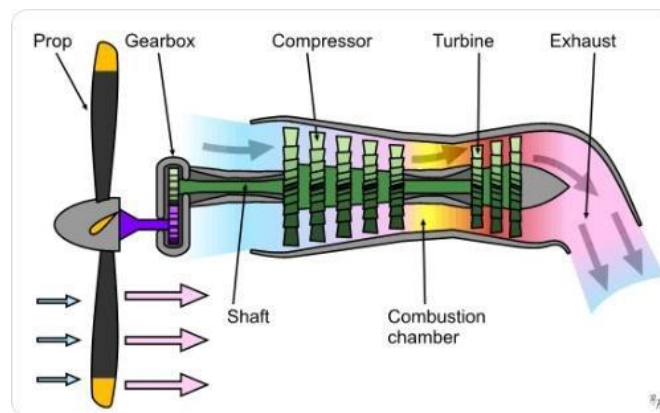


Figure 68: Turbo-Prop Engine

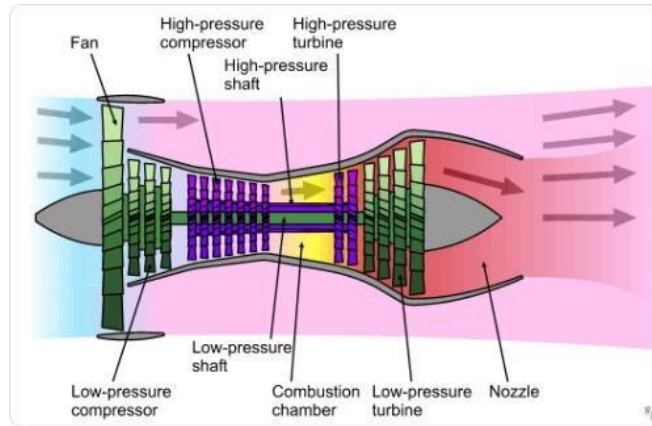
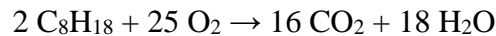


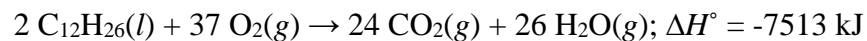
Figure 69: Turbofan Engine

2.3.4 Fuel Engine Power Source

There are multiple types of energy power supply. Fuel energy plays an essential role in the energy field. With the same weight and size, fuel normally can provide more energy than other kind of energy source. Fuel engine can transfer the chemical energy in the fuel to the mechanical energy. By reacting with oxygen, liquid fuel can react violently and create combustion. There are several types of liquid fuel: gasoline, diesel, and kerosene [57]. Gasoline also known as petrol, is a transparent, petroleum-derived flammable liquid. When it is mixed with air and ignited, it has the reaction:



Where both CO_2 and H_2O are in gaseous. Gasoline contains about 42.4MJ/kg with the density of range from 0.71-0.77kg/L. Diesel fuel is widely used and can be categorized by the way it is produced as petroleum diesel, synthetic diesel, and biodiesel. The diesel normally used for aerial engine is petroleum diesel. This kind of diesel is the mixture of multiple components with mostly of saturated hydrocarbons, also called alkane, and aromatic hydrocarbons. When it mixed with air and compressed ignited, it produce gaseous carbon dioxide and water. Diesel has the heating value of 43.1ML/kg with the density of 0.832kg/L. Kerosene is a thin, clear flammable liquid formed from hydrocarbons obtained from fractional distillation of petroleum between 150C and 275C. This kind of fuel is widely used in airlines and can be categorized in several grades such as Avtur, Jet A, Jet A-1, etc. The combustion reaction can be approximated as follows:



It has the density of 0.78-0.81kg/L. Kerosene sometimes is used as an additive in diesel fuel to prevent gelling or waxing in code temperatures [58].

2.4 Cumulative UAV Comparison

In this section, our team analyzed many different types of UAVs that exist in the market or are being used by companies or the military. Our team collected some useful information from each UAV, like the UAV name, type, use, physical properties, physical capabilities and hardware. These parameters will be useful for designing our future UAV design. Following are the tables for each UAV: Table 5 is the datasheet of the Yeair UAV. It is Quad-copter and Dual Powered (Fuel Combustion & Electric Motor), which can delivery services. It is a good reference of quad-copter.

Table 4: The datasheet of Yeair

UAV Name	Yeair
Type	- Quad-copter - Dual Powered (Fuel Combustion & Electric Motor)
Usage	- Delivery services (carrier) - Motion Picture Productions - Documentaries
Physical properties	- Weight: 4.9 kg - Size: 0.9 x 0.75 x 0.5 m - Fuel tank: 1.5 Liters
Physical capabilities	- Speed: 100 km/h - Range: 55 km - Payload: 5 kg - Fuel Engine: 8.6 hp / 6.4 kW - Electrical Motor: 4s 1250mA/h Lippo-Battery for starting the engine - Endurance: 1 hour
Hardware	- GPS: Next generation GPS chip for highest accuracy and quick readiness for use. - WIFI: Integrated WLAN with 100m range for connection with Tablet or Smartphone.

Table 6 is the datasheet of MQ-8. It is UAV helicopter and turbine powered, which is Military use and Reconnaissance. This is a good reference of UAV helicopter.

Table 5: The datasheet of MQ-8

UAV Name	Northrop Grumman MQ-8 Fire Scout
Type	- UAV helicopter

	- Turbine/ Jet Fuel/ Biofuel
Use	- Military use - Reconnaissance - Situational awareness - Aerial fire support - Precision targeting support
Physical properties	- Size: 7.3 x 1.9 x 2.9 m - Weight: 1,430 kg
Physical capabilities	- Payload: 272kg - Speed: 213 km/h - Range: 203.7 km - Endurance: 5-8 hours - Altitude: 6,100 m - Engine: Rolls-Royce 250, 313 kW / 420 hp
Hardware	- Radar: Telephonics AN/ZPY-4 - Other Hardware: TSAR with Moving Target Indicator (MTI) capability, multispectral sensor, SIGINT module, Target Acquisition Minefield Detection System (ASTAMIDS), Tactical Common Data Link (TCDL)

Table 7 is the datasheet of MQ-9. It is Fixed Wing and powered by Turbine, which is Military use and long-endurance. This is a good reference of fixed wing.

Table 6: The datasheet of MQ-9

UAV Name	General Atomics MQ-9 Reaper (formerly named Predator B)
Type	- Fixed Wing - Turbine/ Jet Engine
Use	- Military Use - Long-endurance - High altitude surveillance
Physical properties	- Crew: 0 onboard, 2 in ground station - Length: 36 ft 1 in (11 m) - Wingspan: 65 ft 7 in (20 m) - Height: 12 ft 6 in (3.81 m) - Empty weight: 4,901 lb (2,223 kg) - Max takeoff weight: 10,494 lb (4,760 kg) - Fuel capacity: 4,000 lb (1,800 kg) - Payload: 3,800 lb (1,700 kg) - Internal: 800 lb (360 kg)
Physical capabilities	- Power plant: 1 x Honeywell TPE331-10 turboprop, 900 hp (671 kW) with Digital Electronic Engine Control (DEEC)

	<ul style="list-style-type: none"> - Maximum speed: 300 mph; 260 kn (482 km/h) - Cruising speed: 194 mph; 169 kn (313 km/h) - Range: 1,151 mi; 1,852 km (1,000 nmi) - Endurance: 14 hours fully loaded - Service ceiling: 50,000 ft (15,240 m) - Operational altitude: 25,000 ft (7.5 km)
Hardware	<ul style="list-style-type: none"> - AN/DAS-1 MTS-B Multi-Spectral Targeting System - AN/APY-8 Lynx II radar - Raytheon SeaVue Marine Search Radar (Guardian variants)

Table 8 is the datasheet of CH-3. It is mid-range and mid-altitude UAV, which is Military use and farming use. It is a good reference of self-operation system.

Table 7: The datasheet of CH-3

UAV Name	CH-3
Type	<ul style="list-style-type: none"> - Capable of radio control and self-operation - Mid range - Mid altitude - Large size
Use	<ul style="list-style-type: none"> - Military use (carry weapons, and investigation with cameras) - Farming
Physical properties	<ul style="list-style-type: none"> - 8m in wingspread - 5.5m in length - Piston engine with propeller - Three-pointed landing gear
Physical capabilities	<ul style="list-style-type: none"> - 2400 km non-return, with 12 hours operation time without refueling - Maximum payload 100 kg - Maximum takeoff weight 640kg - Altitude 3000m - 5000m, maximum altitude 6000m - Capable of takeoff both from runway and cat shot - Speed 220km/h - Remote range 200km
Hardware	<ul style="list-style-type: none"> - Control panels are classified - AR-1 missile, high definition camera and investigation pot under both wings

Table 9 is the datasheet of RQ-21. It is mid-range and mid-altitude UAV, which is Military use only. It is a good reference of radio control system.

Table 8: The datasheet of RQ-21

UAV Name	RQ-21
-----------------	-------

Type	<ul style="list-style-type: none"> - Capable of radio control and self-operation - Mid range - Mid altitude - Mid size
Use	- Military use only(carry weapons, and investigation with cameras)
Physical properties	<ul style="list-style-type: none"> - 4.8m in wingspread - 2.5m in length - Piston engine with 2 propeller blades - Three-pointed landing gear - Power: 8 horse power/5.97KW - Power dissipation: 350W
Physical capabilities	<ul style="list-style-type: none"> - 13 hours operation time without refueling - Maximum payload 17kg - Maximum takeoff weight 61kg - Minimum takeoff weight 36kg - Maximum altitude 5944 m - Capable of take off by cat shot - Speed 110km/h, max speed 164.7km/h - Remote range 200km
Hardware	Control panels are classified

Table 10 is the datasheet of EHANG 184. It is short-range and low-altitude UAV, which is personal use only. It is a good reference of short range and low altitude UAV.

Table 9: The datasheet of EHANG 184

UAV Name	EHANG 184
Type	<ul style="list-style-type: none"> - Capable of radio control and self-operation - Short range - Low altitude - Mid size
Use	- Personal use only
Physical properties	<ul style="list-style-type: none"> - Personal use only - 4 foldable arms with 4 motors and each with 2 propellers - High performance electrical motor - Two bar landing gear - Power dissipation: 106kW
Physical capabilities	<ul style="list-style-type: none"> - 23 minutes operation time (without wind) - Maximum payload 100 kg - Maximum takeoff weight 300kg - Maximum altitude 5944 m - Maximum speed (in theory) 100 km/h - Maximum speed (in theory) 100 km/h - cCarrying a person - 2-4 hour recharging time

Hardware	N/A
-----------------	-----

Table 11 is the datasheet of Phantom3. It is short-range and low-altitude UAV, which is can be used in recreational and commercial aerial cinematography and photography. It is a good reference of electric Quad copters.

Table 10: The datasheet of Phantom3

UAV Name	Phantom3
Type	<ul style="list-style-type: none"> - Quad copters or drones - Powered by electric motor - Short range - Short altitude - Capable of radio control and self-operation
Use	- Recreational and commercial aerial cinematography and photography.
Physical properties	<ul style="list-style-type: none"> - Four electric motors mounted at the ends of the x-shaped body. - Rise speed: 5m/s - Fall speed: 3m/s - Maximum speed: 16m/s - Working environmental temperature: 0°C-40°C
Physical capabilities	<ul style="list-style-type: none"> - Endurance: 23mins - Weight: 1.28kg - Payload: 0kg - Maximum flying altitude: 6000m
Hardware	<ul style="list-style-type: none"> - The body frames are made of composite materials. - Control a maximum range of 2,000 meters - Battery capacity: 4480 mAh

Table 12 is the datasheet of Spreading Wings S1000+. It is Octo-rotor UAV, which is can be used in Professional aerial photography and cinematography. It is a good reference of electric Octo-rotor UAV.

Table 11: The datasheet of S1000+

UAV Name	Spreading Wings S1000+
Type	<ul style="list-style-type: none"> - Octo-rotor Aircraft - Powered by electric motor - Short range - Short altitude - Capable of radio control and self-operation
Use	- Professional aerial photography and cinematography.
Physical properties	<ul style="list-style-type: none"> - Frame Arm length - Landing Gear Size:

	460mm(length)*511mm(width)*305mm(height) - Working environmental temperature: -10°C-40°C
Physical capabilities	- Takeoff weight : 6kg-11kg - Total weight: 4.4kg - Endurance: 15min
Hardware	- Motor Max power: 500W - Weight of Motor :158g - A 40A electronic speed controller - 6S 15000mAh battery

Table 13 is the datasheet of Precision hawk. It is powered by single electric motor, which is can be used in Agriculture. It is a good reference of electric UAV.

Table 12: The datasheet of Precision hawk

UAV Name	Precision hawk
Type	- Single electric motor(fixed wing) - Mid range - Mid altitude - Capable of radio control and self-operation
Use	- Agriculture - Energy & Mining - Insurance & Emergency Response - Environment Monitor
Physical properties	- Wingspan: 1.5m - Maximum speed: 22m/s - Max operating temperature: 40°C - Max operating altitude: 2500m - Communication range
Physical capabilities	- Takeoff weight : 3.55kg - Total weight: 2.4kg - Endurance: 45min
Hardware	- Power source 7000 mA/ hr

Table 14 is the datasheet of Zephyr. It is High Altitude Pseudo-Satellite which is can be used in Environmental surveillance and Maritime & Border surveillance. It is a good reference of solar energy UAV.

Table 13: The datasheet of Zephyr

UAV Name	Zephyr
Type	- High Altitude Pseudo-Satellite (HAPS) UAS/UAV, running exclusively on solar power
Use	- Maritime & Border surveillance - Environmental surveillance - In-theatre C4ISTAR relay - Missile detection

	<ul style="list-style-type: none"> - Navigation - SIGINT - Ad-hoc communication bandwidth - Continuous imagery
Physical properties	<ul style="list-style-type: none"> - Capacity: 2.5 kg (5.5 lb) payload - Wingspan: 73 ft 10 in (22.50 m) - Gross weight: 117 lb (53 kg) - Power plant: 2 × Newcastle University custom permanent-magnet synchronous motor, 0.60 hp (0.45 kW) each
Physical capabilities	<ul style="list-style-type: none"> - Max altitude (ASL) : 21 562 m - Having already been airborne permanently for more than 14 days - Cruise speed: 30 kn (35 mph; 56 km/h) - Service ceiling: 70,000 ft (21,000 m)
Hardware	<ul style="list-style-type: none"> - Stores solar energy collected during the day and - Uses it at night to keep the vehicle in the sky and the payload running. - Stay focused on a specific area of interest and - Provide satellite-like communications and earth observation services over long periods of time without interruption.

Table 14 is the datasheet of NASA Helios Prototype. It is solar electric- powered flying wing designed to operate at high altitudes for long duration flight It is a good reference of solar energy UAV.

Table 14: The datasheet of Helios

UAV Name	NASA Helios Prototype
Type	<ul style="list-style-type: none"> - Proof-of-concept solar electric- powered flying wing designed to operate at high altitudes for long duration flight - Ultra-lightweight flying wing aircraft
Use	<ul style="list-style-type: none"> - Two different ways. First, designated HP01, focused on achieving the altitude goals and powered the aircraft with batteries and solar cells. The second configuration, HP03, optimized the aircraft for endurance, and used a combination of solar cells, storage batteries and a modified commercial hydrogen–air fuel cell system for power at night. In this configuration, the number of motors was reduced from 14 to ten
Physical properties	<ul style="list-style-type: none"> - Wingspan: 247 ft - Length: 12 ft - Wing Chord: 8 ft - Wing Thickness: 11.5 in. (12 percent of chord)

	<ul style="list-style-type: none"> - Wing area: 1,976 sq. ft. - Aspect Ratio: 30.9 to 1 - Empty Weight: 1,322 lb - Gross Weight: Up to 2,048 lb, varies depending on power availability and mission profile.
Physical capabilities	<ul style="list-style-type: none"> - Payload: Up to 726 lb, - Propulsion: 14 brushless direct-current electric motors, each rated at 2 hp. (1.5 kW) - 50,000 to 70,000 ft.,
Hardware	N/A

Table 15 is the datasheet of Lockheed Martin Hale-D. It is High-Altitude Long Endurance (HALE) and Re-usable. It is a good reference of solar energy UAV.

Table 15: The datasheet of Hale-D

UAV Name	Lockheed Martin Hale-D
Type	High-Altitude Long Endurance (HALE)
Use	<ul style="list-style-type: none"> - Multi-payload, multi-mission platform, - Reusable, - Solar-based regenerative power system
Physical properties	<ul style="list-style-type: none"> - Length: 240 ft; Diameter: 70 ft - Volume: 500,000 ft³ - Demo duration goal: 5 days - 80 lb payload (commons & camera)
Physical capabilities	<ul style="list-style-type: none"> - 100's kW – 200 kW solar - Developed and flew a very large 40 kw/hr lithium ion
Hardware	<ul style="list-style-type: none"> - Solar Cell - Hull Materials - Regenerative - Fuel cell - Rechargeable batteries

Table 17 is the datasheet of Penguin B. It is fixed wing and high performance unmanned airframe. It is a good reference of fixed wing UAV.

Table 16: The datasheet of Penguin B

UAV Name	Penguin B
Type	- Fixed Wing
Use	- High performance unmanned airframe
Physical properties	<ul style="list-style-type: none"> - Length 2.27 m - Height 0.9 m - Stall Speed <13 m/s - Cruise Speed 22 m/s - Max Speed 36 m/s

Physical capabilities	<ul style="list-style-type: none"> - Empty Weight 10 kg - Endurance 26.5 hour - Payload 4 kg - Payload with fuel 11.5 kg - Takeoff Run 30 m
Hardware	<ul style="list-style-type: none"> - Portable Ground Control Station - Fuel injected engine

Table 18 is the datasheet of Global Hawk. It is fixed wing and provides a broad overview and systematic surveillance using high-resolution synthetic aperture radar. It is a good reference of fixed wing UAV.

Table 17: The datasheet of Global Hawk

UAV Name	Global Hawk
Type	- Fixed Wing
Use	- Provides a broad overview and systematic surveillance using high-resolution synthetic aperture radar (SAR)
Physical properties	<ul style="list-style-type: none"> - Length 14.5 m - Height 4.7 m - Stall Speed <176km/h - Cruise Speed 310 km/h - Max Speed 629 km/h
Physical capabilities	<ul style="list-style-type: none"> - Empty Weight 6781 kg - Endurance 32+ hour - Payload 3000 lb - Takeoff Run 1128 m
Hardware	N/A

From these tables, our team created useful tables that will help us compare the UAV specs. The (Figure 70, Figure 71, Figure 72, Figure 73, Figure 74) are depicting the UAV comparisons on speed, weight, endurance, altitude, and range. These charts will play a significant role in the future UAV design, and it is a good reference point for us to start. For example, if our team wants to design a high speed and endurance UAV for rescue operations, the global Hawk design will be a good reference to start with. In addition, by reading these tables our team found that there was no UAV that was good at all the parameters we studied. After deciding which design fits our needs, we can move to Chapter 3 and start designing our own UAV. Figure 70 shows the speed performance of each UAV, the highest speed of these UAVs is 629km/h. This chart can be used in the future speed reference.

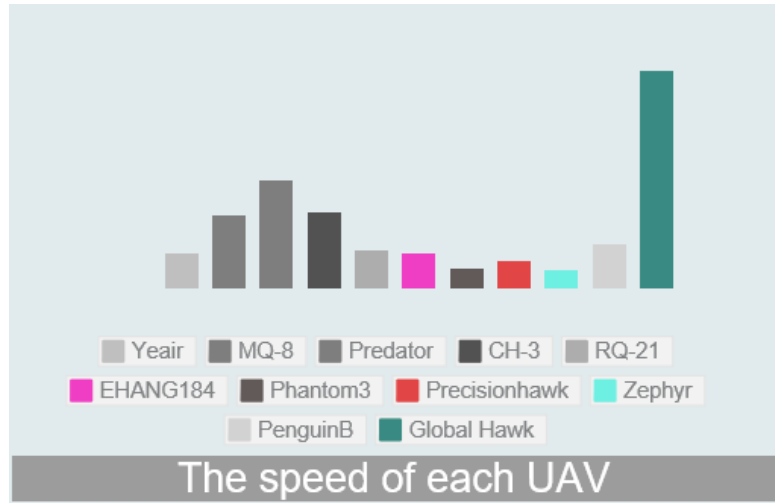


Figure 70: The speed performance of each UAV

Figure 71 is the weight performance of each UAV, the largest weight of these UAVs is 6781kg. This chart can be used in the future weight reference.

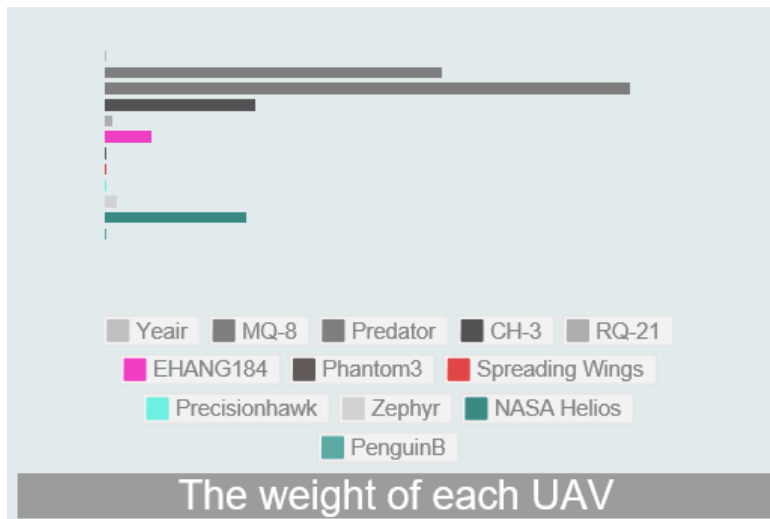


Figure 71: The weight performance of each UAV

Figure 72 is the endurance performance of each UAV, the longest endurance of these UAVs is 32 hours. Some of UAVs are power by the solar energy, which is not listed above. This chart can be used in the future endurance reference.

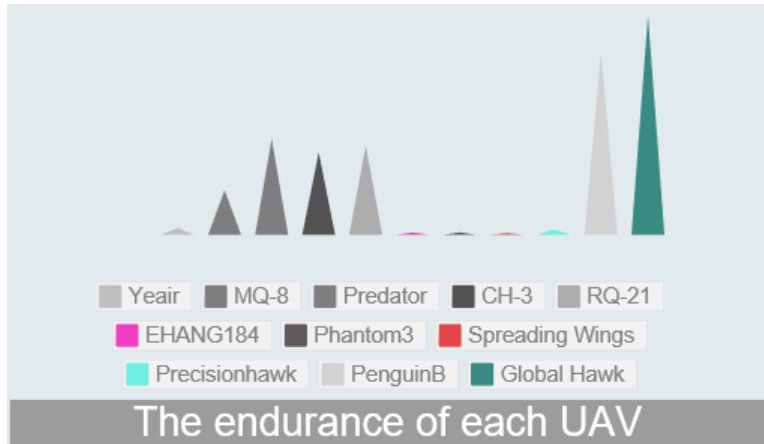


Figure 72: The endurance performance of each UAV

Figure 73 shows the altitude performance of each UAV, the highest altitude of these UAVs is 27200 m. This chart can be used in the future altitude reference.

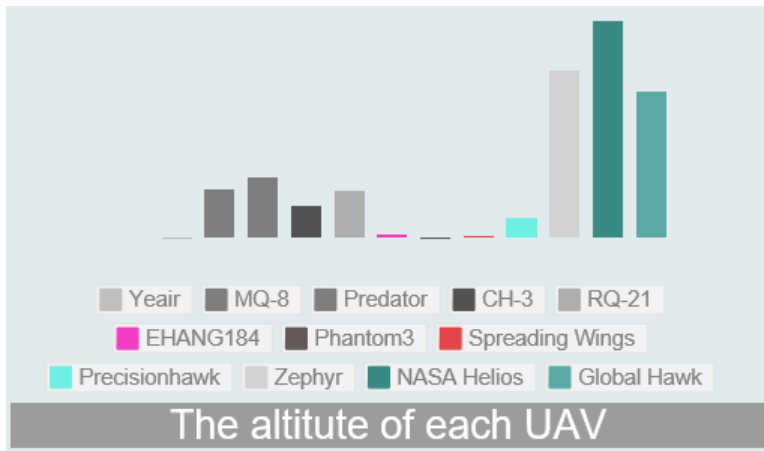


Figure 73: The altitude performance of each UAV

Figure 74 is the communication range performance of each UAV, the highest communication range of these UAVs is 1852 km. This chart can be used in the communication range reference.

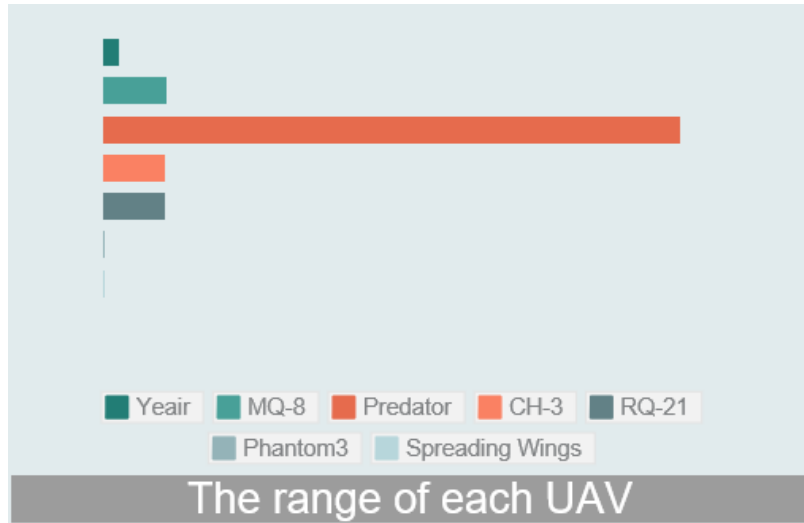


Figure 74: The range performance of each UAV

Below is a cumulative chart of all the UAVs and their specs.

Table 18: Cumulative UAV chart

UAV	Application	Payload Weight(kg)	Speed(km/h)	Endurance(min)	Altitude(m)
Precisionhawk	Mid-range and mid altitude	3.55	79	45	2500
Zephyr	High altitude pseudo-satellite UAV	2.5	56	20160(14 days)	21562
Spreading Wings S1000+	Short range and short altitude	11	-	15	-
NASA Helios Prototype	solar electric-powered flying operates at high altitude and long duration	334	-	-	21000
Lockheed Martin Hale-D	High-altitude long endurance	36	-	7200	15240
Penguin B	High performance unmanned airframe	4	130	1590	-
Global Hawk	Provide a broad overview and systematic surveillance	1360	692	1920	-
Year	Delivery services and motion picture productions	5	100	60	-
Northrop Grumman MQ-8 Fire Scout	Military, reconnaissance, Aerial fire support	272	213	480	6100
General	Military, long	1700	313	840	7500

atomics MQ-9 Reaper	endurance and high altitude surveillance				
CH-3	Military use(carry weapon) and farming	100	220	720	3000-5000
RQ-21	Military use only	17	160	780	5944
EHANG 184	Personal use	100	100	120-240	5944
Phantom 3	Recreational and commercial aerial cinematography	0	606	23	6000

CHAPTER 3. UAV DESIGN SOLUTIONS

3. Introduction

After having completed an extensive research on the topic of Unmanned Aerial Vehicles and Remote Control Aerial Vehicles, it is time to select a type of UAV and based on that design our vehicle. To do so, it is of high importance to define the details of its operation. As we described at the introduction of Chapter 1, the purpose of our drone is to help on rescue operations. To do that, we need it to be able to carry a sufficient amount of payload. This rescue payload can be consisted by life detecting instruments, communication devices and the propulsion systems that will make the vehicle able to fly. Since our team did not receive research funding our design will not include complex detecting and expensive instruments. The team is going to be working on a simplified version of the starting idea, in order to just fulfill the objectives of an Interactive Qualifying Project.

More specifically, our team decided upon an aircraft-like drone, which will carry a battery connected to the propulsion system, a camera with a resolution which will give operators the capability to detect human like objects, and a communications system to transmit the video data from the drone to the operators. The general specifications our team decided that should be matched are the following. The aircraft will be flying in a low speed and altitude as we just need it to scan a given area, and make it possible for operators to detect human life while watching the video transmitted to them. On the other hand, we need a relatively high lift in respect with the size of the UAV, as we want to mount on it instruments that are relatively heavy for the size and power of our battery.

The team will be split in two sub-teams, one responsible for the inner part of the drone, namely, the electrical and computer systems described above, and another team responsible for the outer shape and configuration of the aircraft. In the chapter that follows, we will describe extensively all of the above specifications and designs, as we will end up connecting all the parts together to get our final drone design.

3.1 Preliminary Design and Design Methodology

3.1.1 Wings design

Wing Area: We decided to focus on a large wing area in order to generate enough lift for carrying the payload consisted by the electronics and battery. This led to a total wing area of 0.2 m² with a 0.6 m wingspan and 0.35 m chord length.

Aspect Ratio and Camber: The wing was designed with a fairly high aspect ratio of approximately 1.8 in order to make for more efficient flight, while having a high camber to increase the lift – to – drag ratio and get a higher lift coefficient. The formula to compute the Aspect Ratio of a wing is the following shown in equation 16:

$$A.R. = \frac{b^2}{A} \quad (16)$$

Where b is the wing span (the length of the wings) and A is the area of the wings. So in our case we get an Aspect Ratio of:

$$A.R. = \frac{(0.6 \text{ m})^2}{0.2 \text{ m}^2} = 1.8 \quad (17)$$

On the following picture we have two examples of the same wing with different Aspect Ratio.

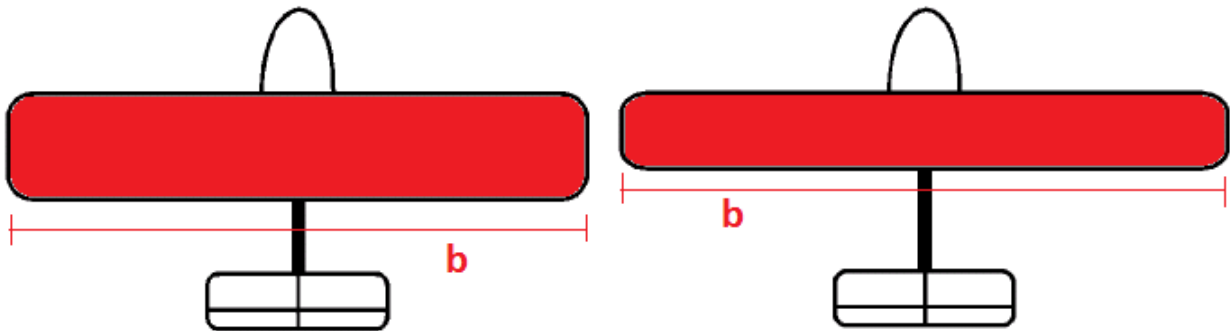


Figure 75: Examples of wings with different aspect ratio.

The wing span at the two airplanes is the same, but the right design has a smaller wing area, thus has a higher aspect ratio. Our design will look more like it the right sketch as we want a high A.R. [59]. The cathedral or dihedral angle is the downward or upward angle of the wing respectively. This angle influences the amount of roll moment on the aircraft when in turn, and is an important stability factor. In our design, we will not take in consideration these effects as we don't need our aircraft to execute complex maneuvers, thus, we will design our wings with the most simple angle configuration, the 0 degrees one.

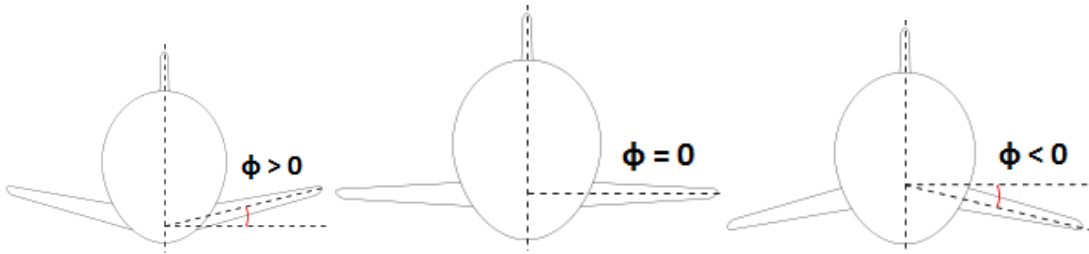


Figure 76: Examples of the three different wing angle cases

On the left graph is an airplane design that has a dihedral wing angle, and on the right is a design that has a configuration. Our design will be similar to the middle one where the angle is 0 degrees. As described above, we need our wing to have a large aspect ratio, which means that the wings are going to be long. That means that in order to support not only the aircraft's weight, but also their own weight, they have to be made out of a material that is strong and light weighted at the same time. Materials with these specifications are most of the times expensive, but in our case, we can assume that our budget is big enough to include these materials. Using the Granta CES Edu Pack materials software, we plotted all the available aerospace materials in respect with the weight and tensile strength and we ended up selecting the Epoxy/aramid fiber as it is the material that is less dense ($1,380 \text{ kg/m}^3$) but has a relatively high tensile strength (about $1.24 \cdot 10^9 \text{ Pa}$). The only drawback is that the material is more expensive than other in market, as it costs approximately 63.3 USD/kg [59].

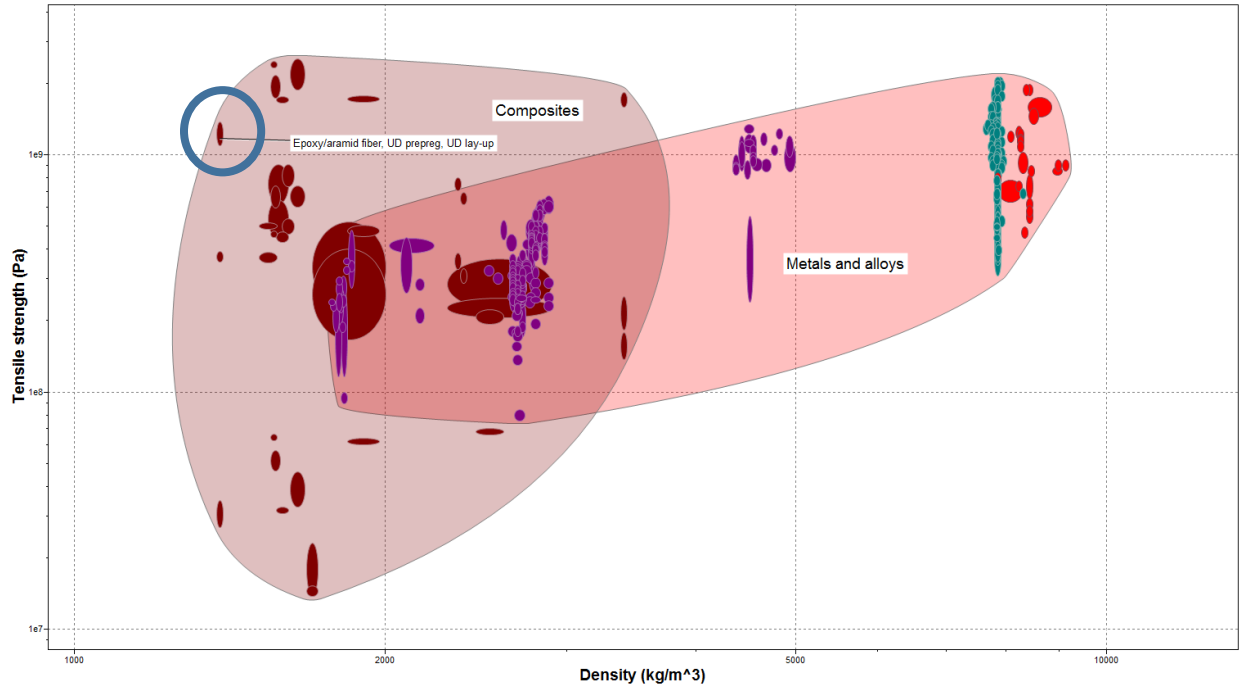


Figure 77: The plot of aerospace materials with respect to strength and density

Our primary goal is to select the proper airfoil that is effective in low speeds and generate enough lift force for the aircraft. For our research, we will use the standardized NACA airfoil and I will modify it to meet our criteria. A key part to get the aircraft flying is our airfoil to generate enough lift when in low speeds. As we will not use flaps and slats to control our aircraft, we will be choosing a standard angle of attack for our airfoil. This is going to be determined using the XFLR5 software. This is our most valuable tool for our airfoil analysis as it simulates the airflow on the foil and it provides us with useful graphs for Lift Coefficient vs. Drag Coefficient and Lift Coefficient vs. Angle of Attack. Based. To get started with our calculations, we will assume and try to build our airplane having as given a -standard for RC aircraft- cruise speed of 70 km/h or approximately 20 m/s.

The next step for our wing design is to figure out which airfoil we will use. Before we model our airfoil in XFLR5 and get accurate measurements for the lift coefficient, we need to calculate the proper Reynold's number and Mach number which will be the inputs for the software calculations. To do so we will use the equation in (2).

In order to provide an accurate lift coefficient (CL), the proper Reynold's number and Mach number are located. Before XFLR5 modeling could be completed, Reynold's number and Mach number are calculated using the equations 2 and 3:

$$Re = \frac{Vc}{\nu}$$

where ν is the flight speed, which in our case is $20 \frac{m}{s}$, c is the chord length (in our case 0.35 m) and the kinematic viscosity of the fluid which the airfoil operates, which is equal to $1.460 \times 10^{-5} \frac{m^2}{s}$ for air at the sea level (a good approximation for our design as we are looking on low altitude flights). To calculate the Reynolds number, we chose a chord length of 0.35 m in order to increase surface area, without making an exceedingly thick airfoil. Thin airfoils are considered to be more effective at low speeds. [59]

$$Re = \frac{20 \frac{m}{s} \times 0.35m}{1.4 \times 10^{-5} \frac{m^2}{s}} = 5 \times 10^5 \quad (18)$$

For the Mach number we have:

$$Mach = \frac{V}{c} \quad (19)$$

Where V is the fight speed (in our case 20 m/s) and c is the speed of sound (343 m/s for the air at 20 degrees Celsius), thus we get:

$$Mach = \frac{20 \frac{m}{s}}{343 \frac{m}{s}} = 0.0583 \quad (20)$$

The Reynolds number and Mach number values are set as inputs to XFLR5 software. For an angle of attack from -10 degrees to +20 degrees we run the software to get data for a variety

of NACA airfoils.

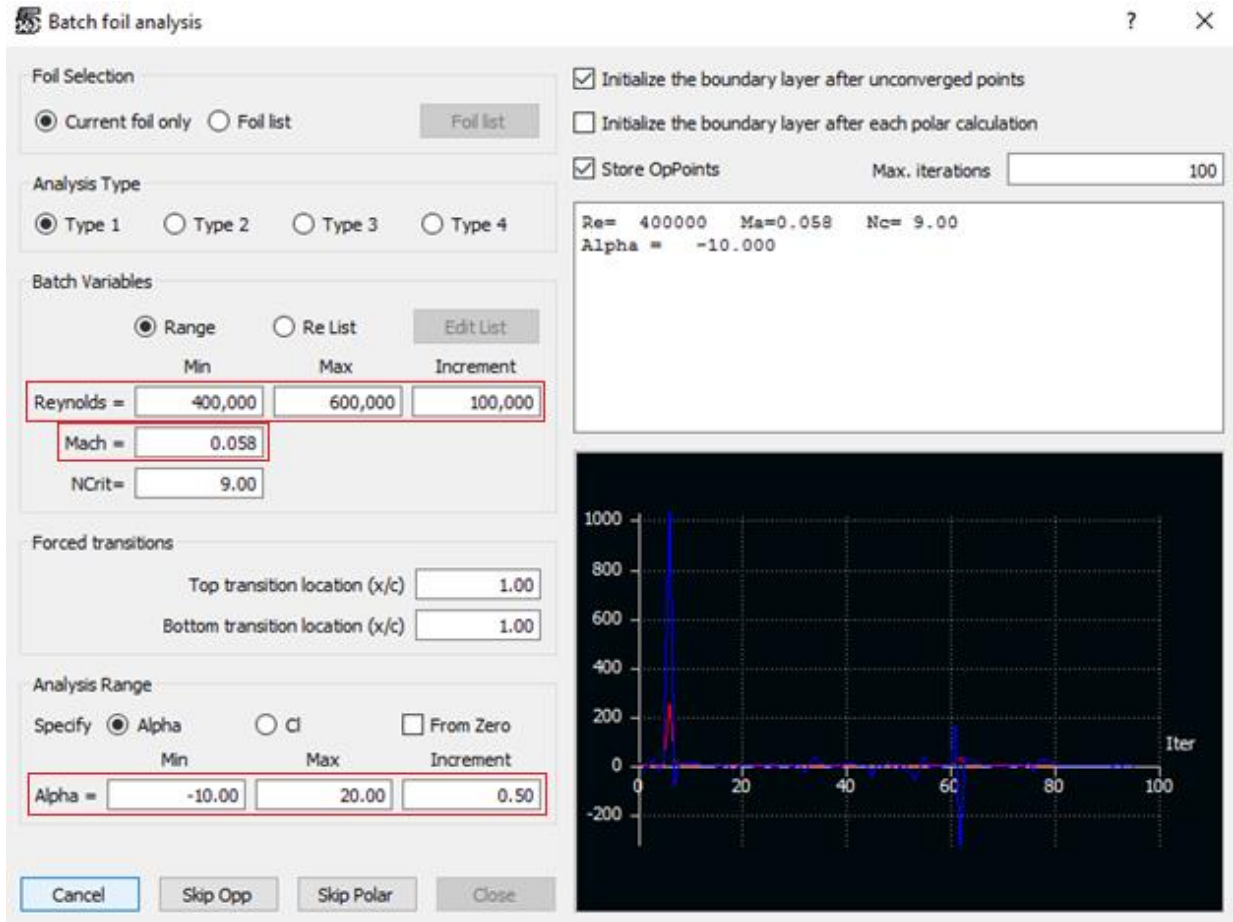


Figure 78: The XFLR5 analysis procedure for the given Reynolds and Mach numbers

We started with the NACA 4412 which is one of the best and most utilized airfoils in aerospace. NACA airfoils are airfoil designs for wings developed by the National Advisory Committee for Aeronautics and their shape is described using a series of digits, each representing a different shape property. NACA 4412 means that the airfoil has a maximum camber of 4% located 40% (0.4 chords) from the leading edge, with a maximum thickness of 12% of the chord. These airfoil specifications work great for simple UAVs like ours, as they are the most standard one is aerospace bibliography, so the only detail we looked on is the camber. As we discussed above, higher camber results to higher Lift Coefficients as shown in the tables below.

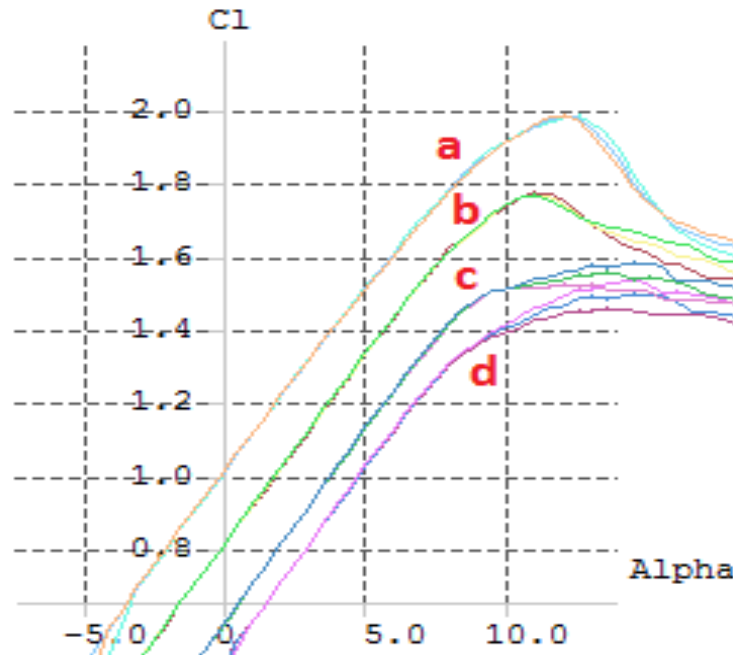


Figure 79: The lift coefficient to angle of attack graph for the four NACA airfoils

Table 19: The values of the maximum lift coefficients for selected airfoil

	Max Lift Coefficient C_L	Angle of Attack α (deg)
NACA 9412 (a)	1.97	12
NACA 7412 (b)	1.77	11
NACA 5512 (c)	1.57	14.5
NACA 4412 (d)	1.53	14.5

To generate as much lift as we can, we selected the NACA 9412 airfoil, which cross section is shown below in green. A concern that was raised while analyzing the lift coefficients for all the airfoils was if by picking the airfoil with the higher lift coefficient, we will get a smaller lift to drag ratio. Plotting on XFLR5 the C_L/C_d with respect to the angle of attack, we saw that the NACA 9412 airfoil gives us a slightly bigger ratio. [60]

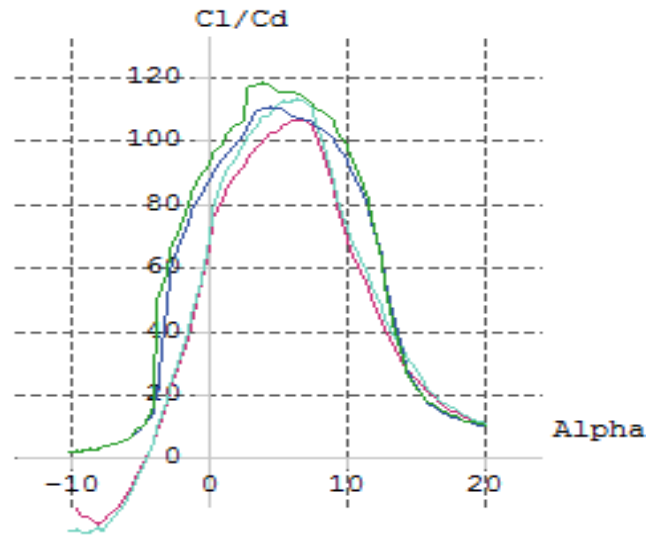


Figure 80: The lift to drag ratio for NACA 4412 and NACA 9412 UAVs

Below is the cross sections of the NACA 4412 in red and the NACA 9412 is green. It is easy to observe how significant the difference in camber for these two airfoils is.

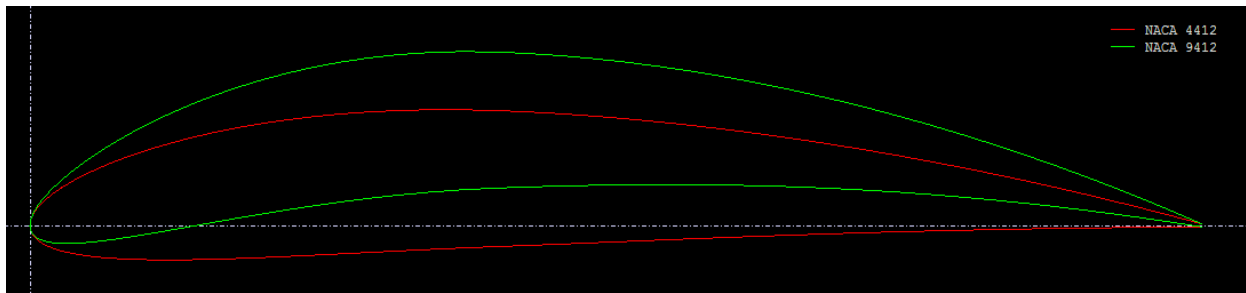


Figure 81: The cross sections of NACA 4412 and NACA 9412 in XFLR5

As previously stated, the most important aspect of our project is our UAV to be able to lift all the payload we want it to carry. As we will discuss further down, at the electronics and communication part of our project, the weight estimate for all the devices on board is going to be approximately 3.5 kg, and adding the weight of the wings and body itself, our UAV will not weight more than 5 kg, so our lift calculations will be based on the assumption that our aircraft's maximum weight is 5kg. Thus, using Newton's first Law (equations 21 and 22):

$$\Sigma F = 0 \tag{21}$$

$$W - mg = 0$$

$$W = mg = 5kg \times 9.81 \frac{m}{s^2} = 49.05 N \quad (22)$$

We need our wings to generate 49.06 Newtons of force in order to be able to fly. Using the lift equation we can finally calculate the area of our wing and knowing the chord length we can solve for the wingspan, and thus we can proceed to the next step, which is designing it. For lift we have equation 6 [60]:

$$L = \frac{1}{2} \rho v C_L A \quad (23)$$

In this case, ρ is the air density which is $1.225 \frac{kg}{m^3}$ for air at the sea level, v is the UAV's speed which we agreed to set as $20 \frac{m}{s}$, C_L is the lift coefficient which for the NACA 9412 at an angle of attack of 12 degrees is 1.97 and A is the wing area, which is our unknown parameter. Thus, we are solving for A :

$$A = \frac{2L}{\rho v C_L} = \frac{2 \times 49.05 N}{1.225 \frac{kg}{m^3} \times 20 \frac{m}{s} \times 1.97} = 0.2 m^2 \quad (24)$$

As we previously mentioned, our chord length is going to be 0.35 m and because we have a rectangular wing, our area equation 25 is simply:

$$A = bc \quad (25)$$

So our aircraft's wingspan b will be shown in Equation 26:

$$b = \frac{A}{c} = \frac{0.2 m^2}{0.35 m} = 0.6 m \quad (26)$$

As soon as we defined all the parameters we needed, we exported the airfoil data to the SolidWorks software, in order to get the cross section of our airfoil which is depicted below.

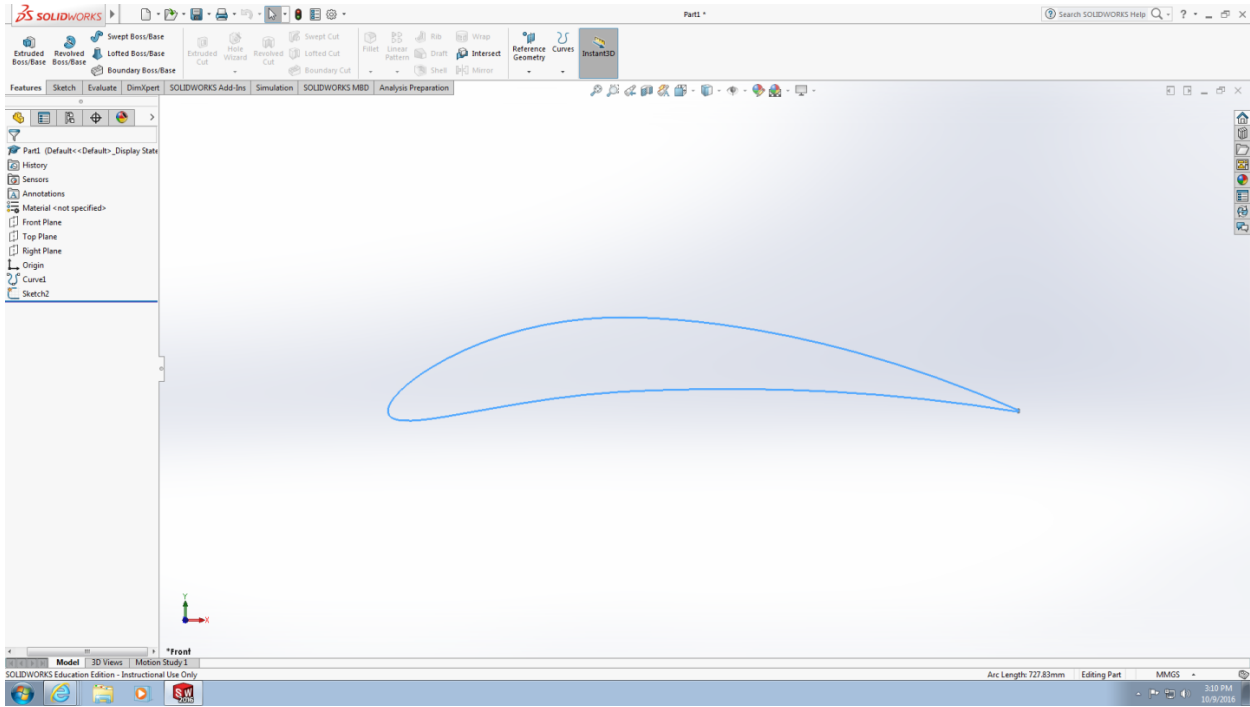


Figure 82: The cross section of NACA 9412 in SolidWorks

Using the Extruded Boss/Base feature in SolidWorks, we converted the 2D sketch into a 3D airfoil, with a wingspan of 600mm (0.6 meters as calculated above). This design has its real dimensions, so it is ready to get assembled with the body. The format of the file allows us to 3D print a sample airfoil. Below are 3 views of the airfoil, each one from a different angle.

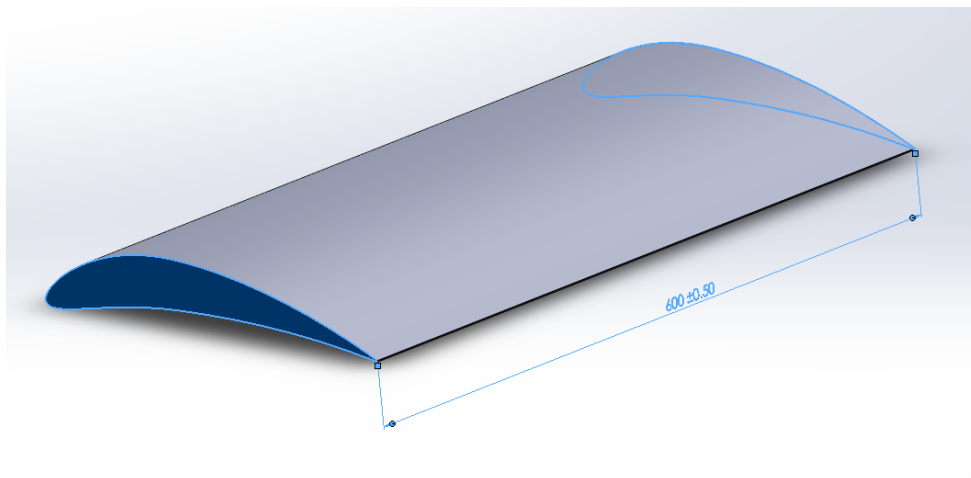


Figure 83: The top back view of NACA 9412 and its wingspan length

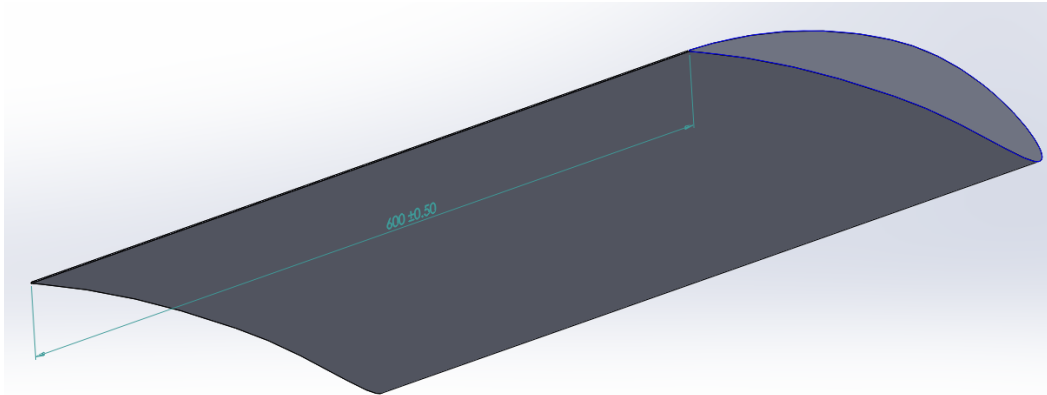


Figure 84: The bottom view of NACA 9412 and its wingspan length

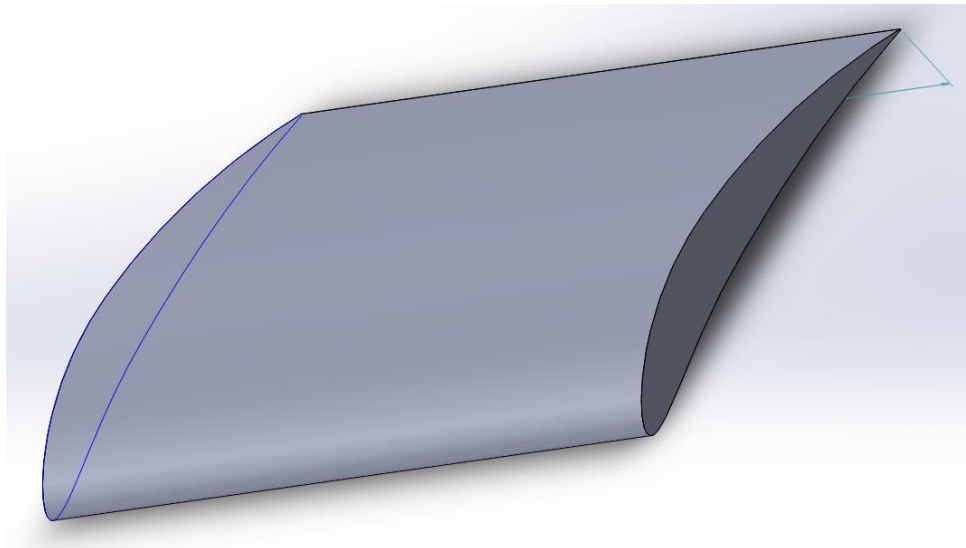


Figure 85: The top front view of NACA 9412

3.1.2 Body Design

Below is a fixed wing UAV model with a length of 46 cm and a width of 50 cm. It has two engines and each has the power of 5W. This UAV can fly within a range of 50 km and have average speed of 100km/h. It can deliver up to 3kg weight and drop 15m above the ground. We put the engine above the wings because at the bottom of the UAV a payload box can be mounted which can carry cameras and other medical supplies. At the front of the UAV it has a

tube shape device. That is a pitot tube used to measure the relative speed between UAV and wind. Another function for that is to break the air and decrease the air resistance. The V shape elevator design is to decrease the number of elevators from 3 to 2 in order to save materials and energy.

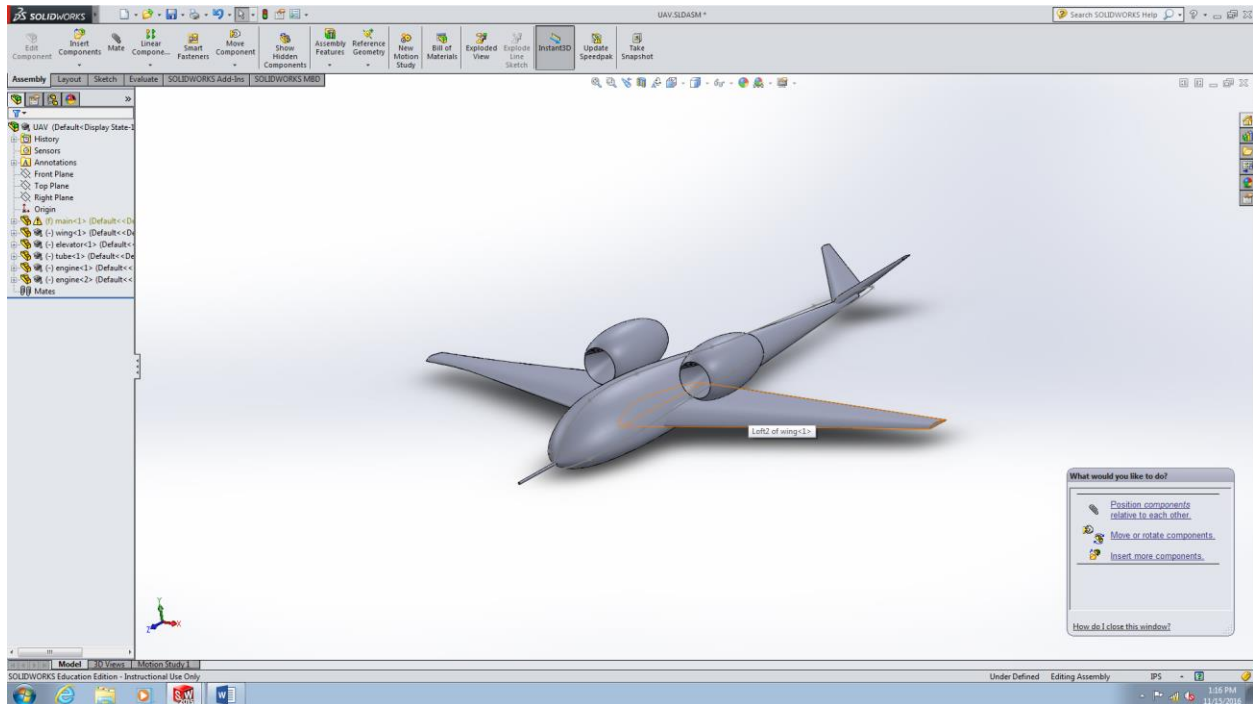


Figure 86: The design of UAV model

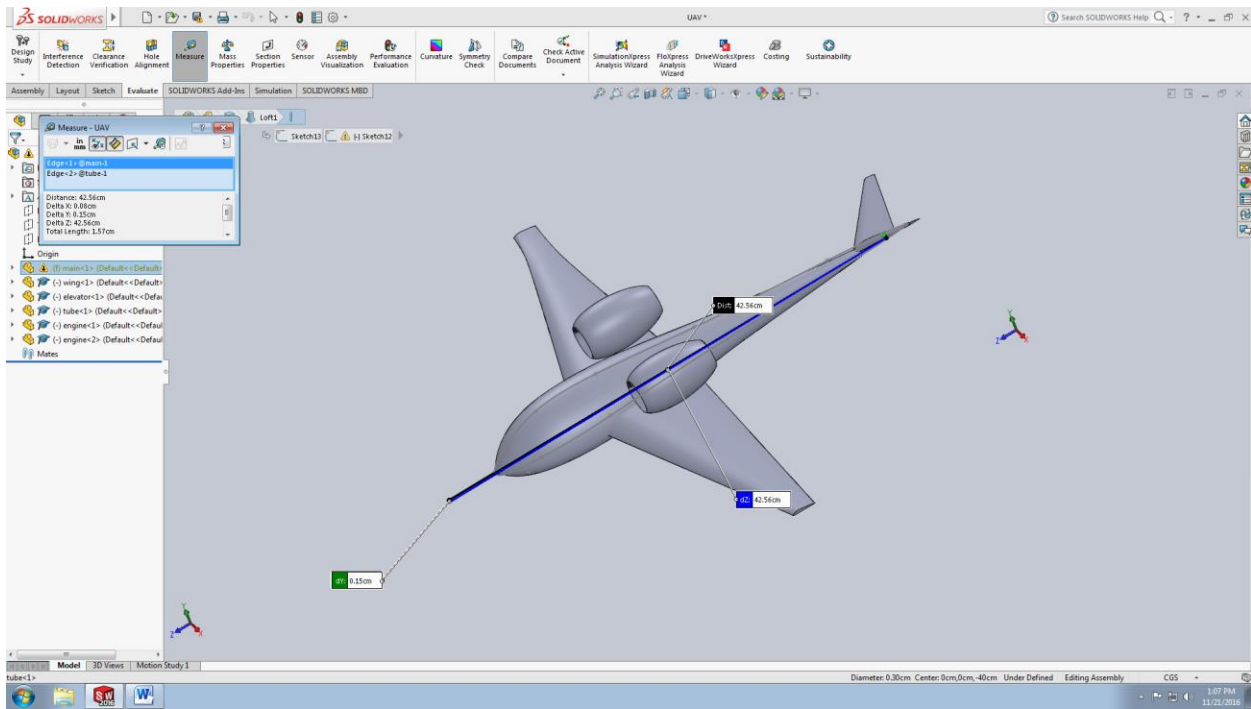


Figure 87: Our model seen from another angle

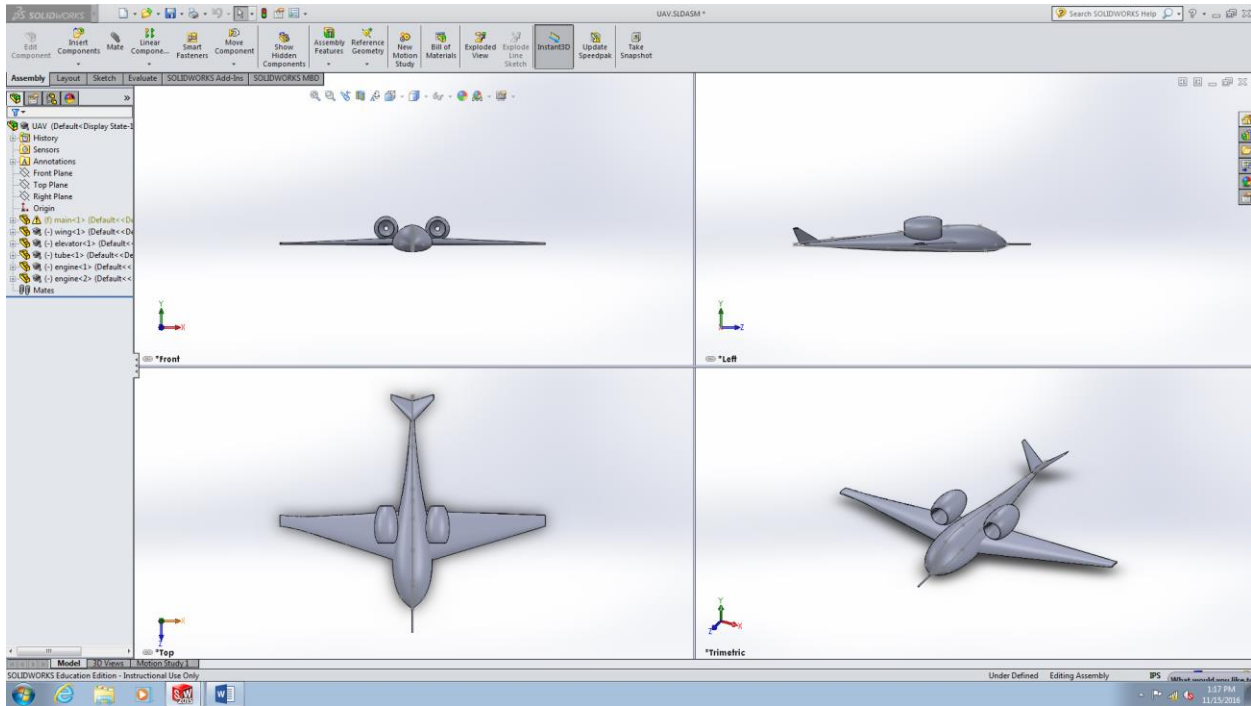


Figure 88: Additional top and side views of the model

3.2 Search and Rescue Methodologies

3.2.1 Transducers and Sensors Descriptions

In this section, sensors and transducers are discussed. In order to make the drone flies in a stable manner, the drone needs to keep sensing the environment and its operating conditions. Sensors such as encoders, potentiometers, oil scale are necessary; however, the exteroptive sensors will be the main focus. It is very important to keep the drone sensing the environment and take actions to different situations. The discussion of some specific sensors will be carried out which are pitot tubes, weather sensors, GPS, accelerometer, gyroscope, and the specific usages. An accelerometer is a device that measures the proper acceleration. That means when the accelerometer is in stationary, the net acceleration is pointing up with the amount of 9.8 m/s^2 . When the accelerometer is in free fall state, the acceleration is 0 m/s^2 . An accelerometer on a UAV can helps it know in which direction is the ground. It also helps the onboard computer to know the acceleration in X, Y, and Z axis. In real situation, the calculations of the actual acceleration are needed especially during flying, raising, or landing. Because the acceleration is proportional to the force, a close loop structural is reasonable to control the UAV and the propeller.

For the structure of the accelerometer, the most common type is a 3D-MEMS (Three-Dimensional Micro Electro Mechanical System) accelerometer. This make use of the piezoelectricity. Piezoelectricity is when a force exerted on a crystal, a current can be created. Inside the accelerometer it is a structure similar to *Figure 89*. When a force exerted, the mass in the middle moves and each pair of green structure locates at top and bottom are charged and have the same function as a capacitor. The ammeter senses the current and can calculate the corresponding force.

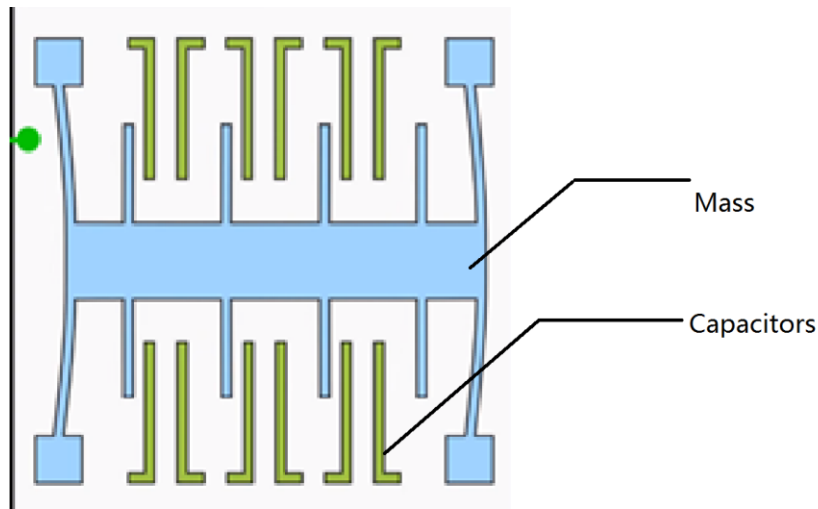


Figure 89: One Dimensional Structure of an Accelerometer

Gyroscope is a device to measure the angular velocity and angle displacement in X, Y, and Z axis. While the UAV is flying, it is necessary to know the angle in each axis. For example, the attack angle can be directly measured by gyroscope. When controlling the UAV, the UAV must keep stable and remain in the same attack angle when it is flying in a straight line.

The most common used gyroscope is also a MEMS [61] (Micro Electro Mechanical System) which also takes advantages of the piezoelectricity. This kind of gyroscope is called vibrating gyroscope. There is a drive arm that keeps a special designed (Double-T shape, tuning fork, H-shape tuning fork) structure crystal keep on vibrating. When a rotational acceleration exerted, the crystal will twist in different direction and amplitude. The crystal is in the middle of a capacitor, so when the voltage potential changes, the current change will be sensed by the ammeter connected with the capacitor.

A pitot tube [62] is a pressure measurement device that used to measure fluid flow velocity. When a UAV is flying, it is important to know what is the velocity related to the air. Sometimes, calculation of the velocity according the data is collected by accelerometer. However, this is the velocity relative to the earth or ground. When the UAV is flying in a steady velocity, most of the forces acting on the UAV is exerted on air. Therefore, in order to control the UAV well, the relative velocity to the air is much more important compare to the ground speed.

A pitot tube is a tube with one open end and one close end. Inside the tube, it cannot measure the flow of the air. However, according to Bernoulli's equations:

Stagnation pressure = static pressure + dynamic pressure

Equations are listed as follow:

$$P_t = P_s + \frac{1}{2}\rho V^2 \quad (27)$$

Therefore the velocity is shown in Equation 28.

$$V = \sqrt{\frac{2(P_t - P_s)}{\rho}} \quad (28)$$

Where V is flow velocity in m/s, P_t is the stagnation pressure in Pascal, P_s is static pressure Pascal, and rho is the fluid density in kg/m. According to the equations above, the velocity of the UAV reverent to the air can be easily retained.

GPS is known as Global Positioning System. It is a global navigation satellite system that can provide location and time in all weather conditions. When the UAV flying by its own, it is necessary to constantly report its precise locations. In addition, while searching for survivors, it has high possibility to search in extreme environment such as heavily rain, extreme cold, and lots of mountains or forest. It is necessary to find a reliable device to find the exact location. GPS just fit for all these requirements. For a GPS receiver modular, crucial properties must be selected such as, size, update rate, power requirement, channels, antennas, and accuracy. These will be discussed more into detail in the next section.

Weather sensors include a lot of sensors. In order to search and save in most efficient way, UAV need to know if the environment is out of its working limit. For example, if UAV searching in polar zone, the temperature could lower than -40 C degrees. That can make the oil freeze, and UAV can fly. Also, in order to save in most efficient way, UAV should report the current weather, so people back at station can decided, when and how to save. Just as the example raised above, UAV needs to check the environment temperature to keep itself safe. Especially, when it is working in extreme cold or warm environment. A thermometer is normally a thermoreceptor with an ammeter. As the resistance of the resistor changes with the temperature, the current changes.

Humidity is the percentage of water in air. The amount of water in air can strongly affect the performance of precise devices. Therefore, the humidity sensing is critical in order to keep the UAV function well. If a UAV enters extreme high moisture zone the UAV should try its best to exit that zone and try not enter next time to keep UAV in good performance. There are two

kinds of humidity measuring units. One is the relevant humidity and another one is absolute humidity. Although there are more than twenty kinds of methods to measure the humidity in air, it is still a hard unsolved task if high precision is required [63]. The extremely high precision for humidity measurement is not necessary. The humidity sensing is just a way to keep UAV safe. One adaptable kind of humidity sensor based on resistive effect. A thick film conductor is shaped to form an electrode. The change of impedance of the conductor is caused by the amount of humidity which is movable ions. In real life, humidity is relevant to the temperature. There is a special device that can measure both temperature and humidity which is called hygromograph or thermohygrograph. However, the size of that device is too large for an UAV, we just use the thermometer and hygromograph separately.

There are also some other sensors that didn't mentioned above. For example, at the joint between the rotatable propellers and the wings both an encoder and potentiometer is needed to control the rotation of the direction of propeller. An infrared camera is need to send the real time image back to saving station to find survivors. Overall, in this section, sensors and transducers needed for UAV are described. In next section, we are going to discuss more about the precision, range, and cost of different kinds and brands of sensors.

3.2.2 Specific Performance Evaluation

The performance of each sensor is directly related to the performance of the UAV. The properties of each sensor also limits the performance of UAV. Therefore, the comparing between sensors is crucial for UAV. We are going to compare the sensors from the following properties: resolution, measuring range, stability, operating temperature, and required input voltage. The chart below is three kinds of different accelerometer that can fit in our UAV.

Table 20: Data description of onboard accelerometers of the UAV [64, 65, 66]

Accelerometer	AKE398B	AKE390	T356M98
Measuring Range (gravity)	±2,±4,±8	±2,±4,±8	±5
Resolution (mg)	1,5,15	1,5,15	0.05
Operating Temperature	-40C to +85C	-40 C to +85C	-20 C to +170C
Input Voltage	9V – 36V	9V – 36V	8-12 V
Max Sample Rate	400 Hz	400 Hz	2000 Hz
Output Signal	4-20 mA	0-5V	8-12V
Cost	250	250	1200

Specific data needs be collected and verified from the data sheet of each accelerometer and build a table that easy for us to compare. First the ranges must be well selected based off of the requirements of the UAV. Because the UAV is not designed to be flying in a constant velocity. In other words, our design does not require difficult high-velocity maneuver. The estimated range of acceleration for our UAV is between -1g to +3g, and all the accelerometer above are fit. For the resolution, it is true that smaller resolution is more precise. However, in some situations, too much decimal of data some times are useless. The resolution usually proportional to the price of device. The first two is absolutely win on this part. Then when the temperature is checked, the first two cases do not fit for the desired requirements. Inside the UAV, the air friction and heat dissipated by the motor is huge, it might go excess the temperature limit. If we want to use the first two accelerometers, we have to build a cooling system. For the output signal, there are two types of output signal. One is current output and another one is voltage output. Therefore, we think voltage output is more stable and reliable. The voltage signal will change less while working in a weak electric field since we can use pull-up resistors to stabilize the voltage signals. In conclusion, we are going to use AKE390 produced by Rion-tech. The following chart is data for different kinds of gyroscope.

Table 21: Three kinds of gyroscopes that fit for the UAV [67, 68, 69]

Gyroscope	TL732D	SDI500	QRS28
Resolution/Range(degree/s)	0.1	0.1-1000	0.02
Input Voltage	9V-36V	10V-42V	-4.75V-5.35V
Operating Temperature	-40C-+85C	-55C-+85C	-55C-+85C
Bias	10 degree/hr	1 degree/hr	N/A
Random Noise degree/s	N/A	0.0003	0.0005

As the same way carried out for accelerometer, chose three best fit gyroscopes are chosen, shown in Table 22. The gyroscope on UAV is just for assisting the UAV maintain its balance and aware of its own position. All the resolution is fit for this UAV. For the input voltage, the second one might require too much voltage, and is very power consuming. All the

working temperature is fit for UAV too. When it comes to bias and noise, even though the exact price cannot be found on internet, it is not hard to get the conclusion that the more precise the more expensive a device is. As I mentioned above, in order to reduce the cost of UAV, TL732D is chosen for our application which is also produced by Rion-tech.

Most pitot tubes are similar and the main differences are size and range. It is fairly reasonable to pick a pitot tube that is commonly used for UAV. It is produced by UAV factory and called Heated Pitot – Static Probe [70]. This has the weight of 58 grams and length of 238mm with the working temperature of -50 C to +85 C. Because this is a digital pitot tube, the operating voltage is 12V and signal output is 5V.

GPS is also an important sensor on UAV because it can send the location of the UAV back to ground station. There are lots of GPS receiver modular selling on internet, the main difference is the sample rate and the number of channels. The Venus GPS [71] produced by SparkFun is selected. This modular has up to 20Hz update rate and precision of 2.5 meter. This is a low power consuming device with only 3.3V required power supply.

The thermos sensor is very cheap and the only thing needs be considered is its operating temperatures. The ideal range should be lower than -70C and higher than 200C. However, the digital thermometers are also need for the electrical wire and chips. It is hard to find a thermometer that works at a temperature lower than -40C. Therefore, temperature lower bound can be assumed as 40C. We choose the cheapest one which is produced by SparkFun called TMP36 [72].

The hydro sensor is a little bit complicated, and it is hard to find a small device that measure precise humidity. The humidity sensor needed is just for protect the devices inside the UAV. HH10D [73] is selected which also produced by SparkFun. It requires 2.7-3.3 volts and with the accuracy of +-3%.

3.2.3 UAV Cooling System

The cooling system on the UAV is very important because all the electrical devices, the motor and the air fraction all produce a lot of heat. It will be a problem that can burn all the chips in UAV if there is a management issue. Therefore, our team decided to use a thermoelectric cooling device that transfer the heat around the chip to the air that going to flow into the turbo engine.

This device takes advantage of thermoelectric effect. When a current is made to flow through a junction between two conductors, heat may be generated or removed at the junction. The cooling side of the modular is attached to the electrical devices. On another side of the cooling device, which the warm side, we use copper to transduce heat. Shown in Figure 91. Our team decided to use 12V 60W cooler called TEC1-12706 [74] cooling Peltier plate.

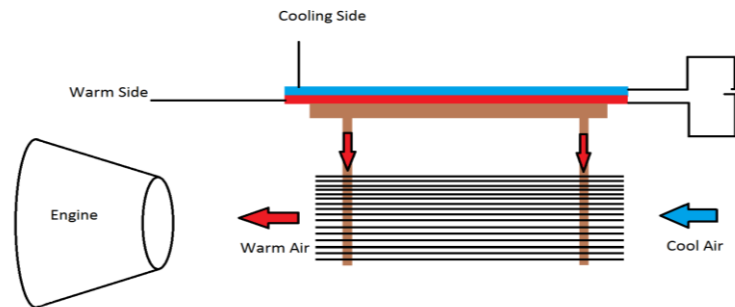


Figure 90: The cooling system in the UAV

3.3 UAV Control and Electric Parts

3.3.1 UAV Control Elements

In this section, the first part is to introduce the relationship between Chapter 3.1, 3.2, 3.3 and 3.4 seen in *Figure 91*. From the *Figure 91*, the embedded board receives all the sensor data and processes to achieve the reliability, safety, motion and tasks. Specifically, for the motion, the GPS, accelerometer, pilot tube and Gyroscope data are sent to the embedded board. The data from GPS includes the altitude of UAV. The data from accelerometer includes the acceleration of UAV. The data from pilot tube includes the velocity of UAV. The data from Gyroscope includes the pose of UAV. These values are important feedback in control system.

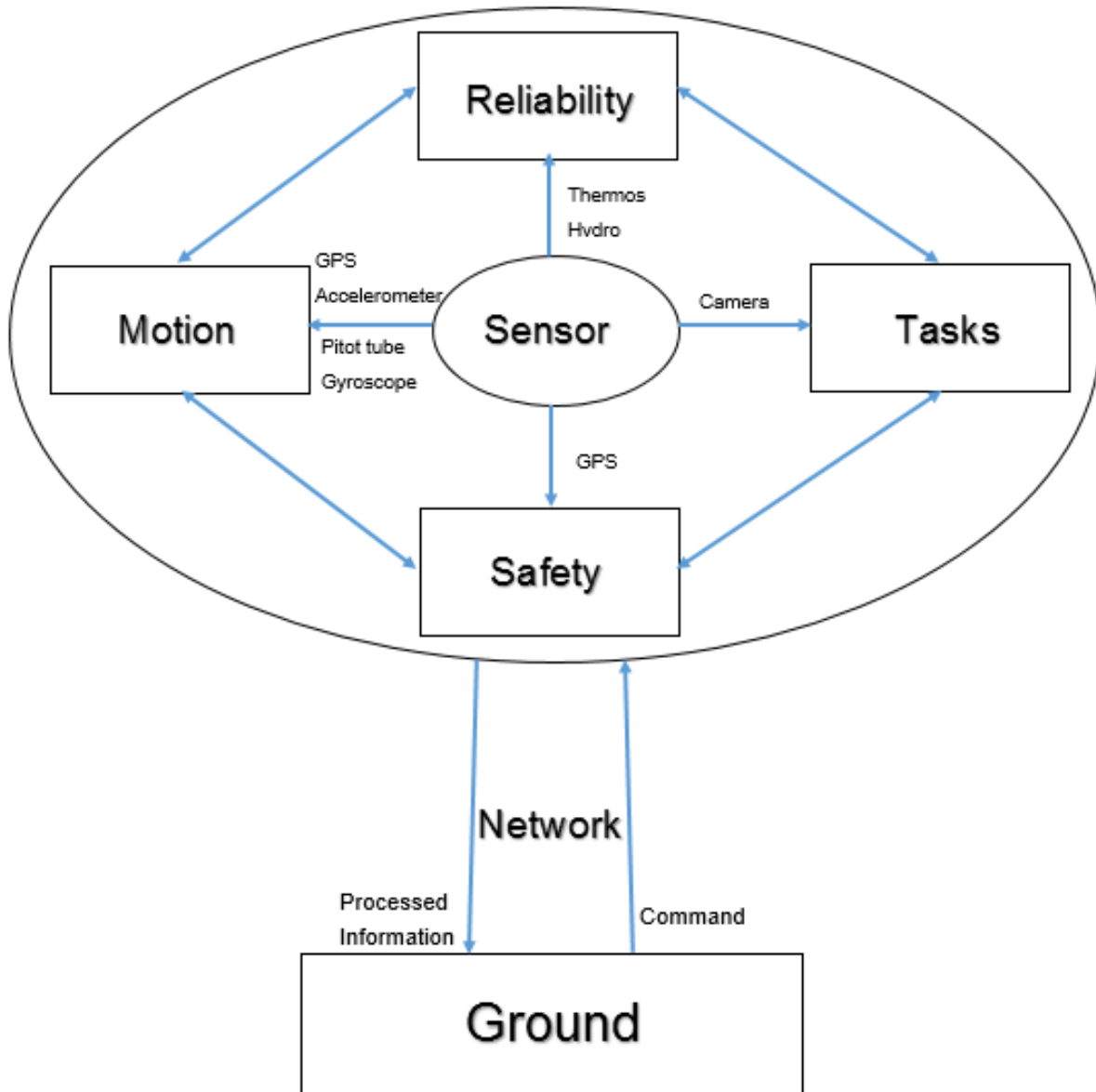


Figure 91: The relationship between each element in UAV

From the concept in the *Figure 91*, the *Figure 92* is brief relationship between devices. Sensor data is discussed in the Chapter 3.2. Data transmission and real-time image will be analyzed in Chapter 3.4. The following section will introduce the electric board battery and control in detail.

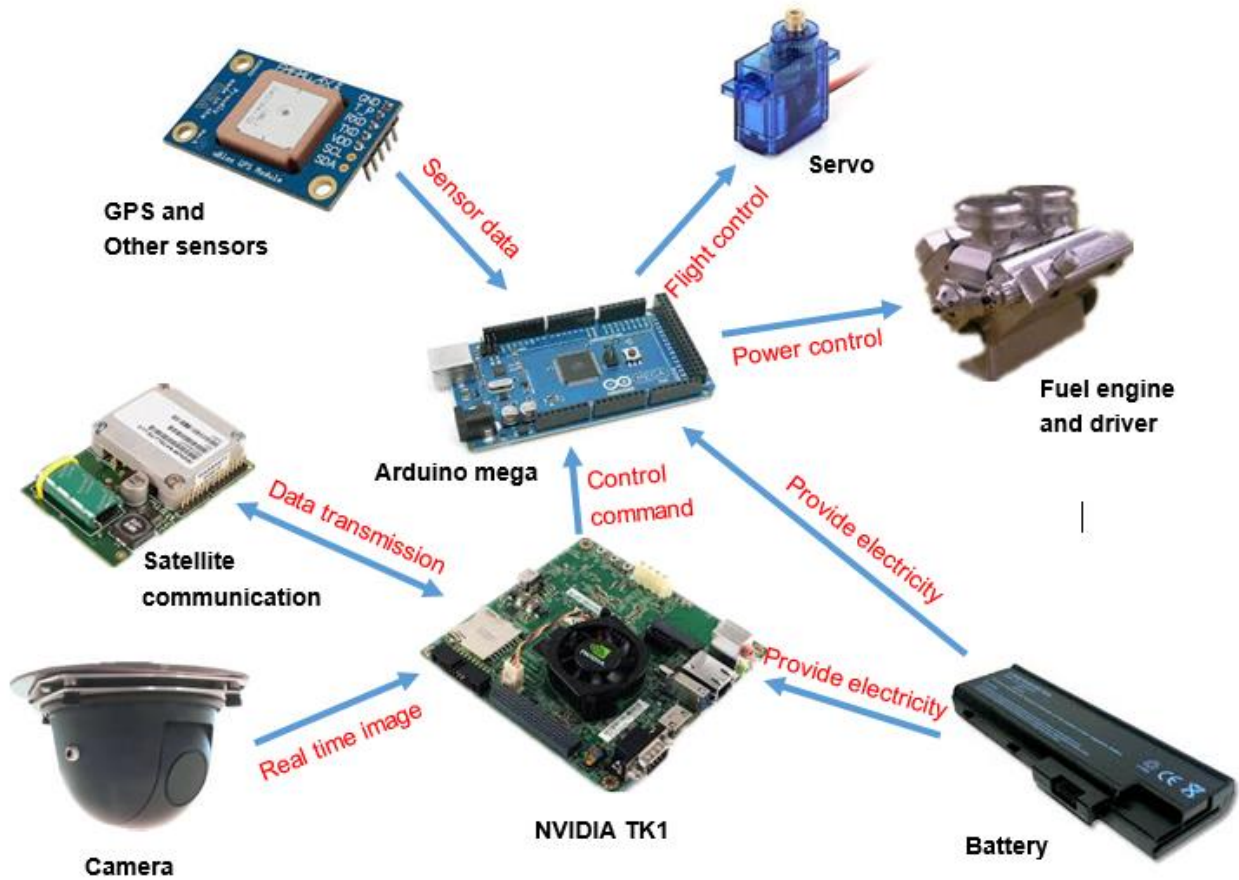


Figure 92: The relationship between each device

The second part is to introduce the electricity our team used in the UAV and discuss them with model our team built. This is important to build 3D model of electrical parts, because these electrical parts can be placed within the UAV in order.

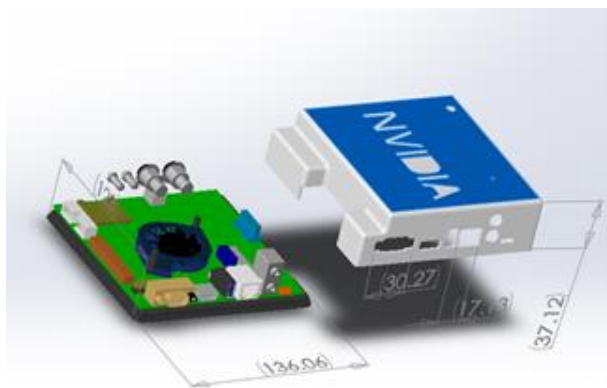


Figure 93: 3D angle of view of the UAV control board



Figure 94: Application of NVIDIA Jetson TK1

The main board the team choose is NVIDIA Jetson TK1. The reason to choose it is that this gives a completely functional NVIDIA CUDA® platform for rapidly developing and deploying compute-intensive systems for computer vision, robotics, medicine, and more. The function of this board is to dispose the data from camera and send the useful data to the station, for example the position of rescue point. From the model our team have, the NVIDIA Jetson TK1 seen in *Figure 93* is like a 136mm* 123mm * 37mm rectangle. The mass is 120g. The power of the board is approximately 7W. The practical application of NVIDIA Jetson TK1 is extensive. For example, it is used in prototype Axiom Gamma 4K open source camera hardware seen in *Figure 94*. And it is widely used in the deep learning, because the computing power of this board is strong. Since there are lots of image computing in UAV, NVIDIA Jetson TK1 would definitely be a good choice. [75] The specific kit content is showing in the Table 23. This table would be helpful for the board communication.

Table 22: NVIDIA Jetson TK1 kit content [76]

Memory	Port	Others
-2 GB x16 Memory with 64-bit Width	-1 Full-Size HDMI Port	-1 ALC5639 Realtek Audio Codec with Mic In and Line Out
-16 GB 4.51 eMMC Memory	-1 USB 2.0 Port, Micro AB	-1 Full-Size SD/MMC Connector
	-1 USB 3.0 Port, A	
	-1 RS232 Serial Port	

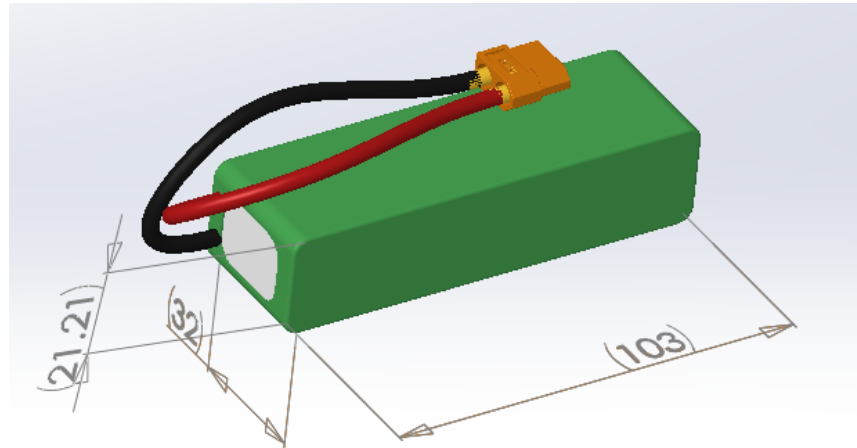


Figure 95: 3D angle of view of battery

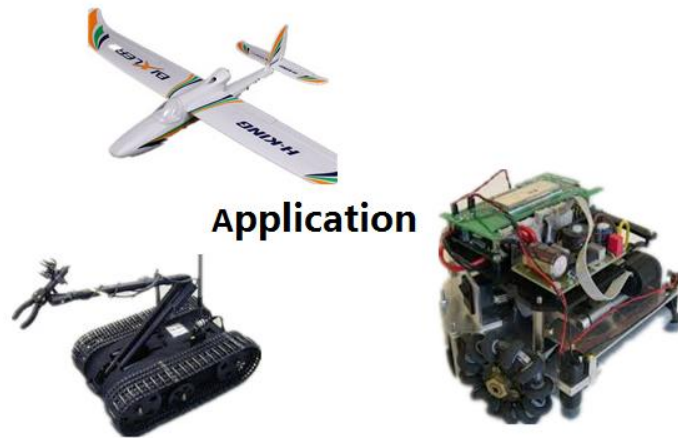


Figure 96: Application of battery

Since the UAV is powered by the fuel engine, the battery just provides power of board in emergency. The size of battery seen in *Figure 95* should be small with low capacity. It is a 103mm*32mm*21mm rectangle. The capacity of this battery is 4000mAh, and the weight is 244g. There are many applications of this battery, which show in the *Figure 96*. It is widely used in the electric car. It has enough power to drive the motor and servo. Other specification is showing in Table 24. This table would be a good material for electrical analysis.

Table 23: The datasheet of the battery of the UAV

Minimum Capacity:	4000mAh
Configuration:	3S1P / 11.1V / 3Cell
Constant Discharge:	10C
Peak Discharge (10sec):	20C
Pack Weight:	244g
Charge Plug:	JST-XH
Discharge Plug:	XT60
Weight (g)	244

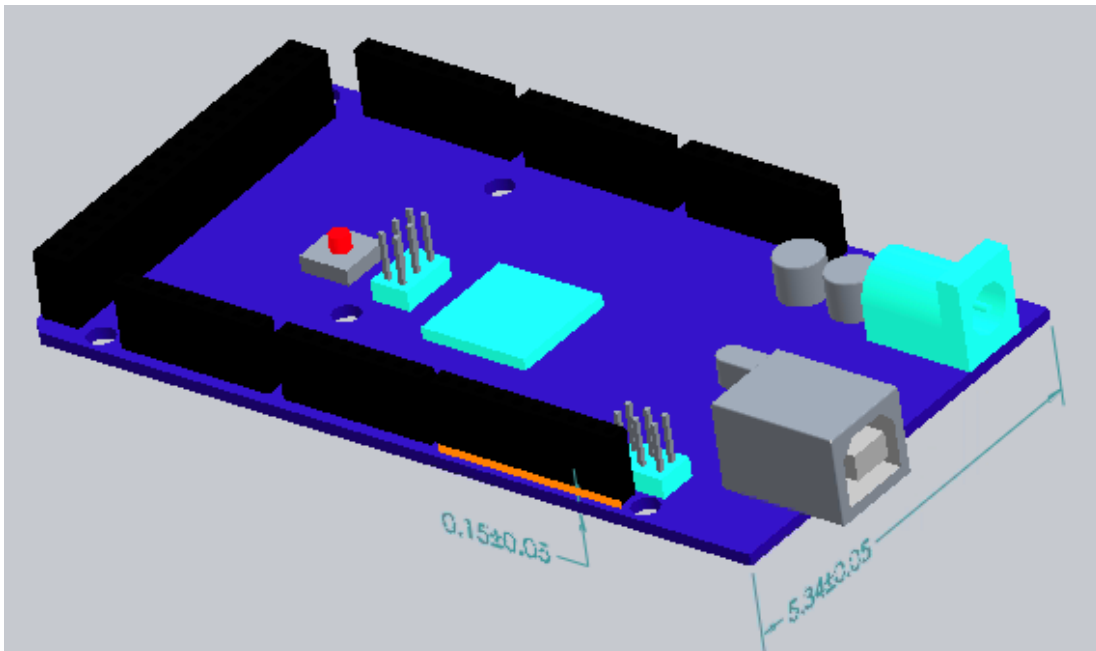


Figure 97: The 3D angle of view of Arduino Mega

The assistant board the research choose is Arduino Mega seen in *Figure 97*. The reason selecting Arduino Mage is that it is light, small and easy to control the UAV. The main function of this board is to control the UAV, like brain, getting the value from the sensors on the UAV and outputting signal to the fuel engine and servo. The size of board is 102×54 mm from the *Figure 97*. Weight is 37g, which is very light. The table 25 is contrast of two similar board. From this table, Microcontroller ATmega2560 has more pin, better to control the servo and more serial port, so ATmega2560 would be better.

Table 24: The data contrast of two small electrical board

Microcontroller	ATmega2560	Microcontroller	ATmega328P
Operating Voltage	5V	Operating Voltage	5V
Input Voltage (recommended)	7-12V	Input Voltage (recommended)	7-12V
Input Voltage (limit)	6-20V	Input Voltage (limit)	6-20V
Digital I/O Pins	54 (of which 15 provide PWM output)	Digital I/O Pins	14 (of which 6 provide PWM output)
Analog Input Pins	16	Analog Input Pins	6
DC Current per I/O Pin	20 mA	DC Current per I/O Pin	20 mA
DC Current for 3.3V Pin	50 mA	DC Current for 3.3V Pin	50 mA
Flash Memory	256 KB of which 8 KB used by bootloader	Flash Memory	32 KB (ATmega328P) of which 0.5 KB used by bootloader
SRAM	8 KB	SRAM	2 KB (ATmega328P)
EEPROM	4 KB	EEPROM	1 KB (ATmega328P)
Clock Speed	16 MHz	Clock Speed	16 MHz
LED_BUILTIN	13	LED_BUILTIN	13

And the camera our team used is like hemispheroid with 69.7mm radius seen in *Figure 98*. The more specific application of this camera will be analyzed in Chapter 3.4

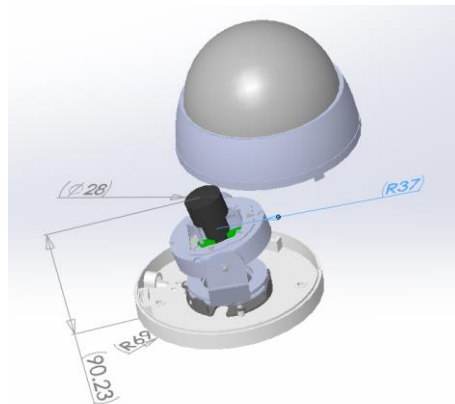


Figure 98: 3D angle of view of the UAV camera

3.3.2 UAV Control Analysis

The importance and theory of PID is analyzed in the Chapter 2.2. In this chapter, it is suggested that gain scheduling has a significant role in the PID controller. Gain scheduling is a PID enhancement that helps the control of a process with gains and time constants that vary according to the current value of the process variable.

A gain scheduler provides the best of both worlds. It allows the controller to be tuned for any number of operating ranges so that an optimal set of tuning parameters can be downloaded into the controller depending on the current value of the process variable [77]. All of the UAV controls are processed by the Arduino Mega. Therefore, it is not allowed to apply the Matlab algorithm directly, for example the PID controller. It supposes to have independent function and library in the Arduino Mega. The Table 26 is an example of how to apply own control function into UAV board.

Table 25: Example code for PID speed and altitude controller in C programming

```
// struct:
pidData pid_Data;

// functions:
void setConst(char Mode, double Kp, double Ki, double Kd);
double calcPID(char Mode, int setPoint, int actPos);
void initPID(unsigned char Mode);

void setConst(char Mode, double Kp, double Ki, double Kd){
    // the function to update the gain settings
    if (Mode == 'A'){ // altitude PID
        pid_Data.Kp_H = Kp;
        pid_Data.Ki_H = Ki;
        pid_Data.Kd_H = Kd;

    } else if (Mode == 'S'){ // speed PID
        pid_Data.Kp_L = Kp;
        pid_Data.Ki_L = Ki;
        pid_Data.Kd_L = Kd;
    }
}

void initPID(unsigned char Mode){
    // the function to initial the PID variable
    if (Mode == 'A') { // altitude PID
```

```

        pid_Data.prev_err_H = 0;
        pid_Data.sum_err_H = 0;
    }
    else if (Mode == 'S') { // speed PID
        pid_Data.prev_err_L = 0;
        pid_Data.sum_err_L = 0;
    }
}

double calcPID(char Mode, double setPoint, double actPos){
    double u;
    double err = setPoint - actPos;; // calculate error
    if (Mode == 'A'){ // altitude PID
        pid_Data.sum_err_H = pid_Data.sum_err_H + err; //
calculate sum of error
        u = (pid_Data.Kp_H * err) + (pid_Data.Kd_H * (err
- pid_Data.prev_err_H)) + (pid_Data.Ki_H *
(pid_Data.sum_err_H));
        pid_Data.prev_err_H = err; // store the last
error
    }
    else if (Mode == 'S'){ // speed PID
        pid_Data.sum_err_L = pid_Data.sum_err_L + err; //
calculate sum of error
        u = (pid_Data.Kp_L * err) + (pid_Data.Kd_L * (err
- pid_Data.prev_err_L)) + (pid_Data.Ki_L *
(pid_Data.sum_err_L));
        pid_Data.prev_err_L = err;// store the last error
    }
    else u = 0;
    return u; // return PID output
}

```

Ziegler-Nichols would be a good method to determine the K_p, K_i, K_d value in the programming. The Ziegler–Nichols tuning method seen in Table 27 is a heuristic method of tuning a PID controller. The "P" (proportional) gain, K_p is then increased (from zero) until it reaches the ultimate gain K_u , at which the output of the control loop has stable and consistent oscillations.

Table 26: PID gain according to Ziegler-Nichols method

PID parameter	K_p	K_p/K_i	K_d/K_p
P	Time/delay time	infinite	0
PI	0.9TC/delay time	Delay time/0.3	0
PID	1.2TC/delay time	2 delay time	0.5 delay time

There are three modes for this UAV: vertical, horizontal and transition seen in Table 28. The horizontal flight mode is most efficient and UAV can take long term operations above a high speed. The transition mode ensures stationary operation. Vertical mode is used to take off and land.

Table 27: The flight mode and speed of the UAV

Fight Mode	Horizontal speed
Vertical	0 – 1.4m/s
Transition	0- 16m/s
Horizontal	10m/s- 35m/s

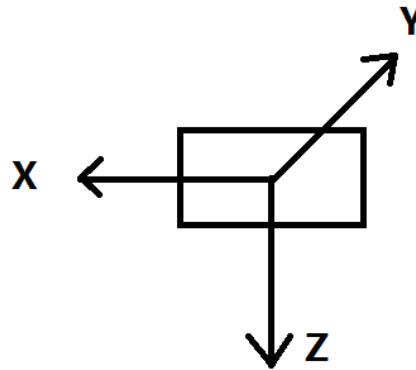


Figure 99: The free body diagram of the UAV

The coordinate system of UAV is depicted in Figure 99. The adaptive control law is designed by taking the pitch channel is

$$\bar{u}_1 = kr + f_0 y_p + f_1 \dot{y}_p \quad (29)$$

In this case, k is the feedforward gain, r is the reference input, f_0 and f_1 are feedback gains. The way is to adjust parameter k , f_0 and f_1 so that the system output can track the simulation. The following is the differential equation

$$\ddot{z} + a_1\dot{z} + a_0z = br \quad (30)$$

Coefficients a_0 , a_1 and b should be gotten based on control performance index of pitch channel.

The equation below is the common two-order system:

$$\varphi(s) = \frac{\omega_n^2}{s^2 + 2\varepsilon\omega_n s + \omega_n^2} \quad (31)$$

The damping analysis and simulation can be done after that

The MatLab Simulink seen in *Figure 100* is very important in the UAV control analysis. The reason is that the UAV flight system is complicated. There are a lot of elements

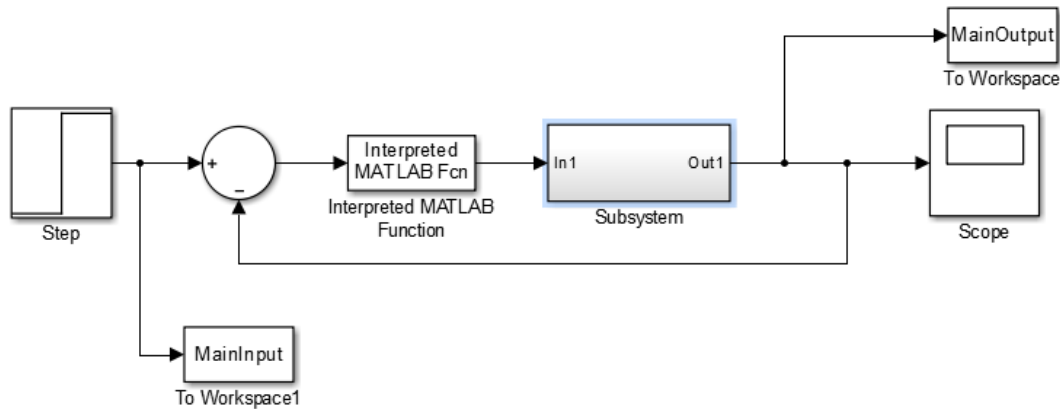


Figure 100: Basic sketch of MatLab Simulink for speed control

3.4 UAV Data Transmission

3.4.1 Long Range Remote Control Description

Different long range remote control systems are suitable for different scenarios. When the required range is below 100 meters, 2.4/5 GHz RC(Radio Control) is the most common solution.



Figure 101: 2.4GHz/5.8GHz frequency wireless communication structure

As *Figure 101* shows Phantom 2 which uses 2.4 GHz to control the UAV and 5.8 GHz to stream video data. Portable NX Pocket Drone, Parrot Disco FPV all used 2.4 GHz wireless communication protocol. Wi-Fi family is one of the most famous protocols on this frequency, which support stable transmission and 10-105 Mbps speed. Modified Wi-Fi, which is an experimental project in UCLA, can support at most 5000 meters range. However, flying range for an UAV usually is larger than that. Satellite communication has very long communication distance, which supports over 1500 kilometers range according NASA 2009 technical report.

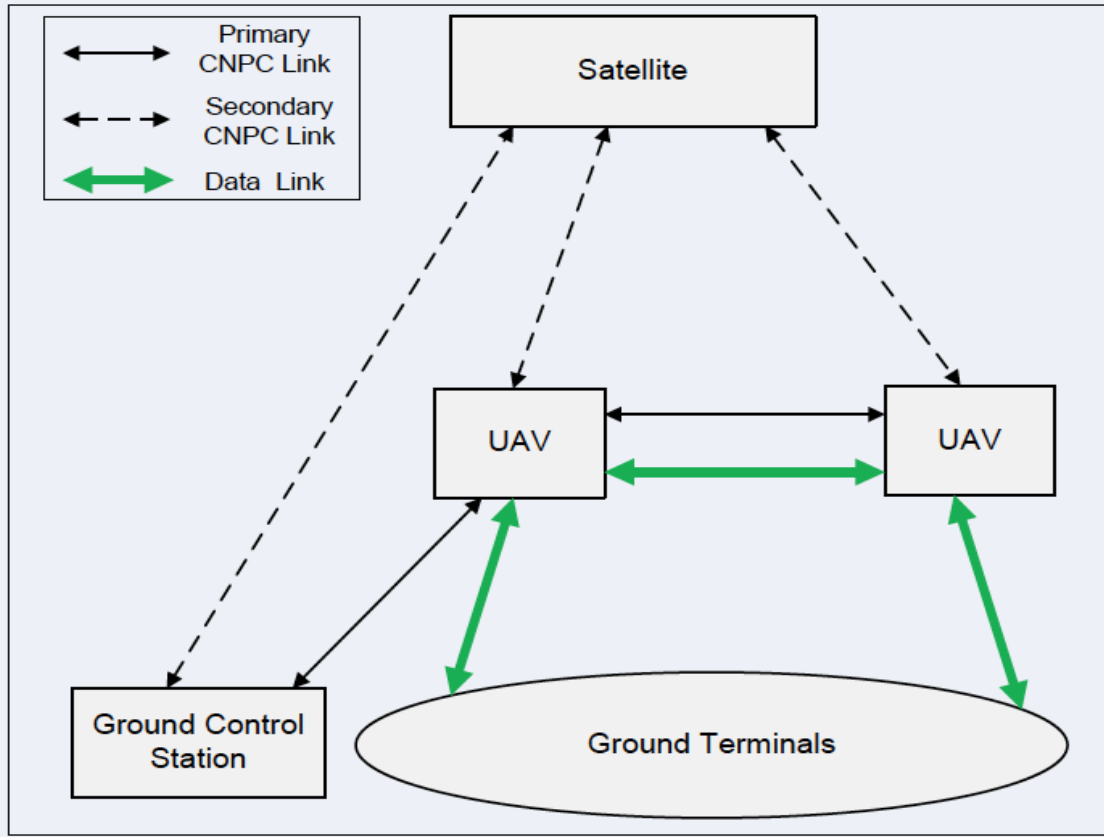


Figure 102: Structure of UAV-Satellite Communication

Figure 102 shows the structure of UAV-Satellite communication. Safe UAV operation is key to operations in shared airspace. Reliable communications between the control station and the aircraft are essential for operators to have feedback control. The CNPC-1000 data link implements the Control and Non-Payload Communications (CNPC) waveform in an optimized package for the small to large unmanned aircraft. This technology is used and recommended by NASA.

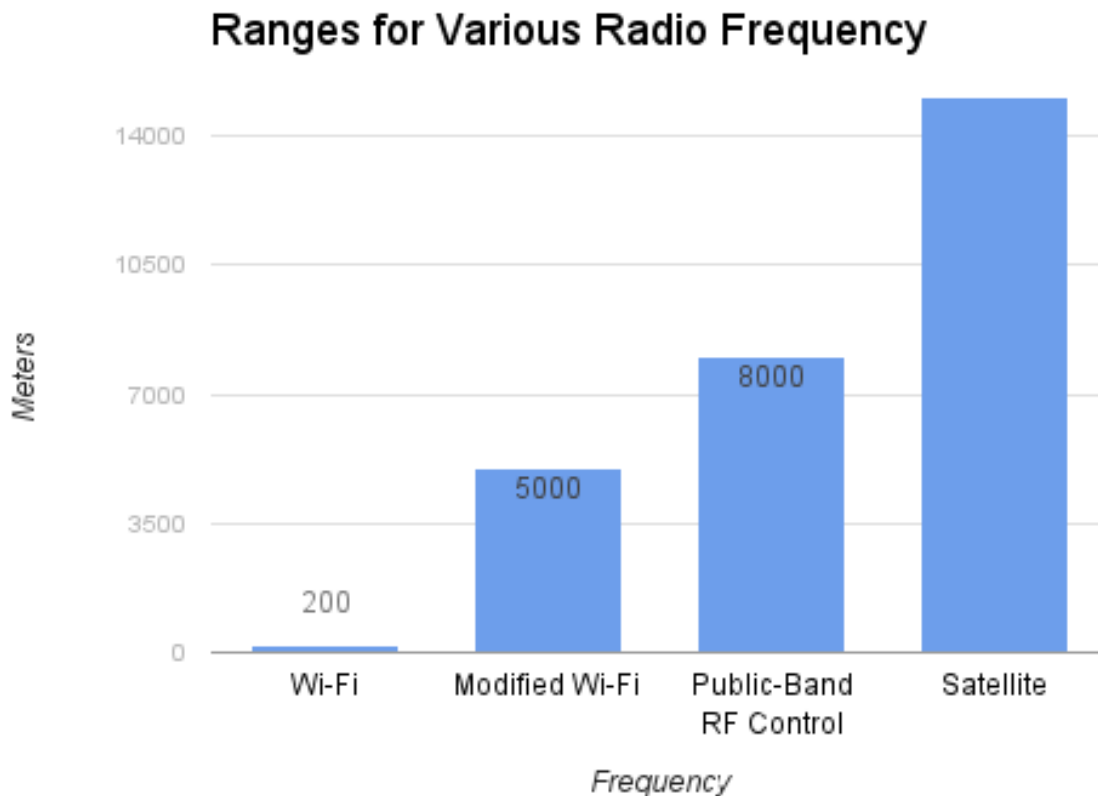


Figure 103: Ranges for various radio frequency

Shown in *Figure 103*, RF (Radio Frequency) control on public band is our best choice for long range control transmission. Range of Wi-Fi is not enough to support long distance for our operation. The real rescuing situation is complex and unpredictable. A distance of 200 meters cannot give relative high probability for rescuing patients in the scene of an incident. Modified Wi-Fi is able to handle the UAV data transmission but lack of stabilities. In rescuing operation, stable communication with base station plays an unsubstituted role. Receiving real time information, including video streaming of circumambient scenario and thermal image, can support the critical clue that shows where the survivals are. Satellite solution, from figure 104, our team believe it is best solution due to its stability. However, huge cost and fundamental setups will make the cost incredibly high. In the other hand, satellite can support almost the best effect among these solutions in summary.

Speed For Various Radio Frequency

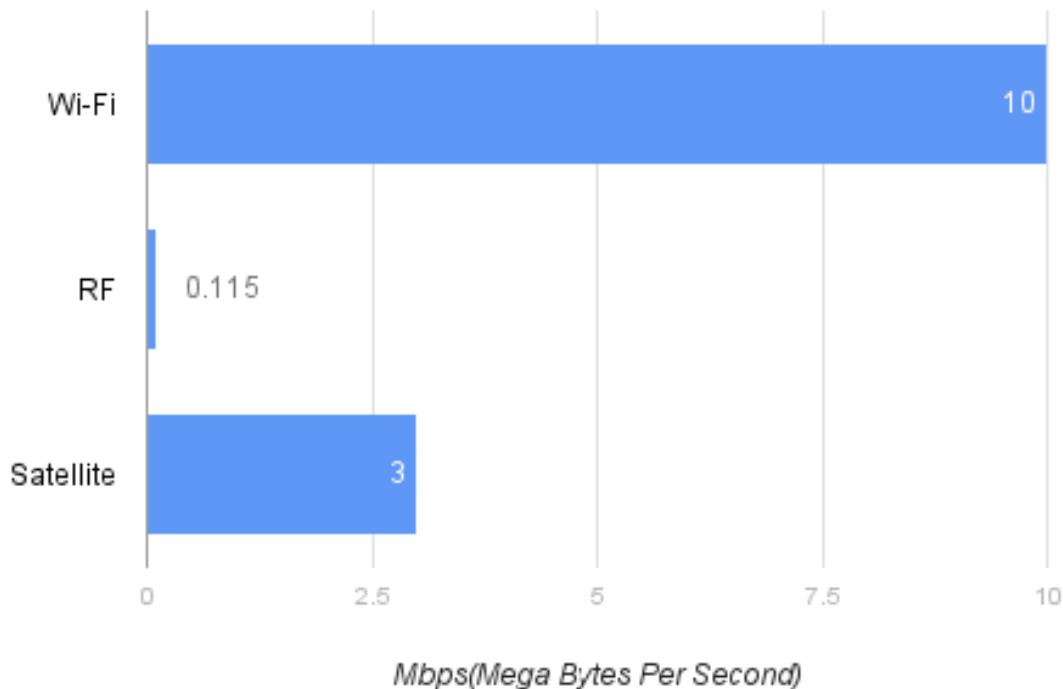


Figure 104: Speed for various radio solution

Figure 104 indicates one problem for RF control. The problem is the effect of low speed data transmission. The RF controlling method is relatively slower than the other two solutions. However, controlling an UAV only require low level of data transmission, only 50 kbps ensured rate can support stable UAV control. Stable video and image transmissions need larger transferring rate of data. To be more specific, a stable 720p video needs transferring rate at least larger than 800 kbps; therefore, 1 mbps would be the ideal rate. Although Wi-Fi protocol can easily achieve this goal, the available communication distance is a critical. Our team self-developed a wireless protocol or wireless module used in wireless transmission which is relied by UAV. Highly customized ability can perfectly fits the complex requirements needed by searching and recurring operation.

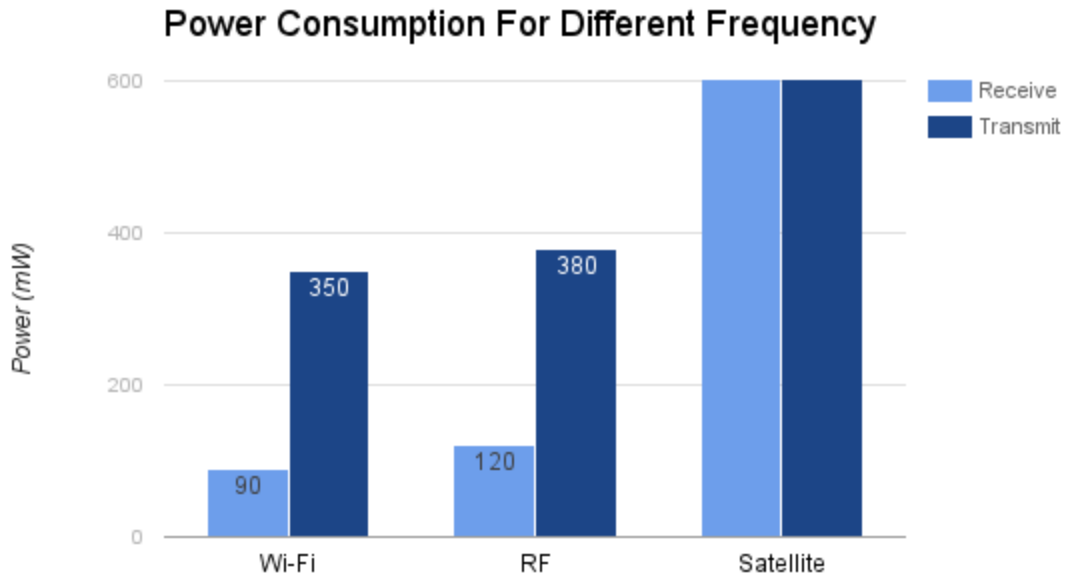


Figure 105: Power consumption for different frequency

From the power consumption point of view, Wi-Fi and other RF family protocols have similar power requirements, because they are all on 2.4 GHz or 5 GHz. Satellite has larger power consumption requirements because it needs signal amplifier to send signal to satellite. In same power consumption requirements, Wi-Fi and RF solutions have better performance and relatively low latency. Low latency is another important factor that affects the quality of wireless communication systems. If the video and the images received by base station are five or 10 earlier, base station will make the decision slower than the expected time. This our team believe will increase the probability of successful search and rescue operations.

3.4.2 On Board Computational Systems

Jetson TK1 embedded system. Support high performance GPU and CPU computation. Powerful port system provides us high scalable ability to extend the functions using sensors attached to the embedded system.

Table 28: List of components onboard the UAV

Items	Port
Time of Flight 3D Camera	Gigabit Ethernet
Thermal Imaging Camera	Gigabit Ethernet
Accelerator	USB
RC Receiver	USB
Battery	Power Port
360 Degree Camera(Panoramic 360° HD Video Camera - Black)	Gigabit Ethernet
Gyroscope	USB

The Table above shows the sensors that are connected to the embedded system. Multiple cameras are used to ensure high probability of finding survivals. The accelerator gives real time feedback about the current status of the UAV.

Different Weights For Different Components

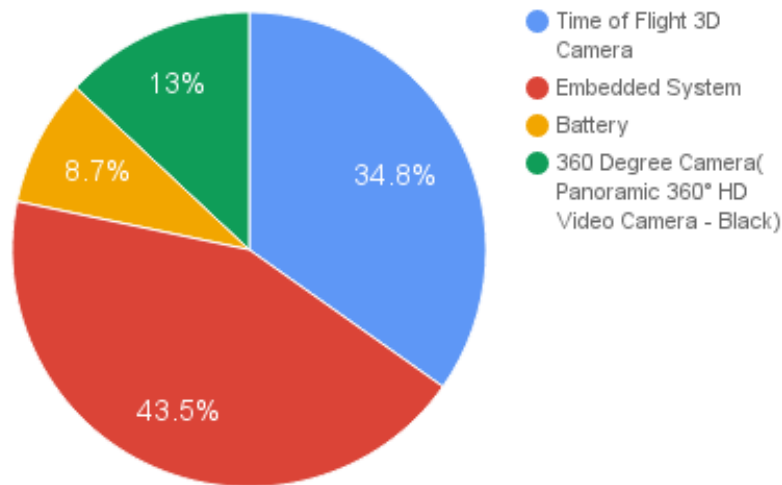


Figure 106: Different weights for different components

According to the *Figure 106*, embedded system takes the most part of weight. It contains many units such as computing unit, wireless unit and storage unit. Compared to embedded system, battery only takes 8.7% of total weight. It means drone can easily extends its power capacity.

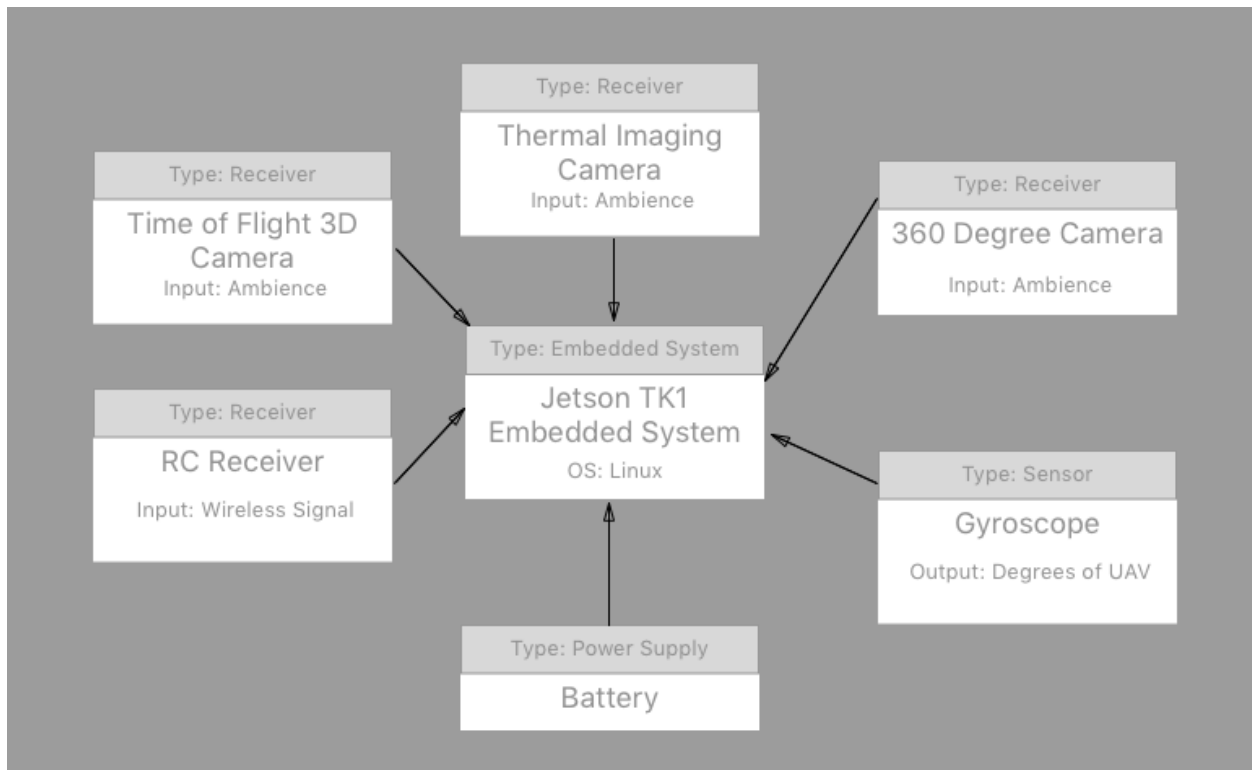


Figure 107: Relations among components in UAV

According to the *Figure 107*, the core of the embedded system is Jetson TK1, which is a kind of Linux embedded system with a strong ability of GPU and CPU computation. One of the most important reasons for choosing Jetson TK1 is its high GPU computing performance. Object detection algorithm and other computer vision related algorithms will get accelerated by using GPU computing. Parallel GPU programming can significantly speed up the processing of the algorithm which support parallel programming. Quicker process speed of graph algorithm performs better understanding of real time situation. Low latency and low delay can help base station quicker and more precise to find possible survivals.

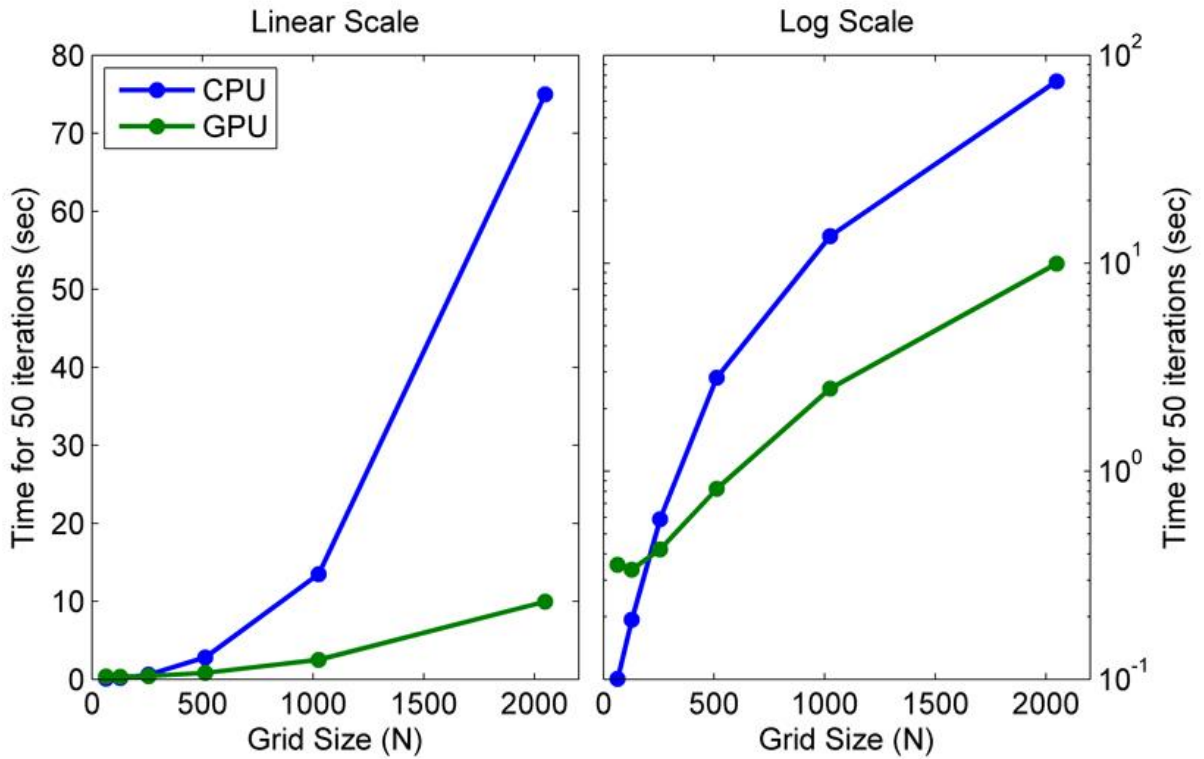


Figure 108: Speed Comparison between CPU and GPU

Gyroscope and GPS are mainly use to detect the status of the UAV. Gyroscope can support the detection of acceleration, rotating angle, and speed. GPS gives base station the global position of the UAV. Combination of these two components would let the base station monitor the status of the UAV in real time. Also, the embedded system will support other critical information systems like battery life and the status of other components such as cameras, wireless communication.

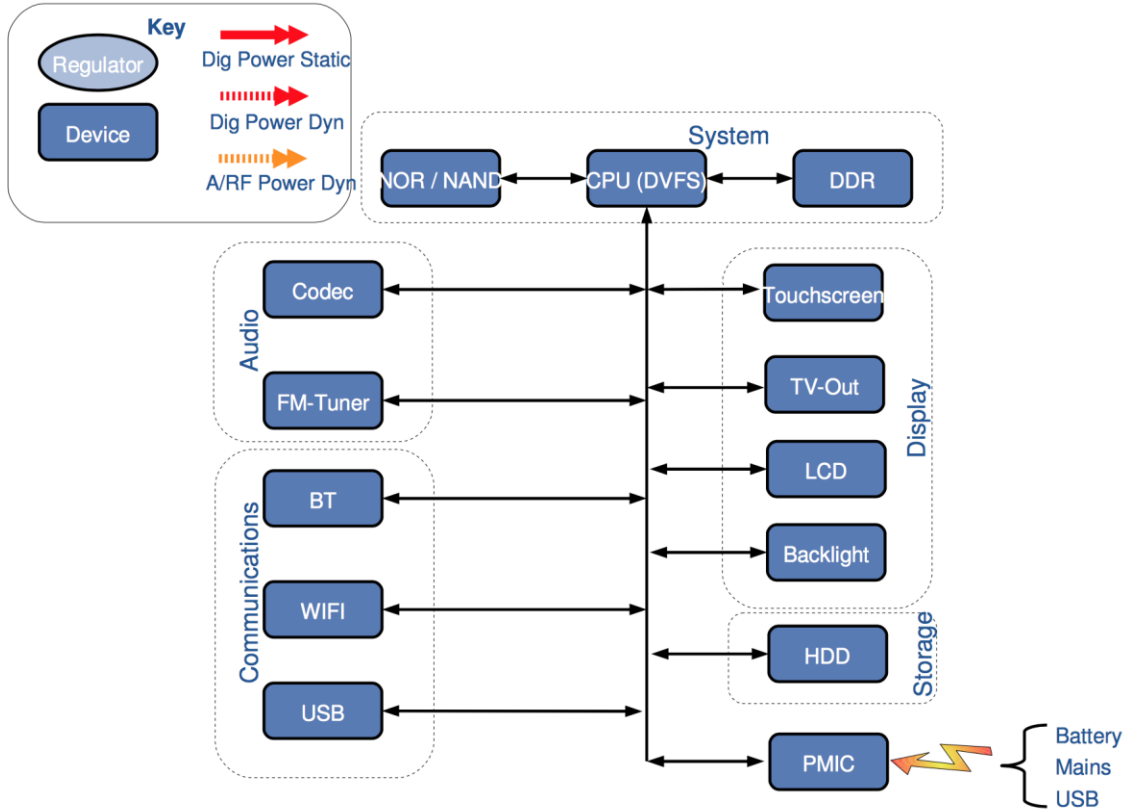


Figure 109: Visual Representation of Power Flow[3333]

Figure 109 shows that although multiple components can support abundant functions that needed by rescuing operations, complexity of system is increasing at the same time, especially for energy transmission. The structure of all of those component connected to the embedded system means all the power output is supported by embedded system. The highly custom ability of Linux kernel support voltage management system. Kernel Regulator framework is designed to solve this problem. This framework provides a standard kernel interface to control voltage and current regulators. It allows systems to dynamically control the power output in order to save power and prolong battery life. The framework is divided into four separate interfaces, namely: consumer interface for device drivers, regulator driver interface for regulator drivers, machine interface for board configuration and sysfs interface for user space. In Linux, kernel space and user space are spate from each other. The reason for that is to protect system stability and give user high scalability to extend the original system kernel at the same time.

Consumers are client device drivers that user regulators to control their power supply. Consumers are constrained by the constraints of the power domain. For view of stability and

scalability, consumers can't request power setting that may damage themselves, other consumers, or the system. If consumers have right to access and change these key information of the system, whole UAV system is vulnerable. This is unexpected when the UAV is in operation.

Table 29: Functions used to control voltage in Linux

Regulator Access:	regulator_get(dev, name)	regulator_put(regulator)
Regulator Control:	regulator_enable(regulator)	regulator_disable(regulator)
	regulator_set_voltage(regulator *, int min_voltage, int max_voltage)	regulator_force_disable(regulator)
	regulator_set_current_limit(regulator *, int min_a, int max_a)	
Regulator Status:	regulator_is_enabled(regulator)	regulator_get_voltage(regulator*)
	regulator_get_current_limit(regulator *)	

From Table 30, Linux system kernel give developers a complete tool chain to control the voltage between component and system port. Depending on those robust application program interface (API), system can customize the output voltage for different component connected to itself.

3.4.3 UAV Data and Signal Transmission

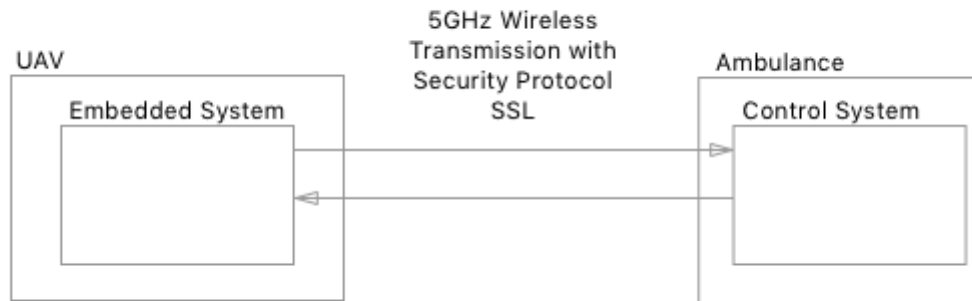


Figure 110: UAV signal transmission structure

UAV data and signal transmission are two independent phases, non-interacting systems. This ensures the stability and security of the UAV when one of them occurs unexpected problem, such as loss of data transmission. If data stream is offline or broken, base station still have backup stream system which is command stream to ensure that the UAV can be properly controlled. Show in *Figure 111*, the data transmission is established by 5 GHz wireless transmission with security protocol SSL; also, there will be two such transmission established between the base and the UAV for failure prove purposes. Specifically, the flight parameters will be transmitted to base station in real time, as well as the thermal image data stream, large data stream like high resolution video and 3D data will be cached directly on storage which is inside the UAV.

CHAPTER 4. CONCLUSION

Based upon research background on UAV applications and designs, our team successfully design a UAV system that can be remotely controlled and operated at a radius of about 50 kilometers. This UAV would provide an opportunity for emergency medicine services teams to respond to a scene of an incident in a timely manner. The UAV is also designed for search and rescue purposes, and delivering medical supplies. It is the understanding of our team that the Rwanda Zip-line UAV has the capability operating within a radius of 30 kilometers and able to maintain a 30 minutes operation time. In the contrast, the UAV designed from this project is able to carry more payload, stay in the air for longer time period, and also equipped with life detecting abilities than the Rwanda Zip-line UAV

Overall this project can be viewed as an improvement with respect to current technologies. However, there are number of areas that can be improved in the future. First and foremost, the UAV design needs to be improved by using wind tunnel examination or air flow simulations. Second, improving the security protocol on wireless transmission is also necessary. This promises a successful search and rescue operation. Finally, an energy recycling system can also be developed in the future. The proposed UAV uses butane as the fuel. Our team hope that renewable forms of energy can be used to enhance the functions and efficiency of the UAV. However, among the design and reasoning given in this IQP, the solution is reasonably acceptable. We believe our suggestions and solutions will enhance the quality of emergency medical UAVs.

REFERENCES

- [1] A. Idries and N. Mohamed, "Towards Risk Knowledge Management in Unmanned Aerial Vehicles Applications Development," Collaboration Technologies and Systems Conference (CTS), June 2015.
- [4] S. Jesse, "How a Quadcopter Works | Clay Allen," 20 January 2015. http://ffden-2.phys.uaf.edu/webproj/212_spring_2014/Clay_Allen/clay_allen/works.html.
- [5] J. Villbrandt, "Illumin - The Quadrotor's Coming of Age," 1 July 2010.
- [6] V. Olivares, F. Cordova, J. M. Sepulveda and I. Derpich, "Modeling Internal Logistics by Using Drones on the Stage of Assembly of Products," 3rd International Conference on Information Technology and Quantitative Management (ITQM), Chile, 2015.
- [8] M. S. Fofana, "Calculating Feedback Controller and Compensator," MyWPI Control Engineering, Class Notes, 15 April 2011.
- [9] T. Takotomamonjy, M. Ouladsine and T. L. Moing, "Longitudinal modelling and control of a flapping-wing micro aerial vehicle," Control Engineering Practice, vol. 18, no. 7, pp. 679-690, July 2010.
- [10] Airforce Technology.com, "X-47 Pegasus UCAV." Accessed April 21, 2016 <http://www.airforce-technology.com/projects/x47/>. <http://www.airforce-technology.com/projects/x47/>.
- [12] "The UAV - The Future of the Sky," 21 April 2016. Website | http://www.theuav.com/fire_scout_uav.html.
- [13] "EADS Talarion - Development and Operational History, Performance Specifications and Picture Gallery," Website | http://www.militaryfactory.com/aircraft/detail.asp?aircraft_id=1087. [Accessed 21 April 2016].
- [14] G. Rob, "Solar Plane Aims for New Record: Three Months Aloft Without a Pilot or Fuel," 7 July 2010. <https://www.element14.com/community/docs/DOC-43347/1/solar-plane-aims-for-new-record-3-months-aloft-without-a-pilot-or-fuel>
- [15] "Official Phantom UAVs specifications.," [http://research.omicsgroup.org/index.php/Phantom_\(UAV\)](http://research.omicsgroup.org/index.php/Phantom_(UAV)), Accessed 7 March 2015
- [18] "Rapid Manufactured Fixed Wing Powered UAV," AMRC Design and Prototyping Group, Available: http://www.amrc.co.uk/wp-content/uploads/AMRC_DPG_PoweredUAV-v2.pdf.

- [19] "Adhesively Bonded Joints in Aircraft Structures," Available: http://link.springer.com/referenceworkentry/10.1007/978-3-642-01169-6_44. [Accessed 21 April 2016].
- [20] "Design Analysis of the Zeke 32 (Hamp - Mitsubishi A6M3)," [Online]. Available: <http://rwebs.net/avhistory/history/zeke32.htm>. [Accessed 21 April 2016].
- [24] H. Chen, X. Dong, X. Xu and M. Mir, "3D Scanning Based on Computer Vision", Quora 2012.
- [25] H.-U. Meier, "Die Pfeilflügelentwicklung in Deutschland bis, Einspruch 1984", Gegen US-Patentschrift NASA über, 1945.
- [26] L. S. PhD, "Common Application of Airplane Wing Tips", ZhiHu Inc, October 17, 2014.
- [27] M. Y. a. A. C, "Air Flow Applications on Fighter Jets", ZhiHu Inc, September 5, 2015.
- [28] S. Ye, "Engine and Propeller Location Applications", ZhiHu Inc, July 25, 2014.
- [29] S. L. a. Z. C. "Changsong Xie, Engine Application Difference for Aircrafts", ZhiHu Inc, May 27, 2013.
- [30] M. Wei, "Structure Difference Between UAVs and Commercial Aircraft", ZhiHu Inc, August 11, 2014.
- [31] A. Salehian, "Vibration Analysis for Quadrotor Arm in an Unmanned Aerial Vehicle (UAV)", University of Waterloo, ON, Canada: Technical report, submitted to Aeryon Labs, December 19, 2012.
- [32] A. Salehian, "System Identification and Active Isolation of a High Altitude Reconnaissance Camera", Illinois, USA: Phase III Technical report, submitted to Recon Optical Inc, March 10, 2005, <http://www.airforce-technology.com/projects/u2/>
- [33] A. Salehian, "System Identification and Active Isolation of a High Altitude Recon Cense Camera", Illinois, USA: Phase I and II Technical report, submitted to Recon Optical Inc, January 7, 2005. <http://www.airforce-technology.com/projects/u2/>
- [34] B. Gunston, "The Cambridge Aerospace Dictionary Cambridge", Cambridge University Press, 2004.
- [37] M. Sadraey, "Aircraft Design: A System Engineering Approach", Wiley Publication, Rudder Design Chapter 12 Design of Control Surfaces, September 2012.
- [38] NASA, National Aeronautics and Space Administration, 5 May 2015. Available: <https://www.grc.nasa.gov/www/k-12/airplane/trbttyp.html>.

- [40] G. W. J. H. G. PinYing Yang, "Design of a Solar Power Management System for an Experimental UAV", Tamkang University, Taiwan, October, 2009.
- [41] "Fuel Cell System with Sodium Borohydride as Hydrogen source for Unmanned Aerial Vehicles," in *Fuel Cells Science & Technology*, vol. 196, 2011, pp. 9069-9075.
- [42] "Energy Information Administration," , US Department of Energy, 29 July 2015, Available: http://www.eia.gov/Energyexplained/?page=about_energy_units.
- [43] "Lead-Free gasoline Material Safety Data Sheet," NOAA., 2008.
- [45] C. Collins, "Implementing Phytoremediation of Petroleum Hydrocarbons," *Methods in Biotechnology (Humana Press)*, pp. 99-108, 2007.
- [46] "Fuel Oil Combustion," *Kerosene Blending*.
- [47] " Emissions Inventory Testing at Long Beach Turbine Combustion Turbine No. 3. CARNOT," Tustin, 1989.
- [49] "GAO-13-294SP, Defense Acquisitions Assessments of Selected Weapon Programs," US Government Accountability Office, Northrop Grumman USAF, 2013, pp. 113-114.
- [50] N. Grumman, "Global Hawk, Specifications (Multi-INT and Wide Area Surveillance Models)," Northrop Grumman Corporation, 2016. [Online]. Available: <http://www.northropgrumman.com/Capabilities/GlobalHawk/Pages/default.aspx>.
- [51] C. R. W. Wilson, "Eyes in the Sky Aerial Systems," *Military Intelligence Professional Bulletin*, 1996.
- [52] Northrop Grumman, "Global Hawk," Aeronautical Systems Center Laboratory, United States Air Force, USA.
<http://www.northropgrumman.com/Capabilities/RQ4Block20GlobalHawk/Pages/default.aspx>
- [53] Northrop Grumman, "Precisionhawk," PrecisionHawk 2016, Aeronautical Systems Center Laboratory, United States Air Force, USA, Available: <http://www.precisionhawk.com/lancaster>.
- [54] "Official Phantom UAVs Specifications.," Dà-Jiāng Innovations (DJI) Science and Technology Co., China , 2015.
- [55] B. Coxworth, "DJI Announces Stabilized HERO Mount, and Camera-Equipped Phantom Quadcopter"n *New Atlas*, 2015.
- [56] A. Fitzpatrick, "Finally, a Drone You Can Own," 30 January 2014,
<http://techland.time.com/2014/01/30/dji-phantom-vision-quadcopter-drone-review/>
- [57] "Spreading-Wings s1000 Plus," DJI Technology. [Online]. [Accessed 2 March 2015].

- [58] "Spreading-Wings s1000 Plus," 22 January 2015. [Online]. Available: http://wiki.dji.com/en/index.php/Spreading_Wings_S1000%2B.
- [59] "Design Build Fly Master Qualifying Project" WPI Aerospace Engineering, 2014.
- [60] J. G. Fairman, "Lift Formula," NASA, [Online]. Available: https://www.grc.nasa.gov/www/k-12/WindTunnel/Activities/lift_formula.html.
- [61] Y. Tan, Y. Dong and X. Wang, "Review of MEMS Electromagnetic Vibration Energy Harvester," Journal of Microelectromechanical Systems, vol. PP, no. 99, pp. 1-16, 2016.
- [62] A. Cho, J. Kim, S. Lee and C. Kee, "Wind Estimation and Airspeed Calibration Using a UAV with a Single-Antenna GPS Receiver and Pitot Tube," IEEE Transactions on Aerospace and Electronic Systems, vol. 47, no. 1, pp. 109-117, 2011.
- [63] O. He, Z. Wang and J. He, "Temperature and Humidity Profiles Retrieving Over Land Using Clear Sky Measurements of Microwave Humidity-Temperature Sounder on Chinese FY-3C Satellite," IEEE International Geoscience and Remote Sensing Symposium, pp. 4161-4164, 2016.
- [64] "MEMS Current Type Accelerometer," RION Tech. http://en.rion-tech.net/products_detail/productId=75.html
- [65] "MEMS Voltage Type Accelerometer," RION Tech. http://en.rion-tech.net/products_detail/productId=75.html
- [66] "Low Outgassing Triaxle ICP Accelerometer Installation and Operating Manual," PCB Piezotronics Inc.. http://www.imi-sensors.com/Products.aspx?m=356M208_NC
- [68] "MEMS Quartz Tactical Inertial Measurement Unit," Syttron Donner Inc., http://www.syttron.com/sites/default/files/sdi510_b.pdf
- [69] "MEMS Quartz Dual Axis Rate Sensor," Syttron Donner Inc., http://www.syttron.com/sites/default/files/sdi510_b.pdf
- [70] Static Pressure Probe A-520 Datasheet, DN520.5, MAMAC System.
- [71] Channel Low Power GPS Receiver VENUS634FLPx 65 Datasheet, Version 0.5, Sky Traq Technology, Inc., Taiwan
- [72] Low Voltage Temperature Sensors TMP36 Datasheet, Analog Devices.
- [73] H. RF, Humidity Sensor Module HH10D Datasheet, Version 2.0.
- [74] L. Hebei, Thermoelectric Cooler., I.T Co., Shanghai, China <http://peltiermodules.com/peltier.datasheet/TEC1-12705.pdf>

[75] Antmicro, “Antmicro at Embedded World 2016 – Sneak Peek”, 18 February, 2016.

[76] Nvidia, “Kitcontents”, 2016. Available: <http://www.nvidia.com/object/jetson-tk1-embedded-dev-kit.html>.

[77] P. Vance VanDoren, “Back to Basics: How gain scheduling works”, 21 December, 2010.

APPENDICE

Dijkstra Functions

```
2
3  create vertex set Q
4
5  for each vertex v in Graph: // Initialization
6      dist[v] ← INFINITY      // Unknown distance from source to v
7      prev[v] ← UNDEFINED    // Previous node in optimal path from source
8      add v to Q              // All nodes initially in Q (unvisited nodes)
9
10 dist[source] ← 0           // Distance from source to source
11
12 while Q is not empty:
13     u ← vertex in Q with min dist[u] // Source node will be selected first
14     remove u from Q
15
16     for each neighbor v of u: // where v is still in Q.
17         alt ← dist[u] + length(u, v)
18         if alt < dist[v]: // A shorter path to v has been found
19             dist[v] ← alt
20             prev[v] ← u
21
22 return dist[], prev[]
```

Any little improvements in this searching algorithm will benefits the UAV to auto-generating flying route.

However, dijkstra's algorithm only can solve problem in idea scenario. When UAV meets some obstacles so that it need to change its direction or altitude. Keeping changing state of UAV will accurate loosing power. What we want is to let UAV can fly in given route as long as possible. In order to avoid that, A-star search algorithm is introduced to solve this problem.

```

function A*(start, goal)
    // The set of nodes already evaluated.
    closedSet := {}
    // The set of currently discovered nodes still to be evaluated.
    // Initially, only the start node is known.
    openSet := {start}
    // For each node, which node it can most efficiently be reached from.
    // If a node can be reached from many nodes, cameFrom will eventually contain the
    // most efficient previous step.
    cameFrom := the empty map

    // For each node, the cost of getting from the start node to that node.
    gScore := map with default value of Infinity
    // The cost of going from start to start is zero.
    gScore[start] := 0
    // For each node, the total cost of getting from the start node to the goal
    // by passing by that node. That value is partly known, partly heuristic.
    fScore := map with default value of Infinity
    // For the first node, that value is completely heuristic.
    fScore[start] := heuristic_cost_estimate(start, goal)

    while openSet is not empty
        current := the node in openSet having the lowest fScore[] value
        if current = goal
            return reconstruct_path(cameFrom, goal)

        openSet.Remove(current)
        closedSet.Add(current)
        for each neighbor of current
            if neighbor in closedSet
                continue // Ignore the neighbor which is already evaluated.
            // The distance from start to a neighbor
            tentative_gScore := gScore[current] + dist_between(current, neighbor)
            if neighbor not in openSet // Discover a new node
                openSet.Add(neighbor)
            else if tentative_gScore >= gScore[neighbor]

```

```

    continue // This is not a better path.

    // This path is the best until now. Record it!
    cameFrom[neighbor] := current
    gScore[neighbor] := tentative_gScore
    fScore[neighbor] := gScore[neighbor] + heuristic_cost_estimate(neighbor, goal)

return failure

function reconstruct_path(cameFrom, current)
    total_path := [current]
    while current in cameFrom.Keys:
        current := cameFrom[current]
        total_path.append(current)
    return total_path

```

A-star algorithm use heuristic way to evaluate the cost of edges. It only keep edge with smallest cost in final route.